MICRORNA FUNCTION DURING ZEBRAFISH RETINA REGENERATION

By

Kamya Rajaram

Dissertation

Submitted to the Faculty of the

Graduate School of Vanderbilt University

in partial fulfillment of the requirements

for the degree of

DOCTOR OF PHILOSOPHY

In

Biological Sciences

August 2014

Nashville, Tennessee

Approved

Ronald B. Emeson, Ph.D.

Joshua T. Gamse, Ph.D.

Douglas G. McMahon, Ph.D.

James G. Patton, Ph.D.

Antonis Rokas, Ph.D.

To my parents, Lalitha and Rajaram

To my sister, Divya

and

To my husband, Siddharth

This would not be possible but for your endless support, encouragement and love

ACKNOWLEDGEMENTS

Throughout my time in graduate school I have interacted with a number of wonderful people who have helped me grow both as a scientist and a human being. First amongst them is my Ph.D. advisor Dr. James Patton without whose support and confidence, this thesis may not have materialized. I want to thank Jim for his excellent mentorship, scientific guidance and for letting me work on projects I enjoyed. I'm thankful to my committee members: Dr. Doug McMahon, Dr. Josh Gamse, Dr. Antonis Rokas and Dr. Ron Emeson, for their expertise, suggestions and willingness to meet and talk to me both during committee meetings and otherwise. I'm grateful to our collaborator Dr. David Hyde at the University of Notre Dame, and his lab members Dr. Rachel Harding and Dr. Travis Bailey for sharing zebrafish lines and helping me learn retina manipulation techniques that have formed the crux of my dissertation. I'm deeply indebted to Dr. Jay Parrish at the University of Washington, for letting me be part of his lab and serving as a surrogate mentor during a decisive year in my graduate career.

Graduate school would not have been fun without the friendship and support of the Patton lab members. I thank Nan, Abby and Chunyao for showing me the ropes about being a grad student when I first joined the Patton lab. I'm fortunate to have overlapped with the current members of the Patton lab, particularly Mahesh, Diana and Nergis. I will surely miss our scientific conversations, our daily lunches and coffee breaks. A special note of thanks to Emily Summerbell, my undergrad, who stuck with me and our project for 3 years, and was always enthusiastic about our midnight time points and weekend experiments.

I appreciate the efforts and care of Qiang Guan in maintaining my zebrafish lines. I'd like to credit the Vanderbilt zebrafish community and the Program in Developmental Biology (PDB) for sharing reagents, protocols and helpful comments and suggestions. I want to thank the Department of Biological Sciences at Vanderbilt University, particularly Leslie Maxwell for her help throughout my duration here. I want to acknowledge my funding sources at Vanderbilt, the MOSIG funds in the Department of Biological Sciences and the Vanderbilt International Scholar Program (VISP) that allowed me to travel to conferences and present my research there.

I'm thankful to my friends both here in Nashville and outside. I'm particularly grateful to Saumitra and Poojitha for being the awesome listeners that they are and for their company during these long years of grad school.

Lastly, I want to thank my family. My parents, for their inspiration, open-mindedness and for letting me follow my interests, my sister for keeping me grounded and always looking out for me, and my dearest husband for his immense patience and belief in me. Without all your support, I would not be here today.

TABLE OF CONTENTS

LIST OF TABLES

Table Page

LIST OF FIGURES

LIST OF ABBREVIATIONS

AMD	age-related macular degeneration
Ascl1a	achaete-scute complex-like 1a
BrdU	bromodeoxyuridine
CE	cone ellipsoids
CGZ	circumferential germinal zone
CMZ	ciliary marginal zone
CNS	central nervous system
DC	double cones
Dot1l	disrupter of telomeric silencing 1 like
EGFP	enhanced green fluorescent protein
ELM	external limiting membrane
ESC	embryonic stem cells
ESCC	embryonic stem cell specific cell cycle regulating
FACS	fluorescence activated cell sorting
GCL	ganglion cell layer
GFAP	glial fibrillary acidic protein
GFP	green fluorescent protein
HSC	hematopoietic stem cell
HTS	high throughput sequencing
IHC	immuno histochemistry
IKNM	interkinetic nuclear migration

ILM	internal limiting membrane
INL	inner nuclear layer
IPL	inner plexiform layer
iPSC	induced pluripotent stem cell
Lsc	long single cones
MG	Müller glia
miRNAs	microRNAs
MO	morpholino
MRE	microRNA recognition element
NGS	next generation sequencing
NSC	neural stem cell
ONL	outer nuclear layer
OPL	outer plexiform layer
Pax	paired homeobox
PCNA	proliferating cell nuclear antigen
qPCR	quantitative real-time polymerase chain reaction
RGC	retinal ganglion cell
RISC	RNA induced silencing complex
RNP	ribonucleoprotein
ROS	rod outer segments
RP	retinitis pigmentosa
RPE	retinal pigment epithelium
SGZ	sub granular zone

Ssc	short single cones
Std Ctl	standard control
SVZ	sub ventricular zone
TUNEL	terminal deoxynucleotidyl transferase dUTP nick end labeling
UTR	untranslated region

CHAPTER I

INTRODUCTION

The retina is a thin, light sensing tissue that lines the back of the eye. It forms as an extension of the central nervous system (CNS) and the development, architecture and function of the retina is highly conserved amongst vertebrates (Cepko et al., 1996). Vision is achieved when light responsive cells in the retina called photoreceptors convert the information in the incident light into electrochemical signals that are relayed via a series of retinal neurons to the brain. Degenerative diseases of the retina such as age-related macular degeneration (AMD), retinitis pigmentosa (RP) and diabetic retinopathy are important causes of vision impairment and blindness in humans. The etiology of retina degenerative diseases is diverse, but in all cases irreparable loss of one or more retinal cell types ultimately impairs visual processing. Interestingly, non-mammalian vertebrates like amphibians, fish and birds to some extent, have inherent abilities to regenerate lost retinal neurons.

The retina of the teleost zebrafish can spontaneously regenerate following different kinds of retinal damage including surgical lesioning (Cameron, 2000), retinal puncture (Fausett and Goldman, 2006), intense light exposure (Vihtelic and Hyde, 2000) (Bernardos et al., 2007), laser ablation (Wu et al., 2001) and chemical or toxin treatment (Fimbel et al., 2007). In all these cases, retinal cell loss stimulates retinal glial cells, Müller Glia (MG), to partially dedifferentiate and generate progenitor cells. The progenitor cells rapidly divide to form progenitor cell clusters, which migrate to the region of damage and differentiate into lost retinal cell types. Since the retinal structure

and cell types are conserved across vertebrates, identifying key players during fish regeneration process can help design strategies to stimulate regeneration in the mammalian retina.

The molecular mechanisms underlying zebrafish retina regeneration are being parsed out. Historically, studies have focused on identifying protein-coding genes and signaling pathways, and only recently moved towards epigenetic or post-transcriptional regulation of retina regeneration. Small non-coding RNAs called miRNAs are important regulators of post-transcriptional gene expression in numerous processes including developmental timing, differentiation, cell proliferation, cell fate determination, apoptosis, metabolism and stem cell maintenance (Brennecke et al., 2003; Lee et al., 1993; Poy et al., 2004; Wang et al., 2008; Wang et al., 2007). Regeneration of different body parts in numerous cold-blooded vertebrates has been shown to be miRNA dependent (Sehm et al., 2009; Thatcher and Patton, 2010; Thatcher et al., 2008). Recently, MG dedifferentiation, an early step integral to retina regeneration, was shown to be dependent on suppression of the miRNA *let-7* (Ramachandran et al., 2010). Still, the overall requirement and functions of miRNAs in zebrafish retina regeneration remain unexplored.

In order to evaluate the requirement of miRNAs for retina regeneration, we inhibited miRNA biogenesis and demonstrated that mature miRNAs are necessary for retina regeneration. By performing high throughput sequencing (HTS) from undamaged, actively regenerating and completely regenerated retinas, I discovered that only a small subset of miRNAs actively changed their expression during retina regeneration, and almost all miRNAs returned to their basal expression levels once regeneration was

completed. To investigate how these differentially expressed miRNAs function during retina regeneration, I performed gain and loss of function studies in the adult zebrafish retina and found that miRNAs regulate both the initiation and progression of retina regeneration. I focused on 2 downregulated miRNAs, *miR-203* and *miR-216*, and discovered that they regulate progenitor cell proliferation and MG dedifferentiation, respectively, during adult zebrafish retina regeneration.

The Zebrafish Retina

Structure and Function

All vertebrate retinas are composed of 7 different classes of cells, 6 classes of neurons and one class of glia that are arranged in three distinct cellular layers (Figure 1). The outermost (most apical) cellular layer is the outer nuclear layer (ONL) that contains the cell bodies of the photoreceptors, rods and cones, which mediate night vision and color vision, respectively. The ONL is closely apposed to a monolayer of cuboidal epithelial cells called the retinal pigmented epithelium (RPE). The middle retinal layer is the inner nuclear layer (INL), which contains 3 classes of interneurons- horizontal, bipolar and amacrine cells- as well as the cell bodies of Müller glia (MG), which are the principal macroglial cell type found in all vertebrate retinas. The innermost (most basal) retinal layer is the ganglion cell layer (GCL) that is mainly composed of the retinal ganglion cells (RGC) and a few displaced amacrine cells. Separating the 3 cellular layers are 2 synaptic layers, the outer and the inner plexiform layer (OPL and IPL).

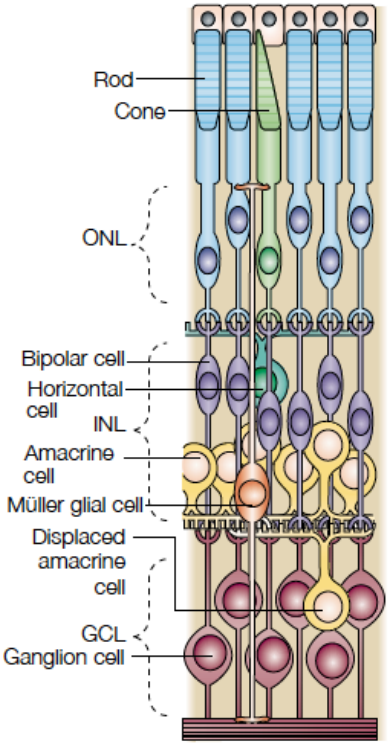

Figure 1. Structure of the vertebrate retina.

The different cell types in the retina are shown. ONL, outer nuclear layer; INL, inner nuclear layer; GCL, ganglion cell layer. Adapted from Dyer and Cepko, 2001.

The visual process begins when incident light enters the eye, passes through the cells in the GCL and the INL and falls on the photoreceptors. The photoreceptors receive the photic information and transduce it into electrochemical signals, which are sent to the RGCs via the bipolar cells (Centanin and Wittbrodt, 2014). Horizontal and amacrine cells perform lateral signal processing at the OPL and the IPL respectively, and help refine and integrate the visual output. The axons of the RGCs form the optic nerve that exits the eye and carries visual information to the brain. The non-neuronal MG, although not directly

involved in visual processing, provide homeostatic and metabolic support to the retinal neurons.

Cell Type Diversity

Although vertebrate retinas contain only seven main classes of cells, retinal neurons exhibit inter and intra species diversity. Extensive work in rabbits and rodents has estimated >60 distinct types of neurons in mammalian retinas, with slight differences in exact cell numbers amongst different species (Masland, 2001, 2012). Cytochemical markers, as well as neuronal arborizations and shape, were used to define cell types (Masland, 2001). So far, most mammalian retinas contain 1 type of rod photoreceptor, 2-3 types of cone photoreceptors (di or trichromatic), 2 types of horizontal cells, 12 types of bipolar cells, ~30 types of amacrine cells and ~20 types of RGCs. Non-mammalian vertebrates like fish and birds are tetrachromatic and contain 4 types of cone photoreceptors (Stenkamp, 2007). Zebrafish retinas contain 17 types of bipolar cells, 28 types of amacrine cells and 3 types of horizontal cells (Connaughton et al., 2004; Jusuf et al., 2011). Importantly, the whole repertoire of retinal cell types is generated from a population of retinal progenitor cells during development.

Development

The retina, like other parts of the CNS, is derived from the embryonic neural tube (Pei and Rhodin, 1970). Vertebrate eyes develop as paired lateral outgrowths of the forebrain called optic vesicles, which grow out to contact the surface ectoderm. This contact induces the cells of each optic vesicle to invaginate to from a double-layered cup-

shaped structure, whose outer cell layer becomes the retinal pigment epithelium (RPE) and the inner cell layer becomes the neural retina.

During early vertebrate eye development, the retina begins as a homogenous sheet of psuedostratified neuroepithelial cells, with processes that contact the apical and basal surfaces of the retina (also called the external limiting membrane, ELM and the internal limiting membrane, ILM). The cells of the neuroepithelium are multipotent retinal progenitor cells that transition through different 'competence' states over time, and give rise to all the retinal cell types in a stereotypical order that is conserved across different species (Cepko et al., 1996; Rapaport and Vietri, 1991; Young, 1985a). RGCs are the first cell types to be produced, followed by amacrine cells, horizontal cells and cone photoreceptors. Rod photoreceptors, MG and bipolar cells are the last to be generated.

Neurogenesis not only generates the different retinal cells, but also crafts the multilayered, highly laminated retinal structure. Multipotent progenitor cells undergo interkinetic nuclear migration (IKNM), where the nucleus of the progenitor migrates in an apical-basal fashion in phase with the cell cycle (Baye and Link, 2008; Young, 1985b). Mitosis always occurs at the apical surface of the retina, effectively 'birthing' all cells in the same location (Sidman, 1961). Cell division can be symmetric or asymmetric producing daughter cells with equivalent or different fates, respectively (Livesey and Cepko, 2001). The daughter cells can be progenitors, which reenter the cell cycle and undergo IKNM, or post-mitotic cells, which exit the cell cycle. The post-mitotic daughter cells undergo nuclear translocation, where they put forth cytoplasmic processes to contact the ILM (or basal retinal surface) and their nuclei migrate to occupy their typical positions within the retina. Thus, even cells born at similar times can end up in different

retinal layers. Both cell intrinsic and extrinsic factors determine the cell fates of retinal progenitors (Harris, 1997).

A characteristic pattern of retinal differentiation is observed across vertebrates (Wong and Godinho, 2003). RGCs near the optic stalk are the first to differentiate, and then differentiation gradients proceed from the inner to the outer retinal layers before moving in a centro-peripheral sequence through the entire retina. In mammals, all the retinal cells are generated early in the animal's life and neurogenesis does not persist subsequently (Lamba et al., 2008). Mammalian eyes grow extensively after completion of neurogenesis, and this results in a thinning of the retina. However, in several non-mammalian vertebrates including zebrafish, persistent neurogenesis is observed throughout the animal's lifespan.

Persistent Neurogenesis

Unlike mammals, teleost fish and urodele amphibians exhibit indeterminate growth, and the eye grows proportionate with body size. In these animals, only the most central part of the retina is generated from embryonic neurogenesis, and most of the retina is generated post-embryonically (Fischer and Reh, 2000; Hitchcock et al., 2004; Moshiri et al., 2005).

In teleost fish, retinal growth is coordinated with the body size via a growth hormone-IGF axis and is achieved through three different mechanisms: (1) hypertrophy of retinal cells, (2) a balloon-like expansion of the retina and (3) persistent neurogenesis (Boucher and Hitchcock, 1998; Johns, 1977). Post-embryonic neurogenesis in teleosts originates from two different 'stem cell' niches in the retina. The primary source is the

ciliary marginal zone (CMZ) or the circumferential germinal zone (CGZ), which is found at the periphery of the retina, where it meets the ciliary epithelium. The CMZ produces all of the retinal cell types, except rod photoreceptors, throughout the lifespan of the fish (Hitchcock et al., 2004; Johns, 1977). New retinal cells are added to the periphery of the retina in concentric annuli, and this pattern of growth generates a perfect ordering of retinal neurons from the peripheral to the central retina, with the newly differentiated cells located at the periphery and the older and more mature cells located in the central retina. Rod photoreceptors, on the other hand, are generated from a population of slowly cycling MG found in the INL (Bernardos et al., 2007). In adult fish retinas, a small population of MG re-enter the cell cycle very infrequently and undergo asymmetric cell division to produce spindle-shaped rod progenitors. These progenitors begin expressing rod photoreceptor markers and migrate to the ONL by associating along radial MG processes. Once in the ONL, these cells (now called rod precursors), proliferate and their progeny differentiate into rod photoreceptors. Thus new rod photoreceptors are constantly added to the differentiated retina and as the fish grows, the ratio of rods to cones in the retina increases (Johns and Easter, 1977).

Urodele amphibians lack a rod progenitor population and all retinal neurons, including rod photoreceptors are generated from stem cells in the CMZ (Mitashov, 1997; Otteson and Hitchcock, 2003). In contrast to fish and amphibians, most of the chick retina is produced during embryonic neurogenesis. However, limited proliferation of cells in the CMZ has been detected in the post hatch chick, and a small number of amacrine and bipolar cells are added at the retinal margin (Fischer and Reh, 2000). No persistent neurogenic zones have been detected in mammalian retinas (Moshiri et al., 2004).

Regeneration

As mentioned above, mammalian retina degeneration is irreversible, while non-mammalian vertebrates are capable to regenerating their retinas. Two modes of retina regeneration have been observed: (1) RPE-mediated regeneration and (2) MG-mediated regeneration.

RPE-mediated regeneration

RPE-mediated retina regeneration is observed in urodele amphibians and the embryonic chick (Karl and Reh, 2010). The RPE is a monolayer of melanin-containing epithelial cells, that are closely apposed to the photoreceptor outer segments and normally supports the retina by absorbing scattered light within the retina, mediating nutrient transfer, visual pigment processing, and phagocytosis of the shed photoreceptor discs. Following surgical removal or devascularization of the urodele retina, a subset of RPE cells lose their pigment, detach from their basement membrane and re-enter mitosis to generate a new layer of psuedostratified cells (Reh and Nagy, 1987; Stone, 1950). This layer behaves like the embryonic neuroepithelium and generates all of the lost retinal neurons in the stereotypic developmental order (Reh and Nagy, 1987). Following damage to a small portion of the retina, RPE cells near the site of injury respond and regenerate lost retinal cells. Normal retinal lamination, retinal cell numbers and visual function are restored following regeneration.

MG-mediated regeneration

Fish and post hatch chick (to a lesser extent) demonstrate MG-mediated retina regeneration after retinal damage. MG, as discussed earlier, are the only glial cells that share a common progenitor with retinal neurons during development. Under normal conditions, MG are post-mitotic and play important supportive roles in the retina (Reichenbach and Bringmann, 2013). Their processes span the entire width of the retina; form the ILM and the OLM, and ensheath retinal neurons. MG functions in the retina are diverse: MG (1) sustain retinal neurons by releasing neurotrophic factors and providing anatomical support, (2) aid in vision by processing visual pigments and by acting as optic fibers that guide light to the photoreceptors, (3) control the extracellular environment in the retina by taking up and processing neurotransmitters, regulating pH, water and ion homeostasis, (4) supply nutrients to the neurons and remove metabolic wastes and (5) contribute to the formation and maintenance of the blood-retinal barrier (Bringmann et al., 2006).

After retinal damage in the teleost zebrafish, post-mitotic MG spontaneously dedifferentiate and asymmetrically divide to produce progenitor cells that can rapidly proliferate, migrate and differentiate into the lost cell types. (Ramachandran et al., 2010; Ramachandran et al., 2011; Thummel et al., 2010). Regeneration restores most of the retinal architecture and complete visual function in the zebrafish retina (Fimbel et al., 2007; Vihtelic and Hyde, 2000).

In the retinas of post hatch chick, MG retain the ability to spontaneously respond to damage by proliferating and producing progenitor cells (Fischer and Reh, 2003). However, fewer progenitor cells are generated compared to the zebrafish retina, and a

very small population of the progenitor cells (<10%) preferentially differentiates into amacrine or bipolar cells. Interestingly, most of the MG derived progenitor cells (>80%) continue expressing progenitor markers without differentiating into a post-mitotic retinal cell type. It remains unknown if newly generated cell types are stably integrated into the chick retinal circuitry and if retinal function is restored (Lamba et al., 2008).

Damage to mammalian retina causes reactive gliosis of MG (Bringmann et al., 2006; Karl and Reh, 2010). Reactive MG change their gene expression pattern, upregulate GFAP expression, undergo hypertrophy and migrate to the region of damage. In some cases, reactive MG can proliferate and form a fibrotic 'glial scar', which precludes neuronal regrowth in the damaged area. Mammalian retinas lack any ability to spontaneously stimulate a regeneration response. However, studies in rodents have shown that retinal injury coupled with transcription factor or growth factor administration can induce some MG to dedifferentiate, proliferate and produce some progenitor cells that can preferentially become bipolar cells or photoreceptors (in rats) and amacrine cells (in mice) (Karl et al., 2008; Ooto et al., 2004). Additionally, the regeneration response is highly dependent on the age of the animal and extent of damage, with younger animals and widespread retina damage stimulating a stronger regeneration response.

Molecular mechanisms underlying regeneration

Retinal damage in the adult zebrafish triggers a spontaneous MG-mediated regeneration response. Regeneration studies performed using retinal puncture and intense light damage models have uncovered many genes and signaling pathways that control distinct steps of the regeneration process. In all these models, retinal damage triggers MG

dedifferentiation and expression of the pro-neural gene Ascl1a (Fausett and Goldman, 2006; Nelson et al., 2013). Activation of canonical Wnt- signaling via β-catenin stabilization (Ramachandran et al., 2011) is necessary for MG dedifferentiation, while suppression of *let-7* miRNAs by Lin-28 has also been detected at this stage (Ramachandran et al., 2010). Dedifferentiated MG express STAT3, TNFα and Alcama, incorporate the thymidine analog BrdU, accumulate PCNA and re-enter cell cycle (Kassen et al., 2007; Nagashima et al., 2013; Nelson et al., 2013). The MG nucleus migrates to the base of the ONL by IKNM, and undergoes a single round of asymmetric division to produce a $PCNA^{+}$/$Alcama^{-}$ progenitor cell (Nagashima et al., 2013). Both the progenitor cell and the MG nucleus migrate back to the INL, and the former rapidly divides *in-situ* to produce clusters of $PCNA^{+}$ progenitor cells that span the length of the INL and associate closely with the MG. Progenitor cell migration to the INL is dependent on N-cadherin expression in the dedifferentiated MG (Nagashima et al., 2013), while progenitor cell proliferation requires expression of *pax6a* and *pax6b* in the progenitor cells (Thummel et al., 2010). The clusters of progenitor cells then migrate along the MG processes and differentiate into the lost retinal cell types.

While most of these molecular markers are conserved in light damaged and punctured retinas, different signals have been identified to communicate with the MG and initiate differentiation. The Goldman lab detected enrichment of the EGFR ligand HB-EGF in MG as early as an hour after retinal puncture (Wan et al., 2012). Regeneration was impaired by HB-EGF knockdown and recombinant HB-EGF stimulated MG dedifferentiation in undamaged retinas, demonstrating that HB-EGF is necessary and sufficient to initiate MG-mediated regeneration. However, other groups have been unable

to replicate this result (Nelson et al., 2013). Additionally, the Hyde lab showed that HB-EGF was not necessary for light-induced retina regeneration (Nelson et al., 2013). They identified TNFα as the activator of MG dedifferentiation. TNFα expression was first detected in the dying photoreceptors and then in the MG. Administration of TNFα to undamaged retinas triggered MG-mediated regeneration, and TNFα knockdown abolished regeneration. It is possible that different damage models use different signals to initiate regeneration. Although genes and signaling pathways have been identified in retina regeneration, very little is known about regulation of these genes and the process of retina regeneration as a whole.

Constant intense light lesioning

Amongst the various retina damage models employed in zebrafish, the constant intense light exposure paradigm pioneered by Hyde and colleagues (Vihtelic and Hyde, 2000) has several advantages: (1) it is highly specific, since it causes photoreceptor apoptosis and leaves the rest of the retina intact (Figure 2), (2) it is non-invasive, (3) photoreceptor cell death is synchronous (Thomas et al., 2012). Light lesioning mimics photoreceptor apoptosis, the final pathway in many human retina degenerative diseases including retinitis pigmentosa (RP) and age-related macular degeneration (AMD). Both rod and cone photoreceptors die within a day of intense light exposure and regeneration begins as early as 3 days after the intense light treatment (Figure 3) (Vihtelic and Hyde, 2000). Regeneration in complete by 28 days after the light exposure and the retina is fully functional.

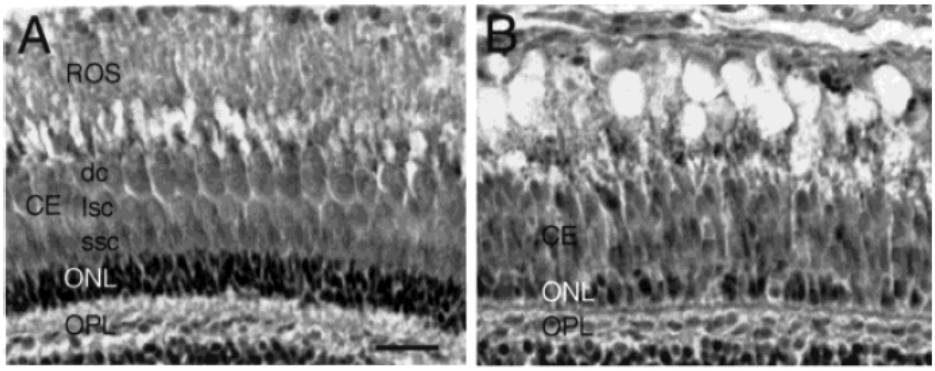

Figure 2. Effects of constant intense light exposure on the adult zebrafish retina.

ONL of hematoxylin-eosin stained retinas obtained from adult *albino* zebrafish prior to light exposure (A), or after 7 days of intense light exposure (B). Following light exposure, the thickness of the ONL is reduced. Long ROS and three distinct cone photoreceptor nuclei are visible in the undamaged retina (A), but destroyed following light damage (B). ROS, rod outer segments; CE, cone ellipsoids; dc, double cones; lsc, long single cones, ssc, short single cones; ONL, outer nuclear layer; OPL, outer plexiform layer. Scale bar 25 um. Adapted from Vihtelic and Hyde, 2000.

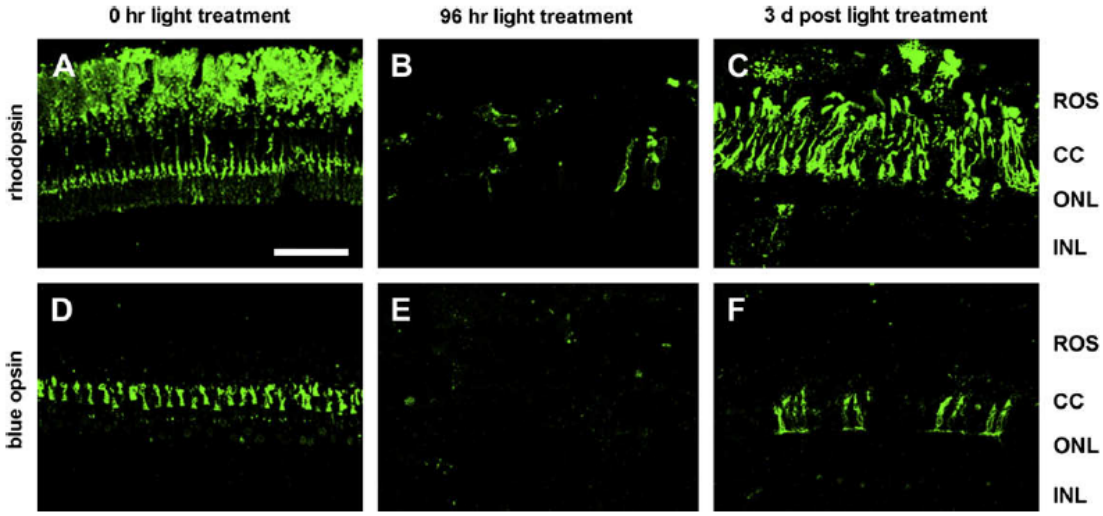

Figure 3. Photoreceptor regeneration following light damage.

Adult *albino* zebrafish retinas were examined by immunohistochemistry for the rod photoreceptor marker rhodopsin (A-C) or the blue cone photoreceptor marker blue opsin (D-F). Photoreceptor staining is detected prior to light exposure (A and D), but lost after 4 days in constant intense light (B and E). Photoreceptors begin to regenerate by 3 days after intense light treatment (C and F). ROS, rod outer segments; CC, cone cells; ONL, outer nuclear layer; INL, inner nuclear layer. Scale bar 25 um. Adapted from Thummel at al., 2008.

Despite its specificity and relatively cheap set-up, the constant intense light leisoning model has only been used in zebrafish of the *albino* genetic background, which lack the pigment melanin in their RPE. This eliminates the use of many valuable transgenic zebrafish lines of the pigmented AB genetic background. Nevertheless, the changes that happen in the retina following light induced photoreceptor degeneration are well documented (Figure 4) and provide a system to exclusively study the molecular mechanisms underlying photoreceptors regeneration.

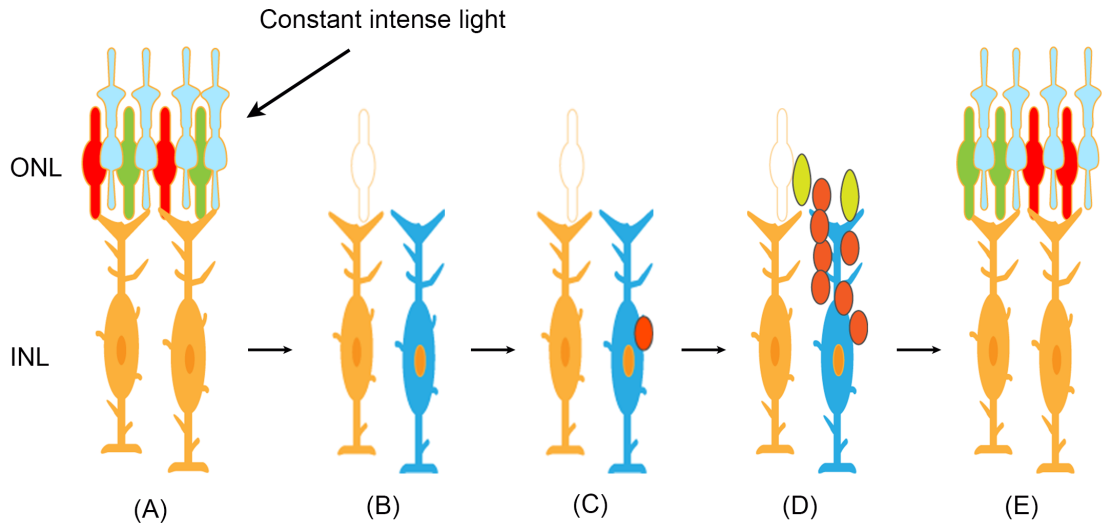

Figure 4. Changes in the retina during regeneration.

(A) Constant intense light exposure induces ONL photoreceptor apoptosis (red, green cells- cones; cyan cells- rods). (B) In response to this, some MG (mustard cells) dedifferentiate into a stem cell like state (dark blue cells). (C) Dedifferentiated MG undergo a single round of asymmetric cell division to generate a progenitor cell (orange cell). (D) The progenitor cell rapidly proliferates to form clusters of progenitor cells (groups of orange cells), which migrate to the ONL and begin to differentiate into new photoreceptors (greenish-yellow cells). (E) 28 days after the constant intense light exposure, the photoreceptors have completely regenerated in the retina. ONL, outer nuclear layer; INL, inner nuclear layer.

microRNAs (miRNAs)

microRNAs (miRNAs) are endogenous, evolutionarily conserved, small non-coding RNAs involved in post transcriptional gene regulation. Initially identified as regulators of developmental timing in the worm *C. elegans,* miRNAs have been discovered in worms, flies, plants and vertebrates, and regulate a myriad of processes from development to disease progression (Ambros, 2003; Chen et al., 2005; Lagos-Quintana et al., 2003; Lee et al., 1993; Pasquinelli et al., 2000; Wightman et al., 1993). They function by partial base pairing in the 3' untranslated region (UTR) of target mRNAs, causing both mRNA downregulation and repression of protein production (Kloosterman and Plasterk, 2006) (Figure 5). Highly complementary base pairing between nucleotides 2-8 in the 5' end of the miRNA (also called miRNA 'seed') and the miRNA recognition element in the mRNA 3' UTR (also called 'MRE') is generally thought to be necessary for efficient miRNA regulation (Bartel, 2004). Their small size, in addition to imperfect base pairing in mRNA 3' UTRs, enables miRNAs to effectively target many transcripts and influence various pathways simultaneously. Computational analyses predict that over a third of human genes are regulated by miRNAs (Lewis et al., 2005).

Roughly 50% of miRNA genes in vertebrate genomes are monocistronic and transcribed from their own promoters, the rest are polycistronic and found in clusters with other related or unrelated miRNA genes and transcribed together from a common promoter (Kim and Nam, 2006; Lagos-Quintana et al., 2001; Olena and Patton, 2010). miRNAs can arise from both introns and exons of protein coding and non-protein coding

genes. In many cases, miRNAs within a cluster contain identical seed sequences and can regulate identical mRNA targets (Zhu et al., 2011). miRNAs with high similarity in precursor sequences (see below) are commonly grouped into miRNA 'families' and members of the same family mostly contain identical seed sequences and target identical mRNAs.

Biogenesis

miRNA biogenesis is a multistep process that results in the incorporation of a single-stranded, ~22nt, mature miRNA into a functional ribonucleoprotein complex (Figure 5). Canonical miRNA genes are transcribed by RNA polymerase II into long primary transcripts called primary or pri-miRNAs that contain multiple imperfect stem loop structures (Cai et al., 2004; Lee et al., 2004). The nuclear 'microprocessor' complex, which minimally consists of the RNase III family enzyme Drosha and its partner DGCR8/Pasha, cleaves the pri-miRNA at the base of the stem loop and releases the hairpin (Denli et al., 2004; Gregory et al., 2004; Han et al., 2004; Lee et al., 2003). The hairpin (also called precursor or pre- miRNA) has a 2 nt overhang in the 3' end that is recognized by the nuclear export receptor Exportin 5 and transported to the cytoplasm (Gwizdek et al., 2001; Gwizdek et al., 2003; Gwizdek et al., 2004). In the cytoplasm, the pre-miRNA is processed by another RNase III family enzyme, Dicer and its partner TRBP/Loquacious (Chendrimada et al., 2005; Forstemann et al., 2005) and the loop of the precursor is cleaved to generate a ~22nt miRNA: miRNA* duplex (Grishok et al., 2001; Hutvagner et al., 2001; Ketting, 2001).

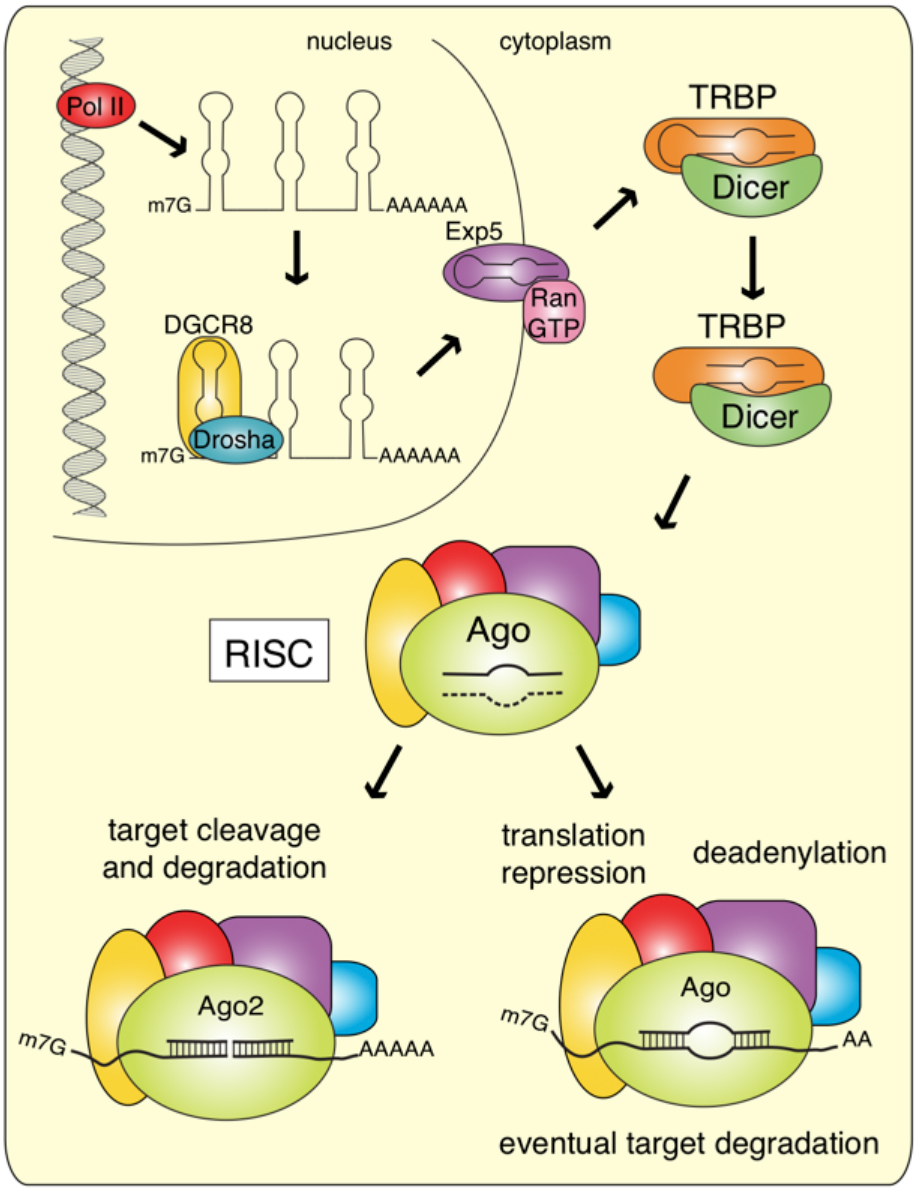

Figure 5. Biogenesis and function of canonical miRNAs

miRNAs are transcribed by RNA polymersase II into primary miRNA transcripts that contain several stem-loop structures. Drosha processes the primary transcripts to generate precursor miRNAs, which are exported to the cytoplasm via exportin 5. In the cytoplasm, Dicer processes the precursor miRNA to generate a duplex mature miRNA. One strand of the duplex is incorporated into the RNA induced silencing complex (RISC) and guided to base pair imperfectly with the 3'UTRs of mRNA targets. The seed (5') region of the miRNA perfectly base pairs with the miRNA recognition element (MRE) in the 3' UTR. miRNA binding results in destabilization of the mRNA target, and/or repression of protein production. Figure by Abby Olena.

One strand of the mature duplex, called the guide strand is preferentially incorporated into a ribonucleoprotein complex called the RNA induced silencing complex (RISC) that contains one or more Argonaute proteins (AGO). The other strand (also called the passenger or * strand) is degraded or loaded as a functional miRNA into a RISC (Matranga et al., 2005; Rand et al., 2005). The miRNA guides the RISC to bind mRNA targets in their 3' UTRs, and together with AGO, GW182 and other RISC proteins, promotes mRNA destabilization and repression of translation.

miRNA profiling using high throughput sequencing

The advent of high throughput sequencing (HTS) or next generation sequencing (NGS) technology has allowed miRNA research to increase dramatically. HTS involves massively parallel sequencing of short RNA (or DNA) fragments obtained from whole transcriptomes (or genomes) (Koboldt et al., 2013). Such high throughput sequencing generates millions of 'reads' or nucleotide sequences that can then be mapped back to the transcriptome to get quantitative and qualitative data about RNA abundance. Compared to hybridization based transcriptome analysis techniques like microarrays, which can only detect known transcripts and have a small dynamic range of detection, HTS directly determines read sequences and frequencies, thereby enabling discovery of novel and low abundance transcripts (Mutz et al., 2013).

A number of HTS platforms are available, including Illumina, 454 Roche and ABI SOLiD. The Illumina technology is based on reversible terminator chemistry where DNA/cDNA molecules are ligated to premade adapters and attached to the surface of a flow cell (Bentley et al., 2008). There, they are used as templates to generate clusters of

identical DNA fragments. These are then sequenced by the process of 'sequencing by synthesis', wherein a modified DNA polymerase is used to incorporate fluorescently labeled nucleotide analogs that also serve as reversible sequencing terminators. Nucleotides are added to the growing chain, one at a time, the fluorescent signal is read, the terminator blockage is reversed and the next nucleotide is incorporated. This process is repeated until the last base is sequenced.

Many groups have used high throughput technology to successfully identify miRNAs in various tissues and cell types, in both animals (Bar et al., 2008; Kuchenbauer et al., 2008; Morin et al., 2008) and plants (Nobuta et al., 2008; Sunkar et al., 2008). NGS technology has also enabled discovery of novel and low abundance miRNAs in different systems (Kozomara and Griffiths-Jones, 2011; Wei et al., 2012).

Functions of miRNAs

miRNAs in embryonic stem cells

Several themes underlie the functions of miRNAs in pluripotent embryonic stem cells (ESCs): (1) different sets of miRNAs are expressed in stem cells and differentiated cell compartments, (2) miRNAs regulate critical decisions between stem cell self-renewal and activation of the differentiation program, and (3) forced misexpression of miRNAs can induce or enhance cell fate switches (Bar et al., 2008; Houbaviy et al., 2003; Sun and Lai, 2013).

The importance of miRNAs for ESC biology was recognized when mouse ESCs lacking canonical miRNAs arrested in G1 and failed to differentiate (Kanellopoulou et al., 2005; Wang et al., 2007). These defects were abolished by introduction of two

different groups of miRNAs. Introduction of the ESC enriched *miR-290* family (also called ESC cell cycle regulating or ESCC miRNAs) rescued the cell cycle arrest phenotype, while introduction of the somatic cell enriched *let-7* family abrogated the resistance to differentiation (Melton et al., 2010; Wang et al., 2008). In ESCs, the decision between ESC self-renewal and differentiation is mediated by a balance between the levels of these two opposing groups of miRNAs. Moreover, introduction of the ESCC miRNAs along with the classic OKSM (Oct3/4, Sox2, Nanog and Myc) reprogramming factors increased the efficiency of somatic cell reprogramming and induced pluripotent stem cell (iPSC) production (Anokye-Danso et al., 2011; Judson et al., 2009; Subramanyam et al., 2011). Recent studies demonstrated that lentiviral delivery of *miR-302/367* miRNAs can generate iPSCs without other protein coding reprogramming factors (Anokye-Danso et al., 2011; Miyoshi et al., 2011). Albeit the controversy surrounding these recent studies, it is clear that certain miRNAs enhance the reprogramming efficiency, although their exact mechanism of action is only beginning to be understood.

miRNAs in adult stem cells and physiological regeneration

Multipotent adult stem cells have been detected in organs and tissues of various vertebrates and are required for proper adult physiology. Regulation of adult stem cell biology is crucial and perturbations can lead to degenerative diseases or cancer. Distinct groups of miRNAs regulate self-renewal, proliferation and differentiation of stem cells in different tissues.

Neural stem cells

The mammalian hippocampus contains two neural stem cell (NSC) niches, the sub ventricular zone (SVZ) and the sub granular zone (SGZ). *miR-124,* by inhibiting its target SOX9, promotes differentiation and inhibits self-renewal of the NSC population in the SVZ (Cheng et al., 2009; Scott et al., 2010). *miR-124* is not expressed in the NSC compartment, but rapidly accumulates as neuronal differentiation proceeds. Ectopic expression of *miR-124* in fibroblast promotes their conversion to neuronal fates, emphasizing the function of this miRNA in promoting neurogenesis (Yoo et al., 2011). Two miRNAs, *miR-7a* and *miR-184*, maintain the SVZ stem cell pool by two independent mechanisms. *miR-7a* represses the transcription factor PAX6 that induces dopaminergic neuron fate and promotes the regionalization of the SVZ stem cells (de Chevigny et al., 2012). In the absence of *miR-7a*, the SVZ stem cells are depleted at the expense or more dopaminergic neurons. *miR-184* promotes self-renewal of the hippocampal NSC (Liu et al., 2010). By targeting numbl, a known inducer differentiation, *miR-184* maintains the balance between proliferation and differentiation.

Hematopoietic stem cells (HSCs)

Transcriptome profiling in different hematopoietic lineages revealed distinct miRNA expression patterns in stem, progenitor and differentiated cells (Chen et al., 2004; Petriv et al., 2010). *miR-125a* is highly enriched in HSCs and is required for their survival (Guo et al., 2010). Several miRNAs control cell fate specification during hematopoiesis. *miR-181* promotes differentiation into B cells (Chen et al., 2004). *miR-150* regulates cell fate commitment in both the lymphoid and myeloid lineages via its

target MYB (Lu et al., 2008; Xiao et al., 2007). In the former, it promotes B-cell formation and in the latter, *miR-150* levels maintain the balance between megakaryocyte and erythrocyte lineages.

Satellite cells and muscle regeneration

Satellite cells are quiescent stem cells found in adult skeletal muscles. Following muscle injury, satellite cells get activated, express the transcription factors PAX7 and PAX3, and proliferate to generate myogenic progenitors. Canonical miRNA biogenesis is required for maintenance of satellite cell quiescence and two miRNAs, *miR-489* and *miR-31* employ two different mechanisms to maintain satellite cell quiescence (Abou-Khalil and Brack, 2010). *miR-489* is enriched in quiescent satellite cells and suppresses the oncogene *Dek,* which promotes myogenic progenitor proliferation (Cheung et al., 2012). *miR-31* maintains satellite cell quiescence by sequestering the myogenic determination factor *Myf5* in cytoplasmic RNP granules (Crist et al., 2012). Upon satellite cell activation, these RNP granules deconstruct allowing the myogenic program to be activated. The activated satellite cell specific transcription factors PAX7 and PAX3 are repressed by several miRNAs as myogenic differentiation proceeds. *miR-1* and *miR-206* repress PAX7, while *miR-27b* represses PAX3 (Chen et al., 2010; Crist et al., 2009).

Skin stem cells

Adult skin homeostasis is maintained by stem cells that reside in the basal layer of the highly stratified skin epithelium. These stem cells self-renew and produce skin progenitors that move up to the supra-basal layer and begin to differentiate into skin cells.

miRNAs are differentially expressed in the stem cell and differentiated cell compartments (Yi et al., 2008). *miR-203* controls the switch between proliferation and differentiation by regulating its target p63. *miR-203* is specifically expressed during differentiation of skin progenitor cells in the supra-basal layers of the skin epithelium, while its target p63 is enriched in the stem cell compartment (Lena et al., 2008; Yi et al., 2008). Overexpression of *miR-203* in skin stem cells triggers cell cycle exit via suppression of p63.

miRNAs in tissue and organ regeneration

In addition to physiological regeneration, several non-mammalian vertebrates like the urodele amphibians and teleost fish exhibit robust abilities to regenerate lost body parts and miRNAs regulate distinct steps in the regeneration process.

Appendage regeneration in amphibians and zebrafish occurs via the formation of a mass of undifferentiated cells called the blastema. Cells in the blastema rapidly proliferate, migrate, and differentiate to generate lost cell types of different lineages and the appendage is re-patterned. miRNAs are differentially expressed during appendage regeneration and both up and downregulated miRNAs play different roles during regeneration (Sehm et al., 2009; Thatcher et al., 2008; Yin et al., 2008). In zebrafish fin regeneration, downregulation of *miR-133* and *miR-203* facilitates blastema proliferation and initiation of regeneration (Thatcher et al., 2008; Yin et al., 2008). *miR-203* was shown to inhibit Wnt signaling by targeting Lef1, and *miR-133* repressed the kinase mps1 during fin regeneration. Overexpression of either miRNA inhibited fin regeneration. In axolotl tail regeneration, *miR-196* is upregulated in the blastema following amputation (Sehm et al., 2009). *miR-196* suppresses Pax7 and supports blastema proliferation.

Interestingly, the *miR-133* family is involved in regeneration of unrelated zebrafish tissues including the heart and spinal cord. Zebrafish can efficiently regenerate their hearts even after genetic ablation of >60% of resident cardiomyocytes (Yin et al., 2012). Heart regeneration does not depend on a stem cell population, but requires proliferation of existing cardiomyocytes to replace lost heart muscle. Under normal conditions, *miR-133* inhibits cardiomyocyte proliferation by targeting mps1 and cx43. However, following heart damage, *miR-133* levels are downregulated, which facilitates cardiomyocyte proliferation and heart regeneration. Intriguingly, studies in zebrafish spinal cord regeneration show an opposite expression pattern for *miR-133*. In this system, injury mediated upregulation of *miR-133* is necessary for spinal cord regrowth (Yu et al., 2011). The authors of the study attributed the opposite roles of *miR-133* to differences in cellular context and mode of regeneration between different tissues. As mentioned above, the role of one miRNA, *let-7* has been studied in zebrafish retina regeneration (Ramachandran et al., 2010). Downregulation of *let-7*, by acting in a loop with Ascl1a and Lin-28, induced MG dedifferentiation during zebrafish retina regeneration.

miRNAs in the retina

Aside from their roles in NSCs, miRNAs regulate various aspects of neural development including differentiation of progenitors, brain patterning, neuronal plasticity, neuronal survival and specification of neuronal identity (Cremisi, 2013). Exploration of miRNA function in the retina has advanced in the last decade primarily due to the availability of high throughput approaches and accessibility of the vertebrate retina to experimental manipulations. miRNA-transcriptome profiling coupled with *in*

situ hybridization studies in developing and adult retinas from mouse and zebrafish revealed variability in miRNA expression across different retinal cell layers (Kapsimali et al., 2007; Karali et al., 2010).

miRNAs are differentially expressed during vertebrate retina development (Hackler et al., 2010). Experiments with conditional Dicer knockout mice, where Dicer was specifically knocked down in retinal progenitor cells at different times in development, revealed varying effects on retinal development. Loss of Dicer in early stage retinal progenitors caused microphthalmia (small eye), apoptosis and an expansion of RGC pool at the expense of later generated retinal cell types (rods and MG), demonstrating that miRNAs are necessary for shifts in the competence state of retinal progenitors as well as proliferation during retinal neurogenesis (Georgi and Reh, 2010; Iida et al., 2011; Pinter and Hindges, 2010) (La Torre et al., 2013). Dicer loss in late stage progenitors caused retinal disorganization, loss of ERG responses from retinal neurons and retinal degeneration, indicating the importance of miRNAs for maintenance and normal functioning of retinal neurons (Damiani et al., 2008).

Studies in amphibians, fish and mice have identified specific miRNAs and miRNA families with distinct roles in retina development and function. *miR-204* regulates vertebrate eye patterning, *miR-24a* promotes retinal progenitor survival, *miRs-129, -155, -214* and *-222* regulate retinal cell identity, *miR-124a* is required for survival of newly differentiated cone photoreceptors and the *miR-183* cluster promotes photoreceptor protection under light induced stress conditions (Conte et al., 2010; Decembrini et al., 2009; Sanuki et al., 2011; Walker and Harland, 2009; Zhu et al., 2011).

Perturbations in miRNA expression profiles have been detected in mouse models of retina degenerative diseases like retinitis pigmentosa, diabetic retinopathy, AMD and Stargardt disease, suggesting that miRNA dysregulation could lead to disease progression (Kovacs et al., 2011; Organisciak and Vaughan, 2010; Sun and Nathans, 2001; Zack et al., 1999) (Loscher et al., 2007; Loscher et al., 2008; Lumayag et al., 2013; Wu et al., 2012). Recently, secreted miRNAs have been detected in the aqueous and vitreous humor, with some miRNAs being differentially expressed in patients suffering from ocular diseases compared to normal patients (Dunmire et al., 2013; Ragusa et al., 2013).

Summary

Work presented in the following chapters explores the expression and function of miRNAs during zebrafish retina regeneration. Chapter II illustrates the global requirement of canonical miRNA biogenesis for progression of retina regeneration and demonstrates that miRNA expression is dynamic during regeneration. Chapter III describes a constant light lesioning model that induces analogous photoreceptor apoptosis and initiates regeneration in both pigmented and *albino* zebrafish. Chapters IV and V focus on specific miRNAs, *miR-203* and *miR-216*, respectively, and characterize their function in retina regeneration. Overall, this thesis demonstrates that miRNAs are important regulators of distinct steps of zebrafish retina regeneration.

CHAPTER II

DYNAMIC miRNA EXPRESSION PATTERNS DURING RETINA REGENERATION IN ZEBRAFISH: LOSS OF DICER INHIBITS REGENERATION [a]

Kamya Rajaram[1]*, Rachel L. Harding[2]*, Travis Bailey[2], James G. Patton[1, #], and David R. Hyde[2,#]

[1]Department of Biological Sciences, Vanderbilt University, Nashville, TN

[2]Department of Biological Sciences and the Center for Zebrafish Research, University of Notre Dame, Notre Dame, IN

---

[a] This work has been submitted to Developmental Dynamics.

* These authors contributed equally to this work.

KR, RLH, DRH and JGP conceived and designed the experiments and analyzed the data. KR, TB and RLH performed the experiments. KR, DRH and JGP wrote the paper.

Abstract

Background: Adult zebrafish spontaneously regenerate their retinas after damage. Although a number of genes and signaling pathways involved in regeneration have been identified, the extent of mechanisms regulating regeneration is unclear. Small non-coding RNAs, microRNAs (miRNAs), that regulate regeneration of various tissues in lower vertebrates were examined for their potential roles in regulating zebrafish retinal regeneration.

Results: To investigate the requirement of miRNAs during zebrafish retinal regeneration, we knocked down the expression of the miRNA-processing enzyme Dicer in retinas prior to light-induced damage. Dicer loss significantly reduced proliferation of Müller glia-derived neuronal progenitor cells during regeneration. To identify individual miRNAs with roles in retina regeneration, we collected retinas at different stages of light damage and performed small RNA high-throughput sequencing. We identified subsets of miRNAs that were differentially expressed during active regeneration but returned to basal levels once regeneration was completed. To validate the roles of differentially expressed miRNAs, we knocked down 6 different miRNAs that were upregulated in expression during regeneration and demonstrated that they have distinct effects on neuronal progenitor cell proliferation and migration during retina regeneration.

Conclusions: miRNAs are necessary for retinal regeneration. miRNA expression is dynamic during regeneration. miRNAs function during initiation and progression of retinal regeneration.

Introduction

Following damage, the zebrafish retina undergoes spontaneous regeneration mediated by Müller glia (MG) (Fausett and Goldman, 2006; Mensinger and Powers, 2007). Damage to the retina stimulates normally post-mitotic MG to reenter the cell cycle, dedifferentiate and asymmetrically divide to generate retinal progenitor cells (Fausett and Goldman, 2006; Nagashima et al., 2013; Thummel et al., 2008a). The progenitor cells rapidly proliferate, migrate to the region of damage and differentiate into lost retinal cell types (Thummel et al., 2010). While MG are found in all vertebrate retinas (Lamba et al., 2008), the mammalian retina is largely incapable of regeneration; damage normally triggers glial hypertrophy and proliferation leading to scarring (Bringmann et al., 2009). A number of proteins and signaling pathways have been shown to be necessary for zebrafish retinal regeneration (Gorsuch and Hyde, 2014, Gemberling et al., 2013, Lenkowski and Raymond, 2014).

In order to precisely control the regeneration response in the zebrafish retina, multiple modes of regulation are employed. microRNAs (miRNAs) have emerged as an important class of post-transcriptional regulators of various biological processes including development, differentiation, cell specification, proliferation and regeneration (Ambros, 2003; Bartel and Chen, 2004; Lee et al., 1993; Morris and McManus, 2005; O'Donnell et al., 2005; Plasterk, 2006; Reinhart et al., 2000; Slack et al., 2000; Slack and Weidhaas, 2006; Thatcher and Patton, 2010). miRNAs are evolutionarily conserved, small non-coding RNAs that arise from RNA polymerase II-derived endogenous hairpin precursors (Cai et al., 2004; Lee et al., 2004). These transcripts are sequentially processed by the RNaseIII-like enzymes Drosha and Dicer into small, ~22 nt, mature miRNAs

(Chendrimada et al., 2005; Gregory et al., 2004; Lee et al., 2003). miRNAs function by imperfect base pairing with the 3' untranslated region (UTR) of target mRNAs, causing mRNA destabilization and decay and/or repression of protein production (Kloosterman and Plasterk, 2006). Complex tissue or organ regeneration in a number of species is regulated by miRNAs (Thatcher and Patton, 2010; Thatcher et al., 2008; Yin et al., 2012; Yin et al., 2008). In zebrafish, *miR-203* regulates fin regeneration (Thatcher et al., 2008), while *miR-133* family members regulate fin, spinal cord and heart regeneration (Yin et al., 2012; Yin et al., 2008; Yu et al., 2011). The *let-7* miRNA was demonstrated to repress the expression of several proteins that are necessary for MG dedifferentiation and proliferation in the puncture-damaged zebrafish retina, which suggests that *let-7* expression must be repressed for the MG to initiate a regeneration response (Ramachandran et al., 2010). Additionally, we showed that an intact miRNA biogenesis pathway is necessary for zebrafish caudal fin regeneration (Thatcher et al., 2008). However, it remains unexplored if there is a similar global requirement of miRNAs for successful retinal regeneration.

Here, we demonstrate that the Dicer-dependent miRNA biogenesis pathway is essential for normal retinal regeneration in zebrafish. Using small RNA high-throughput sequencing, we show that distinct subsets of miRNAs are differentially expressed during retinal regeneration, but return to basal expression levels after completion of regeneration. Using loss-of-function studies in the regenerating retina, we illustrate that differentially expressed miRNAs function to regulate adult zebrafish retinal regeneration.

Experimental Procedures

Fish maintenance and adult zebrafish light lesioning

Zebrafish were maintained in 14h:10h–light:dark cycles at 28.5°C. Constant intense light lesioning of *albino* zebrafish was performed as described (Vihtelic and Hyde, 2000). Briefly, adult *albino* zebrafish were dark-adapted for 14 days and then transferred to constant intense light (~20,000 lux) with the temperature maintained at 30-33°C. Eyes were collected at 0, 16, 35, 51, 68, 72 or 96 hours of light damage (h). For the recovery time points, fish were returned to normal light conditions (14h-light, 10h-dark cycles; 28.5°C) after 96h of intense light exposure and allowed to recover for 28d.

Small RNA library preparation and high-throughput sequencing

Zebrafish were sacrificed in groups of 100 at each time point: i) before (0h) ii) during intense light exposure (35h and 72h), and iii) following recovery (28d). Retinas were collected in TRIzol reagent and total RNA was extracted and size fractionated on 15% urea acrylamide gels. 15-30 nt small RNAs were size selected, ligated to 3' and 5' end adapters and amplified by RT-PCR to generate small RNA libraries as described (Wei et al., 2012). Libraries were sequenced on the Illumina Genome Analyzer II and Hiseq platforms at the Vanderbilt VANTAGE sequencing core. Raw data has been submitted to the NCBI GEO database.

3′ ligation adaptor: AMP-5′ pCTGTAGGCACCATCAATdideoxyC 3′

5′ ligation adaptor: 5′ ACACUCUUUCCCUACACGACGCUCUUCCGAUC 3′

RT primer: 5′ ATTGATGGTGCCTACAG 3'

PCR forward primer:

5′ AATGATACGGCGACCACCGAACACTCTTTCCCTACACGACG 3′

PCR reverse primer:

5’ CAAGCAGAAGACGGCATACGATTGATGGTGCCTACAG 3’.

Small RNA read processing and miRNA expression profile generation

Sequencing reads were processed to remove adapter sequences and mapped to the ZV9 zebrafish genome. Bowtie (Langmead et al., 2009) was used to map the resulting reads to miRNA hairpin sequences from miRbase (www.miRbase.org), followed by further filtering to remove reads derived from precursor miRNA loop regions or passenger strands, as described (Wei et al., 2012). Reads that mapped back to mature miRNA sequences but did not contain the miRNA ‘seed’ sequence (nucleotides 2-6 from the 5’ end of the mature miRNA) or that mapped to the mature miRNA sequence only in the 3’ region were excluded. Mature miRNA reads were normalized to the total number of mappable reads per sequencing run. Normalized reads were $\log_2$ transformed and the resulting values were displayed using heat maps (Multi experiment viewer) (Saeed et al., 2003) (Figure 3) and plotted in scattergrams (Figure 4A-C).

Taqman real-time PCR

Quantitative real-time PCR (qPCR) for miRNAs was performed using Taqman probes (Applied Biosystems, Grand Island, NY), as per the manufacturer’s instructions. qPCR was performed for *miR-21*, *miR-133b*, *miR-7a* and relative miRNA levels were

determined using the ΔΔCt method and normalized to the levels of *miR-9*. The qPCR was performed on a Biorad CFX 96 Real time system.

Morpholino injection and electroporation

3'- Lissamine tagged morpholinos (MOs) (Gene Tools, Philomath, OR) were injected and electroporated into adult *albino* zebrafish eyes prior to light lesioning as previously described (Thummel et al., 2008b). The following 3'-lissamine tagged MOs were used:

MO name	MO sequence (5'-3')
dicer 5-mis MO	5' CTCTAGGCCTGCCATCCTTAGTGAC 3'
dicer MO	5' CTGTAGGCCAGCCATGCTTAGAGAC 3'
Standard control MO	5' CCTCTTACCTCAGTTACAATTTATA 3'
miR-7a	5' ACAACAAAATCACTAGTCTTCCA 3'
miR-27c	5' GCAGAACTTAACCACTGTGAA 3'
miR-31	5'CAGCTATGCCAACATCTTGCC 3'
miR-142b	5' AGTAGTGCTTTCTACTTTAT 3'
miR-146a	5' CCATCTATGGAATTCAGTTCTCA 3'
miR-2190	5' GATCCGAGCGCACCGGAC 3'

The *dicer* and *5-base mismatch* morpholinos (*dicer 5-mis*) were described previously (Wienholds et al., 2003). The sequences of the remaining morpholinos were selected in consultation with GeneTools.

Immunohistochemistry

Immunohistochemistry was performed as described previously (Nelson et al., 2012).

Adult zebrafish eyes were fixed in 9 parts 95% ethanol, 1 part 37% formaldehyde (9:1 fix) overnight at 4°C before being washed in 95%, 80%, 70% and 50% ethanol for 5 minutes each, followed by a 15 minute wash in 5% sucrose/ 1X PBS and an overnight wash in 30% sucrose/ 1X PBS. Eyes were then placed in 2 parts Tissue Freezing Medium (TFM, Triangle Biomedical Sciences, Inc., Durham, NC) to 1 part 30% sucrose/ 1X PBS overnight at 4°C. Finally, eyes were allowed to incubate for 1 hour at room temperature in 100% TFM and then embedded in 100% TFM and frozen at -80° C. Frozen eyes were cryo-sectioned at -20°C (Microm HM550) at 14 μm and retinal sections were collected on Superfrost plus slides (VWR; Radnor, PA) slides as described (Thummel et al. 2010). Sections were dehydrated on a warming plate at 50°C for 40 minutes before being stored at -80°C. Prior to labeling, slides were warmed on a 50°C slide warmer for 20 minutes and then rehydrated for 20 minutes with 1X PBS. Sections were blocked in 0.2% Triton X-100/ 2% normal goat serum/ 1X PBS for 1 hour at room temperature. Primary mouse anti-proliferating cell nuclear antigen (PCNA) monoclonal antibody (1:1,000 dilution, clone PC10, Sigma-Aldrich, St. Louis, MO), rabbit polyclonal anti-PCNA (1:750 dilution, clone C19, Abcam, Cambridge, MA) or mouse anti-green fluorescent protein (GFP) monoclonal antibody (1:1,000 dilution, clone 3E6, Invitrogen, Grand Island, NY) were incubated in blocking buffer overnight at room temperature. Following primary antibody labeling, sections were washed three times for 10 minutes in 0.05% Tween-20/ 1X PBS. Alexa-fluor conjugated (488, 594 or 647) anti-goat secondary antibodies (Invitrogen) were diluted at 1:500 in blocking buffer for 1 hour at room temperature. When necessary, sections were counterstained with TOPRO3 or DAPI nuclear stain (both diluted 1:1,000, Invitrogen), applied concurrently with secondary antibodies. Secondary

antibody labeled sections were washed in 0.05% Tween-20/ 1X PBS three times for 10 minutes, followed by a final wash in 1X PBS for 5 minutes. Coverslips were mounted with ProLong Gold antifade reagent (Invitrogen) and left overnight to allow the ProLong Gold to set.

Image Analysis

Confocal imaging was performed on a Leica TCS SP2 confocal microscope. Only retinal sections containing optic nerve or adjacent sections were imaged to maintain consistency of measurements. Images were taken of one 40X field of view (equivalent to a 320 μm linear distance) equidistant between the CMZ and optic nerve of the dorsal retina for each section. Sections were imaged as z-stacks between 5 and 6 μm of depth. Following image acquisition, levels were adjusted equally across panels to enhance low fluorescence intensity in Adobe Photoshop CS 5.1. Statistical significance was calculated using a two-way ANOVA and Tukey's HSD post-hoc test (Holliday, 2012) with p values less than or equal to 0.5 considered significant. At least 3 retinas from independent fish were examined for each condition.

Results and Discussion

Loss of Dicer inhibits retina regeneration

Pre-miRNAs are processed in the cytoplasm by an RNAse III-like enzyme, Dicer. To determine if miRNAs are important for zebrafish retina regeneration, we knocked down Dicer protein expression in adult *albino* zebrafish retina prior to constant intense light damage using morpholinos (MO). Dark-adapted zebrafish retinas were intravitreally

injected and electroporated with either 5-mismatch control or a *dicer* MO that was described previously (Wienholds et al., 2003). Retinas were collected at 0, 16, 35, 51, 68 and 96 hours of light damage and PCNA (Proliferating Cell Nuclear Antigen) was immunolocalized as a marker for proliferating cells (Figure 6).

At the start of light damage (0 hours of light), PCNA expression was nearly absent in the INL of *dicer* (0.1±0.1) and *5-mis* control morphant (0.2±0.1) retinas (Figure 6I), while very few PCNA-positive nuclei cells were detected in the ONL of *dicer* and *5-mis* control morphant retinas (9.9±0.1, 10.4±2.5, respectively; Figure 6J). After 16 hours of light damage, when photoreceptor cell death is nearing its maximal level (Nelson et al., 2013), only a limited number of PCNA-positive nuclei were present in the ONL in the *5-mis* and *dicer* morphants (10±1 and 8±2, respectively; Figure 6J). These likely represent rod precursor cells that are committed to differentiate into rod photoreceptors during persistent neurogenesis (Lenkowski and Raymond, 2014). In contrast, PCNA-positive INL cells were largely absent in both the *5-mis* control and *dicer* morphant retinas (1±0.2 and 1±0.4, respectively; Figure 6I).

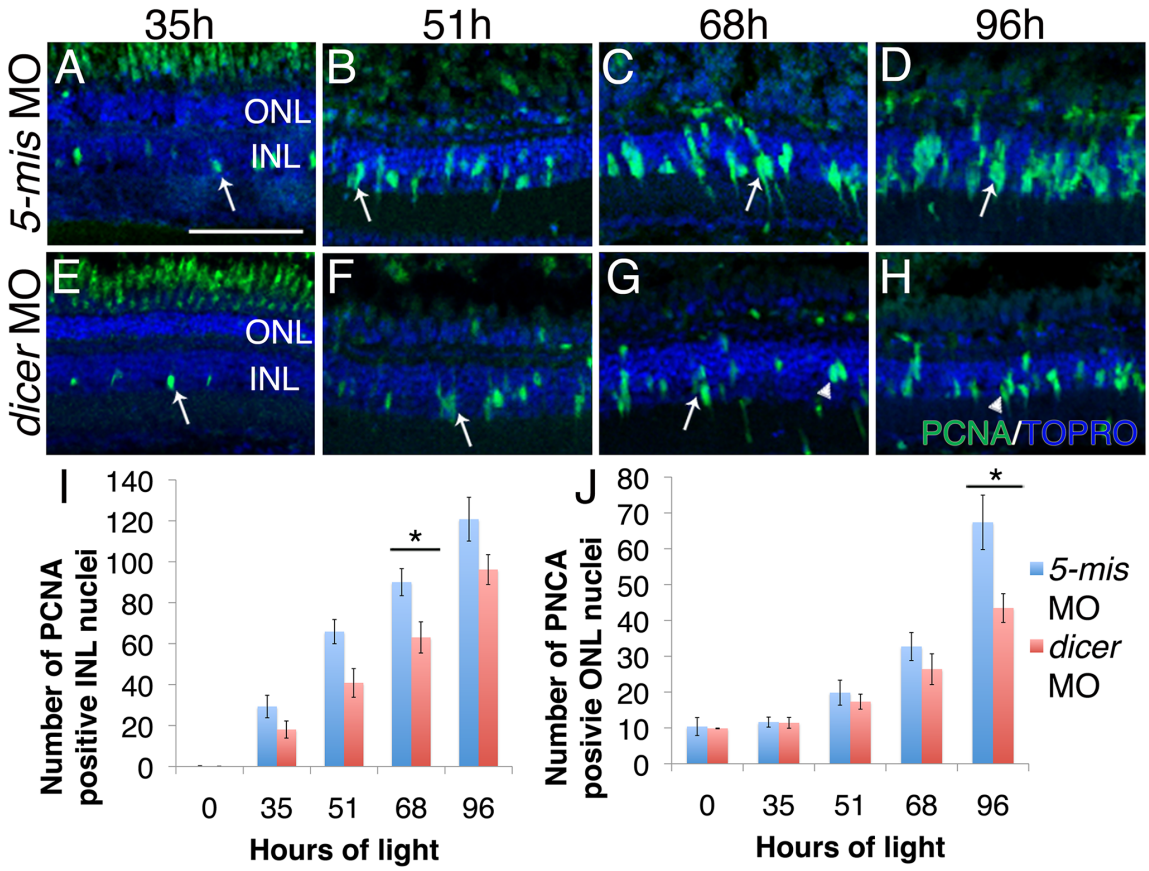

Figure 6. Dicer knockdown decreased INL proliferation in the light damaged retina.

Lissamine-tagged *dicer* 5-base mismatch (*5-mis*) control morpholino or *dicer* morpholino were intravitreally injected and electroporated into dark-adapted adult *albino* zebrafish. Retinas were collected at 0, 16, 35, 51, 68 and 96 hours of light damage and immunostained with anti-PCNA (green) antibodies and TOPRO3 nuclear stain (blue). (A, E) Single PCNA-positive MG were observed in the INL of *dicer 5-mis* control and *dicer* morphant retinas (arrows). (B, F) Both *dicer 5-mis* control and *dicer* morphant retinas contain doublet nuclei at 51 hours of light damage (arrows). (C) Clusters of proliferating progenitor cells are present in the INL of *dicer 5-mis* control retinas (arrow) at 68 hours of light damage. (G) Single (arrow) or doublet (arrowhead) nuclei predominated in *dicer* morphant retinas. (D) Columns of proliferating progenitors were observed in the INL of *dicer 5-mis* morphant retinas at 96 hours of light damage. (H) At 96 hours of light damage, doublet nuclei (arrowhead) predominated the INL of *dicer* morphants. (I) Significantly fewer PCNA-positive INL cells were present in *dicer* morphant retinas compared to *dicer 5-mis* control morphant retinas beginning at 51 hours of light damage. (J) *dicer* morphant retinas contained significantly fewer PCNA-positive ONL cells at 96 hours of light damage. *dicer 5-mis* MO*, dicer* 5-base mismatch morphant*; dicer* MO*, dicer* morphant; INL, inner nuclear layer; ONL, outer nuclear layer; scale bar in panel A is 50 mm and is the same for panels B-H; data represent mean +/- s.e.m; *, p< 0.05 using Tukey's post-hoc test following 2-way ANOVA, n=11.

After 35 hours of constant light, when the MG reenter the cell cycle (Kassen et al, 2007), nearly equivalent numbers of PCNA-positive cells were present in the INL of both *5-mis* control and *dicer* morphant (29±6 and 18±4, respectively), as well as in the ONL of both *5-mis* control and *dicer* morphant (12±1 and 11±2, respectively) retinas (Figure 6A, E, I, and J). After 51 hours of light damage, when the MG began producing neuronal progenitor cells (Kassen et al., 2007), we observed two closely associated (doublet) PCNA-positive nuclei in the INL of both *5-mis* control and *dicer* morphant retinas (arrows, Figure 6B and 6F, respectively). However, the *dicer* morphant contained fewer PCNA-positive INL cells relative to the *5-mis* control morphant (41±7 and 66±6, respectively, p=0.116) retinas (Figure 6I). In contrast, nearly equivalent numbers of PCNA-positive ONL cells were present in the *5-mis* control morphant (20±3 and 17±2, respectively) retinas (Figure 6J).

At 68 hours of constant light, when clusters of proliferating PCNA-positive neuronal progenitor cells were observed in the INL of *5-mis* control morphants (Figure 6C arrow), only individual or doublet PCNA-positive INL nuclei persisted in *dicer* morphant retinas (Figure 6G, arrow and arrowhead, respectively). This suggested that either the MG or initial neuronal progenitor cells failed to continue proliferating. Additionally, the *dicer* morphants contained significantly fewer PCNA-positive INL cells relative to the *5-mis* morphants (63±8 and 90±7, p=0.042; Figure 6I). In contrast, there was no statistically significant difference in the number of PCNA-positive ONL cells in the *dicer* and *5-mis* control retinas (26±4 and 33±4, respectively; Figure 6J). By 96 hours of light treatment, single, doublet (Figure 6H arrowhead), and small clusters of PCNA-positive INL cells persisted in *dicer* morphant retinas relative to the primarily large

clusters of PCNA-positive cells migrating from the INL to ONL in the *5-mis* control morphant retinas (Figure 6D, arrow). The *dicer* morphant contained fewer PCNA-positive INL cells compared to the *5-mis* control morphant retinas (96±7 and 121±11, respectively: Figure 6I), but significantly fewer PCNA-positive ONL cells (43±4 and 67±8, respectively, p=0.01: Figure 6J). This could result from the significant difference in the number of PCNA-positive INL cells that were observed at 68 hours that began migrating to the ONL by 96 hours. Overall, these observations indicated that loss of Dicer expression reduced MG-derived neuronal progenitor cell proliferation in the light-damaged retina.

We confirmed that the reduced proliferation observed in the *dicer* morphant retina was not due to the loss of MG by knocking down Dicer expression in *Tg(gfap:egfp)*^{nt11} transgenic zebrafish that express EGFP in all MG from the *gfap* (glial fibrillary acidic protein) promoter (Kassen et al., 2007). We immunostained for EGFP (Figure 7A-D, I-L) and PCNA (Figure 7E-L) in *dicer* morphants after 35 (Figure 7B, F, and J) and 51 hours of constant light (Figure 7D, H, and L). We compared the *dicer* morphant with the standard control morphant (Figure 7A, C, E, G, I, and K), which uses a morpholino that is not complementary to any known sequence in the zebrafish genome. As expected, there was no statistical difference in the number of EGFP-positive MG in either the INL or the ONL between the *dicer* and standard control morphant retinas (Figure 7O and P, respectively), demonstrating that the reduction in PCNA-positive cells in the *dicer* morphant was not the result of fewer MG. The EGFP-positive ONL cells represent MG that migrated from the INL to the ONL through interkinetic nuclear migration (Nagashima et al., 2013; Lahne and Hyde, personal communication). As observed in the

albino retinas, the *dicer* morphant did not exhibit any statistically significant difference in the number of PCNA-positive cells in either the INL or ONL, relative to the standard control morphant retinas after 35 hours of constant light (Figure 7M and N, respectively). However, the *dicer* morphant did exhibit significantly fewer PCNA-positive cells in the INL relative to the standard control morphant retinas after 51 hours of constant light (Figure 7M, 53±9 and 79±6, respectively, $p=0.011$), when the MG-derived neuronal progenitors are beginning to amplify in number. Thus, both the *albino* and *Tg(gfap:egfp)*^{nt11} transgenic retinas reveal that knockdown of Dicer expression results in significantly fewer proliferating neuronal progenitor cells.

Figure 7. Dicer knockdown does not affect MG in light damaged retinas.

Adult *albino Tg(gfap:egfp)*^{nt11} zebrafish were intravitreally injected and electroporated with standard control or *dicer* morpholino prior to the start of light damage. (A-L) EGFP-positive MG (arrows) were observed in comparable numbers between *dicer* and standard control morphants at all time points (A-D, I-L, O, P). (E, F) PCNA-positive INL cells were observed as mainly single nuclei in *dicer* and standard control morphant retinas at 35 hours of light damage (arrows). (I, J) Overlay of these images revealed that many MG co-labeled with PCNA as they re-entered the cell cycle. (G) Standard control morphant retinas at 51 hours of light damage exhibited doublets or early columns of PCNA-positive INL cells. (H) Single PCNA-positive INL cells rather than doublets predominated in *dicer* morphant retinas (arrows). (M, N) Differences in proliferation in *dicer* morphants resulted in significantly fewer PCNA-positive INL cells at 51 hours of light, but no difference in PCNA-positive ONL cells. Std Ctl MO, Standard Control morphant; *dicer* MO*, dicer* morphant; INL, inner nuclear layer; ONL, outer nuclear layer; scale bar in panel A is 50 mm and is the same for panels B-L; *, $p<0.05$ using Tukey's post-hoc test following 2-way ANOVA, n=7.

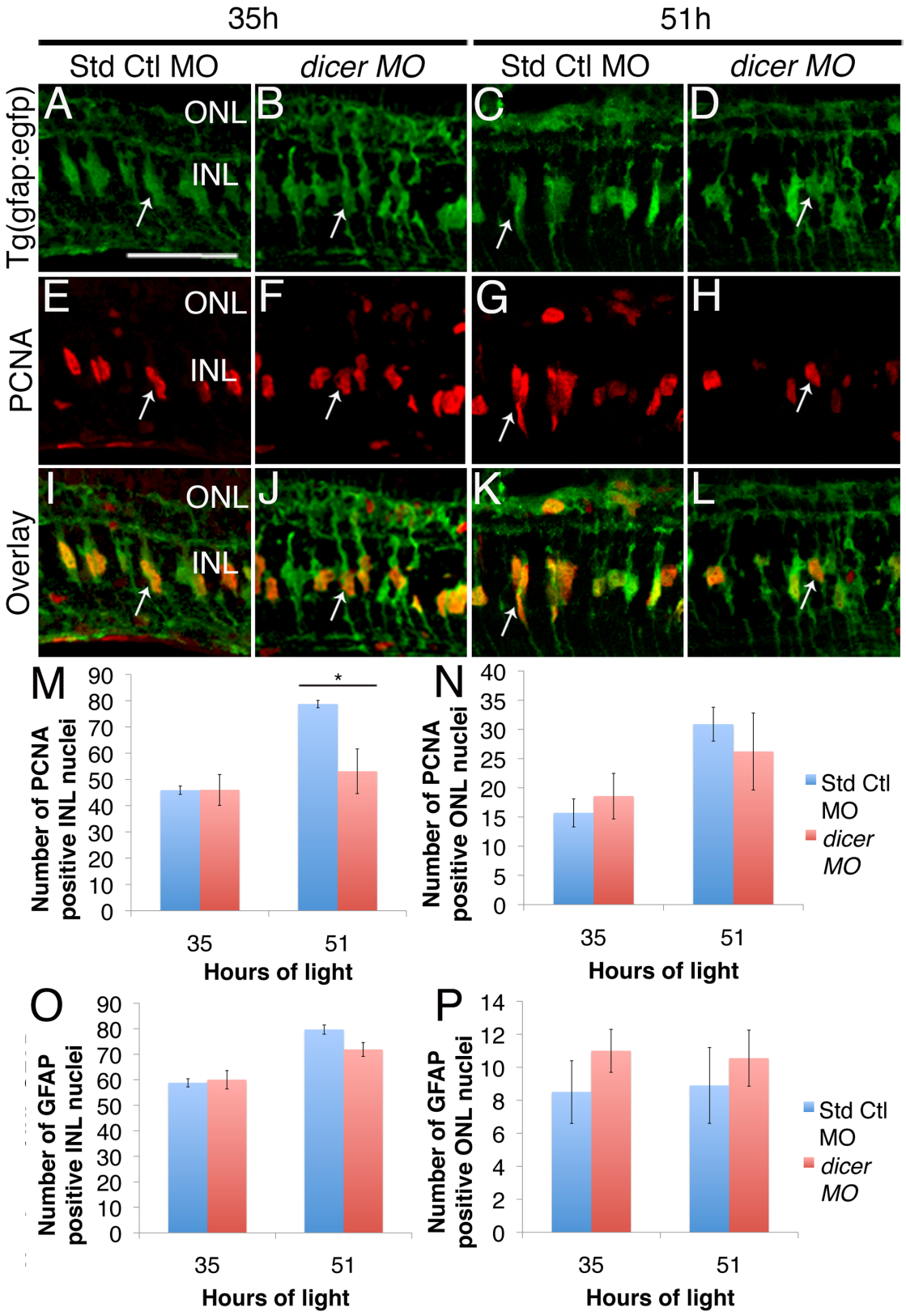
35h
51h
Std Ctl MO
dicer MO
Std Ctl MO
dicer MO
Tg(gfap:egfp)
PCNA
Overlay
A
B
C
D
E
F
G
H
I
J
K
L
ONL
INL
M
Number of PCNA positive INL nuclei
90
80
70
60
50
40
30
20
10
0
*
35
51
Hours of light
N
Number of PCNA positive ONL nuclei
40
35
30
25
20
15
10
5
0
35
51
Hours of light
Std Ctl MO
dicer MO
O
Number of GFAP positive INL nuclei
90
80
70
60
50
40
30
20
10
0
35
51
Hours of light
P
Number of GFAP positive ONL nuclei
14
12
10
8
6
4
2
0
35
51
Hours of light
Std Ctl MO
dicer MO

miRNAs are differentially expressed during retina regeneration

The Dicer loss-of-function experiments suggest that miRNA biogenesis is necessary for proliferation of the MG-derived neuronal progenitors. To identify specific miRNAs that are critical for retina regeneration, we performed small RNA high-throughput sequencing. RNA was isolated and sequencing libraries were prepared from *albino* zebrafish retinas before damage (0 hour of light), at two different time points during active retina regeneration (35 hours and 72 hours of light) and after completion of regeneration (28 days post recovery). These time points were chosen because MG dedifferentiate and reenter the cell cycle by 35 hours of light exposure and the MG-derived neuronal progenitors are maximally proliferating and forming clusters that begin migrating to the ONL by 72 hours of light exposure (Kassen et al., 2007). To confirm the reliability of library preparation and sequencing, we prepared and sequenced two independent small RNA libraries from undamaged retinas (0 hour of light). Global miRNA expression was nearly identical between the replicate libraries (Pearson's correlation r=0.98; R^2=0.97). Additionally, we sequenced the second library on two different Illumina machines (GAII and HiSeq) and found that the datasets were highly comparable (Pearson's correlation r=0.99; R^2=0.99), ensuring consistent and reliable library production.

Sequencing identified a total of 199 unique miRNAs that are expressed in the adult zebrafish retina. Global miRNA expression changes during regeneration are illustrated in the heat map in Figure 8. Most miRNA expression levels remained unchanged or underwent only small changes during regeneration (Figure 9A-C). However, small subsets of miRNAs were both up and down regulated during active

regeneration (Pearson's correlation r=0.88 for 0h vs. 35h and 0.94 for 0h vs. 72h; R^2=0.78 for 0h vs. 35h and 0.88 for 0h vs. 72h). Significantly, nearly all of these miRNAs returned to their baseline expression (0h) levels following completion of regeneration by the 28d time point (Figure 9C) (Pearson's correlation r=0.96; R^2=0.97 for 0h vs. 28d). 36 miRNAs had over a 2-fold change in expression during regeneration (Figure 9D-F), including 13 upregulated miRNAs (Figure 9D), 22 downregulated miRNAs (Figure 9E) and one miRNA that was both up and downregulated at different stages of regeneration (denoted by ** in Figure 9D-E).

Figure 8. Global miRNA expression patterns during retina regeneration.

Dark-adapted zebrafish (0h) were placed in constant intense light for 35 or 72 hours (35h and 72h, respectively) or standard light conditions for 28 days after 96 hours of constant light (28d). RNA was isolated from the retinas at all four timepoints and analyzed by high-throughput small RNA sequencing. Log_2 values of normalized miRNA reads from each sequencing time point (0h, 35h, 72h, 28d) are represented in the heat map. Yellow indicates high expression, blue indicates low expression and grey indicates no expression.

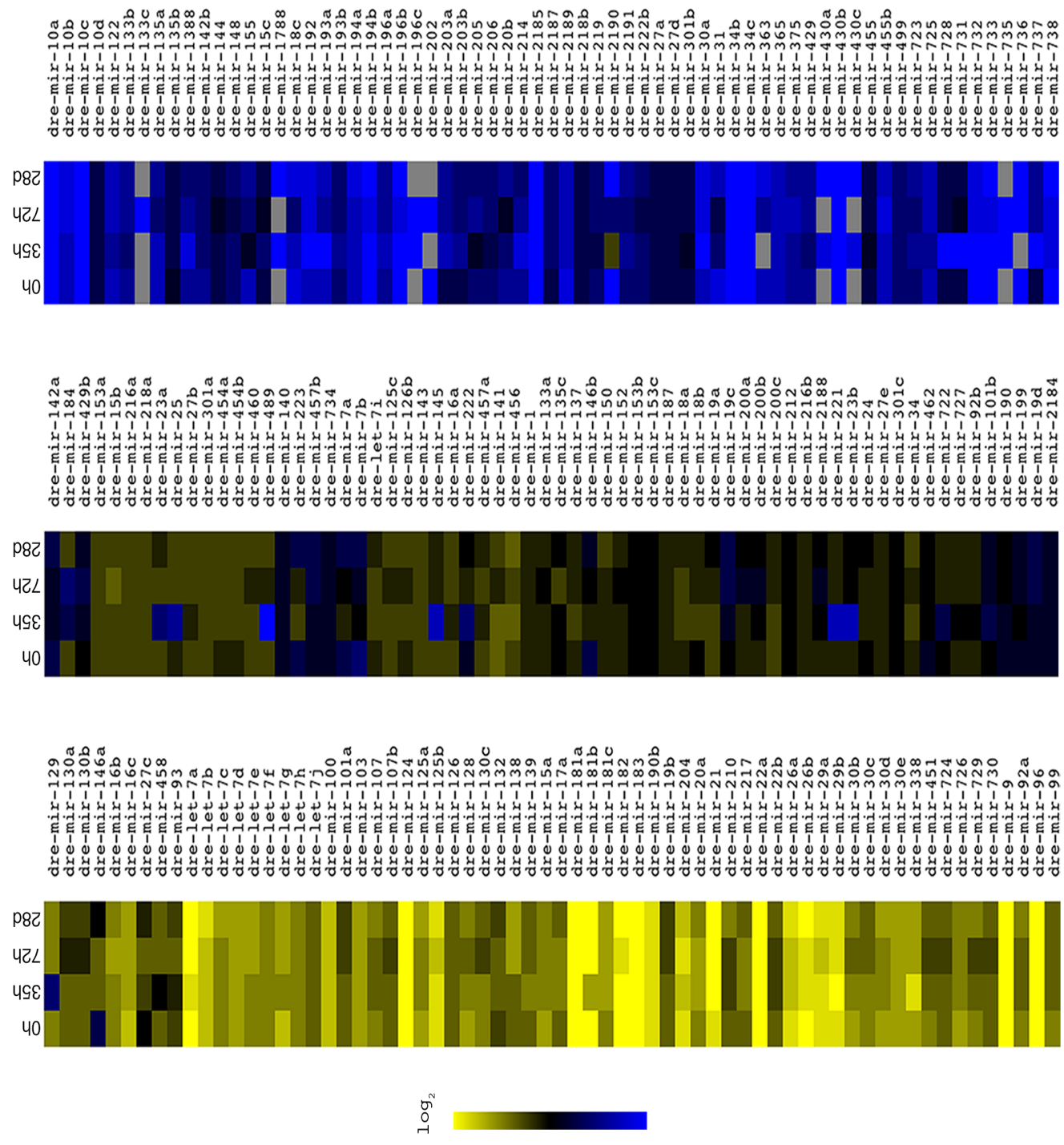
0h
35h
72h
96h
log2
dre-mir-129
dre-mir-130a
dre-mir-130b
dre-mir-146a
dre-mir-16b
dre-mir-16c
dre-mir-27c
dre-mir-458
dre-mir-93
dre-let-7a
dre-let-7b
dre-let-7c
dre-let-7d
dre-let-7e
dre-let-7f
dre-let-7g
dre-let-7h
dre-let-7j
dre-mir-100
dre-mir-101a
dre-mir-103
dre-mir-107
dre-mir-107b
dre-mir-124
dre-mir-125a
dre-mir-125b
dre-mir-126
dre-mir-128
dre-mir-130c
dre-mir-132
dre-mir-138
dre-mir-139
dre-mir-15a
dre-mir-17a
dre-mir-181a
dre-mir-181b
dre-mir-181c
dre-mir-182
dre-mir-183
dre-mir-190b
dre-mir-19b
dre-mir-204
dre-mir-20a
dre-mir-21
dre-mir-210
dre-mir-217
dre-mir-22a
dre-mir-22b
dre-mir-26a
dre-mir-26b
dre-mir-29a
dre-mir-29b
dre-mir-30b
dre-mir-30c
dre-mir-30d
dre-mir-30e
dre-mir-338
dre-mir-451
dre-mir-724
dre-mir-726
dre-mir-729
dre-mir-730
dre-mir-9
dre-mir-92a
dre-mir-96
dre-mir-99
dre-mir-142a
dre-mir-184
dre-mir-429b
dre-mir-153a
dre-mir-15b
dre-mir-216a
dre-mir-218a
dre-mir-23a
dre-mir-25
dre-mir-27b
dre-mir-301a
dre-mir-454a
dre-mir-454b
dre-mir-460
dre-mir-489
dre-mir-140
dre-mir-223
dre-mir-457b
dre-mir-734
dre-mir-7a
dre-mir-7b
dre-let-7i
dre-mir-125c
dre-mir-126b
dre-mir-143
dre-mir-145
dre-mir-16a
dre-mir-222
dre-mir-457a
dre-mir-141
dre-mir-456
dre-mir-1
dre-mir-133a
dre-mir-135c
dre-mir-137
dre-mir-146b
dre-mir-150
dre-mir-152
dre-mir-153b
dre-mir-153c
dre-mir-187
dre-mir-18a
dre-mir-18b
dre-mir-19a
dre-mir-19c
dre-mir-200a
dre-mir-200b
dre-mir-200c
dre-mir-212
dre-mir-216b
dre-mir-2188
dre-mir-221
dre-mir-23b
dre-mir-24
dre-mir-27e
dre-mir-301c
dre-mir-34
dre-mir-462
dre-mir-722
dre-mir-727
dre-mir-92b
dre-mir-101b
dre-mir-190
dre-mir-199
dre-mir-19d
dre-mir-2184
dre-mir-10a
dre-mir-10b
dre-mir-10c
dre-mir-10d
dre-mir-122
dre-mir-133b
dre-mir-133c
dre-mir-135a
dre-mir-135b
dre-mir-1388
dre-mir-142b
dre-mir-144
dre-mir-148
dre-mir-155
dre-mir-15c
dre-mir-1788
dre-mir-18c
dre-mir-192
dre-mir-193a
dre-mir-193b
dre-mir-194a
dre-mir-194b
dre-mir-196a
dre-mir-196b
dre-mir-196c
dre-mir-202
dre-mir-203a
dre-mir-203b
dre-mir-205
dre-mir-206
dre-mir-20b
dre-mir-214
dre-mir-2185
dre-mir-2187
dre-mir-2189
dre-mir-218b
dre-mir-219
dre-mir-2190
dre-mir-2191
dre-mir-222b
dre-mir-27a
dre-mir-27d
dre-mir-301b
dre-mir-30a
dre-mir-31
dre-mir-34b
dre-mir-34c
dre-mir-363
dre-mir-365
dre-mir-375
dre-mir-429
dre-mir-430a
dre-mir-430b
dre-mir-430c
dre-mir-455
dre-mir-455b
dre-mir-499
dre-mir-723
dre-mir-725
dre-mir-728
dre-mir-731
dre-mir-732
dre-mir-733
dre-mir-735
dre-mir-736
dre-mir-737
dre-mir-738

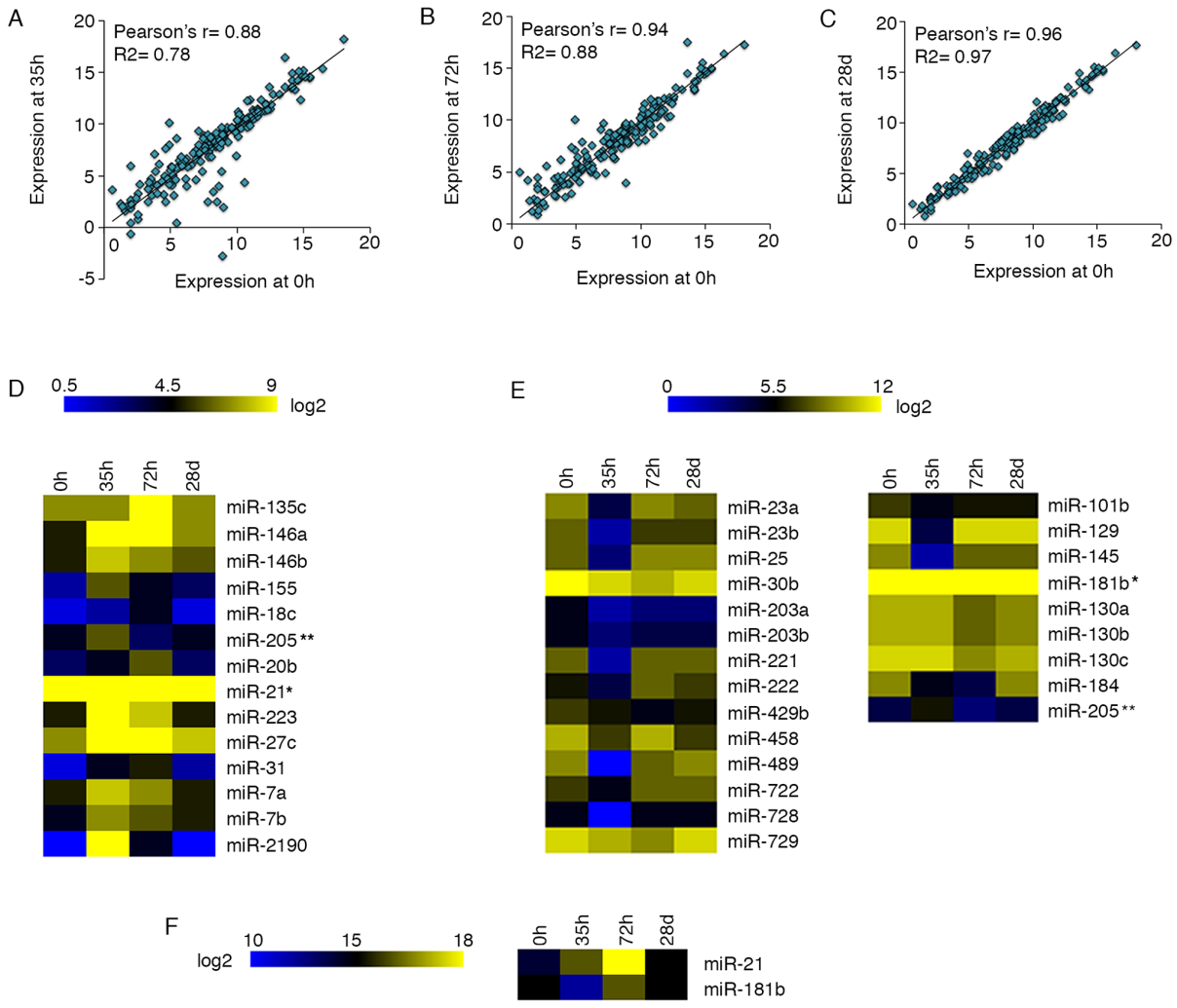

Figure 9. miRNAs are differentially expressed during intense light damage induced retina regeneration.

(A-C) Global miRNA expression changes during and after retina regeneration. miRNA expression at 35 hours (A) and 72 hours (B) of intense light exposure, and after 28 days of recovery in normal light conditions (C) was compared to the control expression levels (0 hours in intense light). Each data point represents one miRNA. Pearson's correlation (r) and R^2 values are indicated. (D-F) miRNAs with >2-fold change in expression during regeneration. (D) Upregulated miRNAs, (E) downregulated miRNAs, (F) expression changes for miRNAs out of scale in panels D and E (indicated with * symbol). One miRNA that is both upregulated and downregulated at different stages of regeneration is denoted with **.

To validate the sequencing results, we examined expression of three random miRNAs (*miR-21, miR-130b, miR-7a*) using Taqman qPCR. To normalize the expression of these miRNAs across different time points, we compared expression levels to *miR-9*, a miRNA with mid-range expression levels in the high-throughput sequencing dataset and whose expression did not change across the time points used. The relative miRNA expression changes detected by qPCR agreed with those revealed by high throughput sequencing (Figure 10).

Upregulated miRNAs are necessary for maximal neuronal progenitor cell proliferation during retina regeneration

Based on the sequencing results, we randomly selected 6 upregulated miRNAs that illustrate different expression patterns (Figure 11, Table 1). These patterns suggest that individual miRNAs possess distinct functions during retina regeneration (Figure 11A). *miRs-7a, -142b,* and *-146a* were upregulated to the same level at both 35 and 72 hours (Figure 11A), which suggests that they play roles in MG dedifferentiation and proliferation, as well as neuronal progenitor cell proliferation and migration. *miRs-27c* and *-31* were upregulated by 35 hours light damage and peaked at 72 hours, implying important roles in neuronal progenitor cell proliferation and migration (Figure 11B). *miR-2190* expression peaked at 35 hours and decreased by 72h of light, which suggested a possible role in MG dedifferentiation and proliferation (Figure 11C).

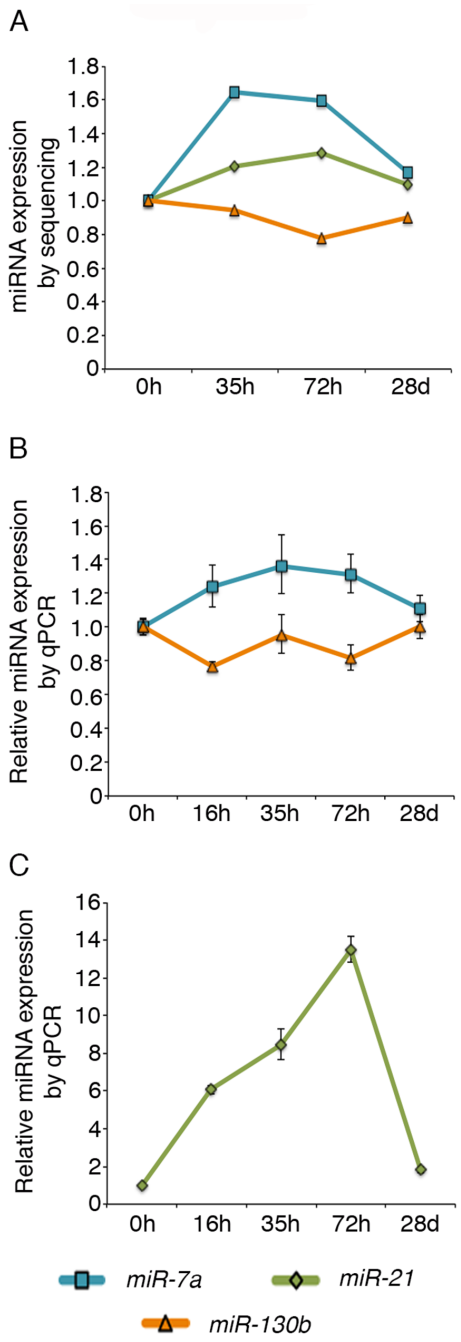

Figure 10. Validation of sequencing results.

Three miRNAs were randomly selected for validation of the sequencing results using Taqman qPCR. The expression of these miRNAs across different time points was normalized to *miR-9* expression, which exhibits mid-range expression levels in the high-throughput sequencing dataset and whose expression did not change across the time points used. (A) miRNA expression patterns during regeneration by high-throughput sequencing. (B-C) qPCR verification of miRNA expression levels relative to *miR-9* is shown. Data represent mean +/- s.e.m.

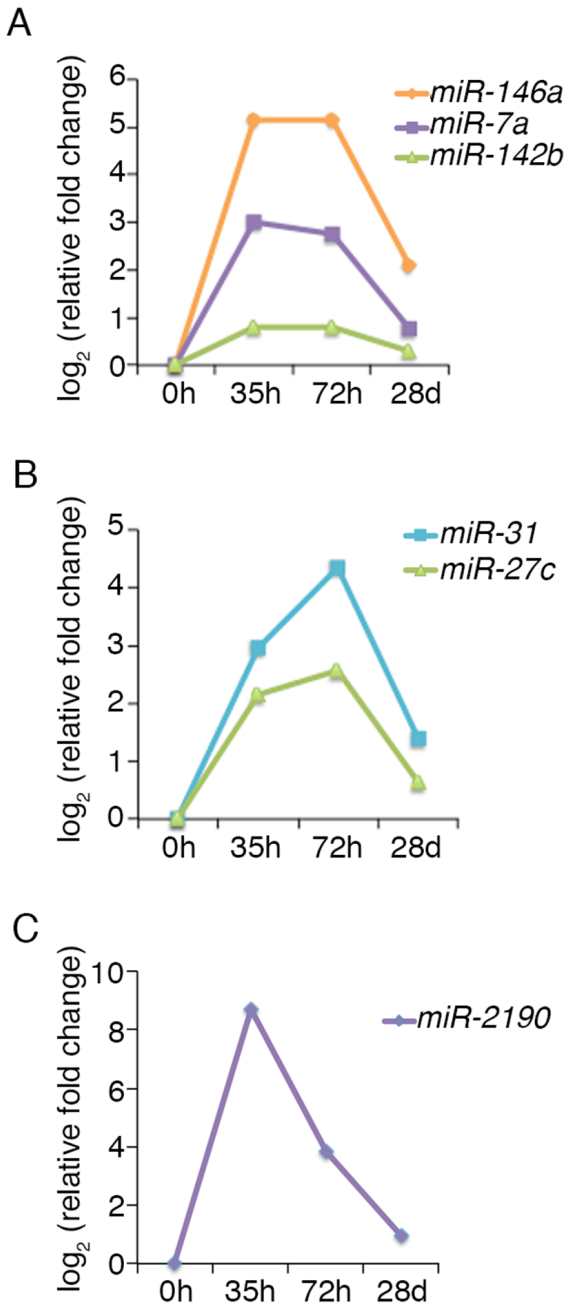

Figure 11. Expression patterns of miRNAs chosen for MO mediated knockdowns.

Six miRNAs were randomly selected for morpholino-mediated knockdown. Log_2 values of miRNA fold changes relative to 0h control values are shown. (A) miRNAs that are upregulated at both 51h and 72h. (B) miRNAs that peak at 72h. (C) miRNAs that peak at 35h.

Table 1. Top upregulated miRNAs tested in loss-of-function experiments.

miRNA	Peak upregulation time point	Log_2 (Peak fold change)
miR-7a	35h, 72h	3
miR-27c	72h	3
miR-31	72h	4
miR-142a	35h, 72h	1
miR-146a	35h, 72h	5
miR-2190	35h	9

We focused on testing the role of these miRNAs during MG-derived neuronal progenitor cell proliferation because knockdown of Dicer expression exhibited reduced neuronal progenitor cell proliferation, without affecting the number of proliferating MG. To test the potential roles of the miRNAs, dark-adapted *albino* zebrafish retinas were intravitreally injected and electroporated with MOs prior to starting intense light exposure. We did not examine the effect of the morpholinos at 35 hours, when the MG dedifferentiate and reenter the cell cycle because knockdown of Dicer expression did not reveal any effect on MG proliferation (Figures 6 and 7). We assessed the effects of reduced miRNA expression at two different time points (51 hours and 72 hours of light) during regeneration (Figure 12-15). At 51 hours of light exposure, the MG-derived neuronal progenitors are beginning to proliferate; while by 72 hours of light exposure, the MG-derived neuronal progenitor cells are rapidly proliferating and generating clusters of PCNA-positive neuronal progenitor cells that are beginning to migrate to the ONL. We sought to determine what effect loss of miRNA function would play early and late in neuronal progenitor cell amplification.

miR-142b: Regulation of both Proliferation and Migration

Of the six miRNAs tested, loss of *miR-142b* had the most dramatic effect relative to the standard control morphant retina (Figure 12A-D), with a significant reduction in the number of PCNA-positive INL cells at 51h (42±9 and 86±5, respectively, p=0.016, Figure 12E) and 72h (77±10 and 117±9, respectively, p=0.026, Figure 12E). This suggests that *miR-142b* is necessary for the early proliferation of the neuronal progenitor cells. The *miR-142b* morphant also possessed significantly fewer PCNA-positive ONL cells at 72h relative to the standard control morphant (33±6 and 58±5, respectively, p=0.017, Figure 12F), although there was not a significant difference at 51h (22±3 and 30±3, respectively, Figure 12F). This difference of PCNA-positive ONL cells at 72 h, but not at 51h, could be due to either a reduced number of MG-derived neuronal progenitor cells that are migrating to the ONL during IKNM of the cell cycle or a role for *miR-142b* in the proliferation of resident ONL rod precursor cells.

Previously, *miR-142* was suggested to play a role in liver regeneration (Lu et al., 2013). *miR-142* was also shown to regulate the balance between mesenchymal progenitor cell proliferation and differentiation through the regulation of Wnt signaling (Carraro et al., 2014). This is of interest because Wnt signaling was previously shown to play an important role in MG dedifferentiation and proliferation in the regenerating zebrafish retina (Ramachandran et al., 2010; Wan et al., 2012). It will be interesting to determine if loss of *miR-142b* suppresses MG proliferation and progenitor cell generation, thereby indirectly contributing to reduced progenitor proliferation and migration at later stages, or

if loss of *miR-142b* directly affects neuronal progenitor cell proliferation through the Wnt signaling pathway.

miR-146a: Regulation of Progenitor Cell Generation

Loss of *miR-146a* reduced the number of INL PCNA-positive cells at 51h, but not at 72h, relative to the standard control morpholino (Figure 13A-D). At 51h, the *miR-146a* morphant possessed significantly fewer PCNA-positive INL cells compared to the standard control morphant (30±6 and 86±5, respectively, p=0.006, Figure 13E), indicating that expression of this miRNA is crucial for maximal progenitor cell generation from dedifferentiated MG. However, there was no difference in the number of PCNA-positive ONL cells at either 51h or 72 h in the *miR-146a* morphant and standard control morphant (Figure 13F). The ability of the *miR-146a* morphant to reach the same number of proliferating INL neuronal progenitor cells as the standard control morphant at 72h could be due to (1) compensation of the early *miR-146a* loss by additional miRNAs, most likely by the similar family member, *miR-146b,* that is also upregulated during regeneration (Figure 4D), (2) cell cycle re-entry of additional MG to compensate for the lack of progenitors, or (3) the short half life of *miR-146a* MO that could lead to de-repression of *miR-146a* (Miska et al., 2007; Selbach et al., 2008).

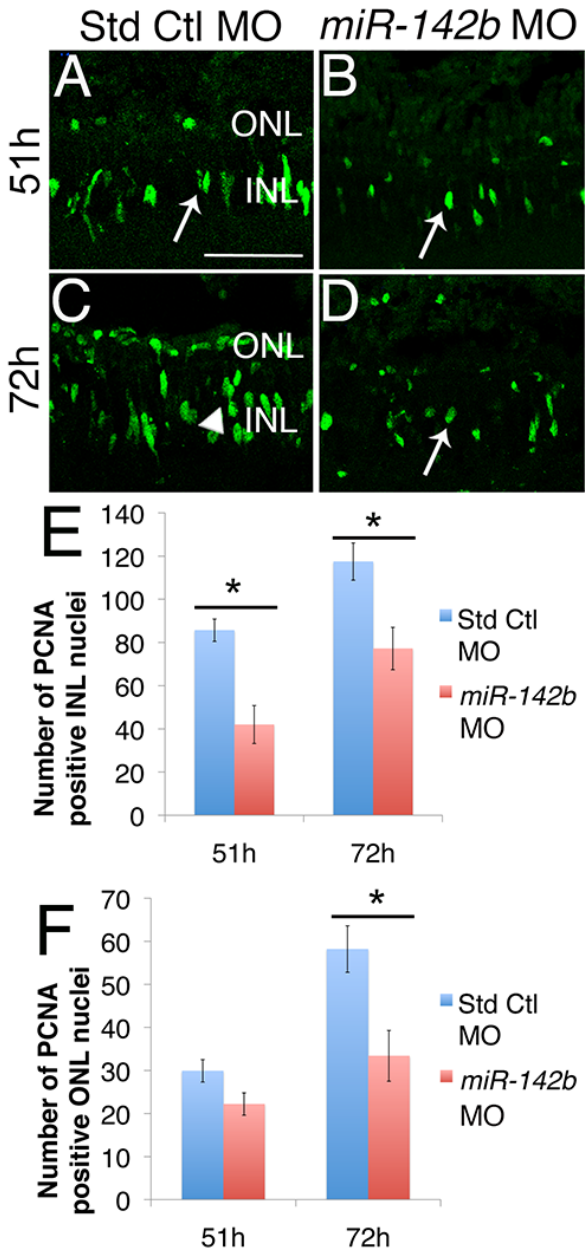

Figure 12. Knockdown of *miR-142b* reduces proliferation.

(A-B) Doublet PCNA-positive INL cells (arrows) are present in both the standard control and *miR-142b* morphant retinas at 51h. (C-D) PCNA-positive INL cell clusters are present in standard control morphants at 72h (C, arrowhead) but doublet or fewer PCNA-positive INL cells (D, arrow) remained in *miR-142b* morphant retinas. (E-F) *miR-142b* knockdown significantly reduced the number of PCNA-positive INL cells at both 51 and 72h and ONL cells at 72h. INL, inner nuclear layer; ONL, outer nuclear layer; scale bar in panel A is 50 mm and is the same for panels B-D; data represent mean +/- s.e.m. *, $p < 0.05$ using Tukey's post-hoc test following 2-way ANOVA. n=3.

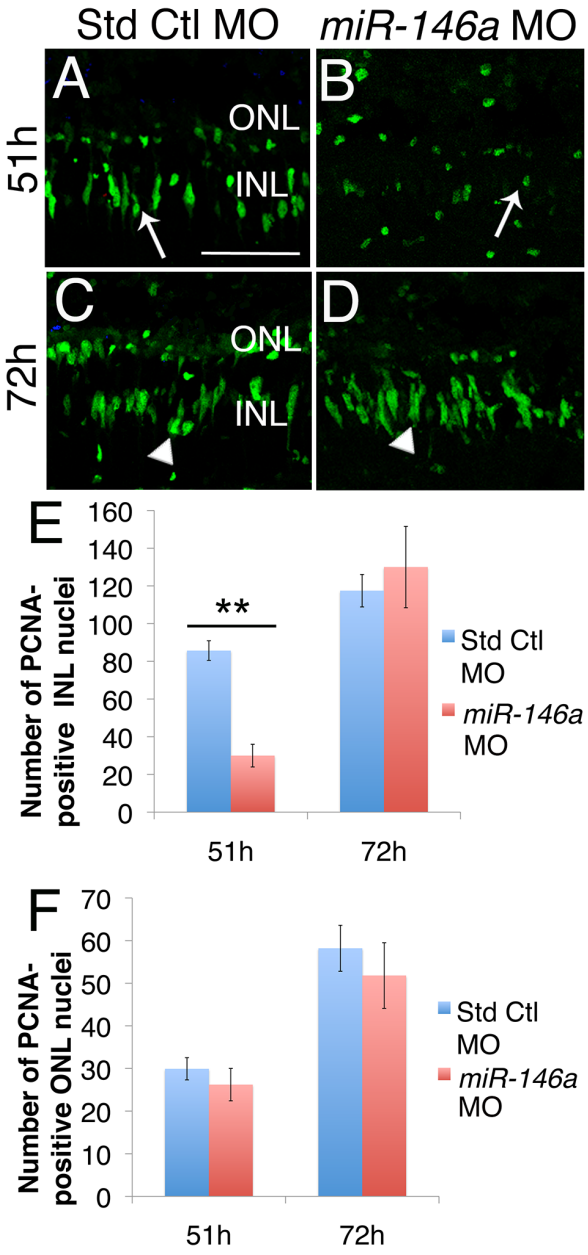

Figure 13. Knockdown of *miR-146a* reduces proliferation at 51h.

(A-B) Doublet PCNA-positive INL cells are present in standard control morphants at 51h (arrow), but mainly single PCNA-positive INL cells are present in *miR-146a* morphants (arrow). (C-D) By 72h, both standard control and *miR-146a* morphants contained columns of INL proliferating nuclei (arrowheads). (E-F) *miR-146a* knockdown significantly reduced the number of proliferating nuclei at 51h, but not at 72h. There was not significant difference in the number of PCNA-positive INL cells at either 51h or 72h between the *miR-146a* and standard control morphant retinas. INL, inner nuclear layer; ONL, outer nuclear layer; scale bar in panel A is 50 mm and is the same for panels B-D; data represent mean +/- s.e.m. **, $p < 0.01$ using Tukey's post-hoc test following 2-way ANOVA. n=3.

miR-7a, miR-27c, and *miR-31*: Regulation of Progenitor Cell Proliferation

Knockdown of either *miR-7a*, *miR-27c,* and *miR-31* resulted in statistically equivalent numbers of PCNA-positive INL and ONL cells at 51h relative to the standard control morphant (Figure 14A-D, I-N). However, the *miR-7a*, *miR-27c,* and *miR-31* morphant retinas contained fewer PCNA-positive cells than the standard control retina at 72h (Figure 14E-H). At 72h, the *miR-7a* morphant contained statistically fewer PCNA-positive relative to the standard control morphant in the INL (53±13 and 117±9, respectively, $p=0.001$, Figure 14I) and the ONL (18±6 and 58±5, respectively, $p<0.001$, Figure 14L). Similarly, the *miR-27c* morphant contained statistically fewer PCNA-positive relative to the standard control morphant in the INL (41±14 and 117±9, respectively, $p=0.001$, Figure 14J) and the ONL (23±5 and 58±5, respectively, $p<0.001$, Figure 14M).

The reduced number of PCNA-positive INL cells in both the *miR-7a* and *miR-27c* morphants at 72h relative to 51h suggests that both of these miRNAs may be necessary for maintaining the viability of the proliferating neuronal progenitor cells, possibly by preventing the neuronal progenitor cells from remaining in the cell cycle without allowing the cells to differentiate. Interestingly, this effect is reminiscent of the role of *miR-27c* family members *miRs-27a* and *-b* in muscle satellite cell activation, where they promote muscle progenitor cell migration, proliferation and delay differentiation (Crist et al., 2009; Lozano-Velasco et al., 2011). *miR-7a* has also been implicated in neuronal stem cell (NSC) maintenance and cell fate determination in the mouse brain, where it restricts Pax6 protein to NSCs (de Chevigny et al., 2012). In the regenerating zebrafish retina, Pax6 upregulation in progenitors is required for their proliferation and its loss leads to

inhibition of progenitor proliferation and phenocopies *miR-7a* knockdown (Thummel et al., 2010). Importantly, the *miR-7a*, *pax6a*, and *pax6b* morphants all exhibit a similar neuronal progenitor cell phenotype of PCNA-positive two- or four-cell clusters relative to the larger clusters in the standard control morphant at 72h (Figure 14E-H) (Thummel et al., 2010), which may suggest a complex regulatory network between *miR-7a* and Pax6 in the regenerating zebrafish retina.

Similarly, the *miR-31* morphant contained statistically fewer PCNA-positive relative to the standard control morphant in the INL (76±3 and 117±9, respectively, p=0.02, Figure 14K) and the ONL (31±4 and 58±5, respectively, p=0.014, Figure 14N) at 72h. The effect generated by the *miR-31* morphant suggests that this miRNA plays a role in neuronal progenitor cell proliferation or migration. The exact regulation of proliferation by *miR-31* remains unclear, as both anti- and pro-proliferative roles of *miR-31* have been reported (Cekaite et al., 2012; Valastyan and Weinberg, 2011).

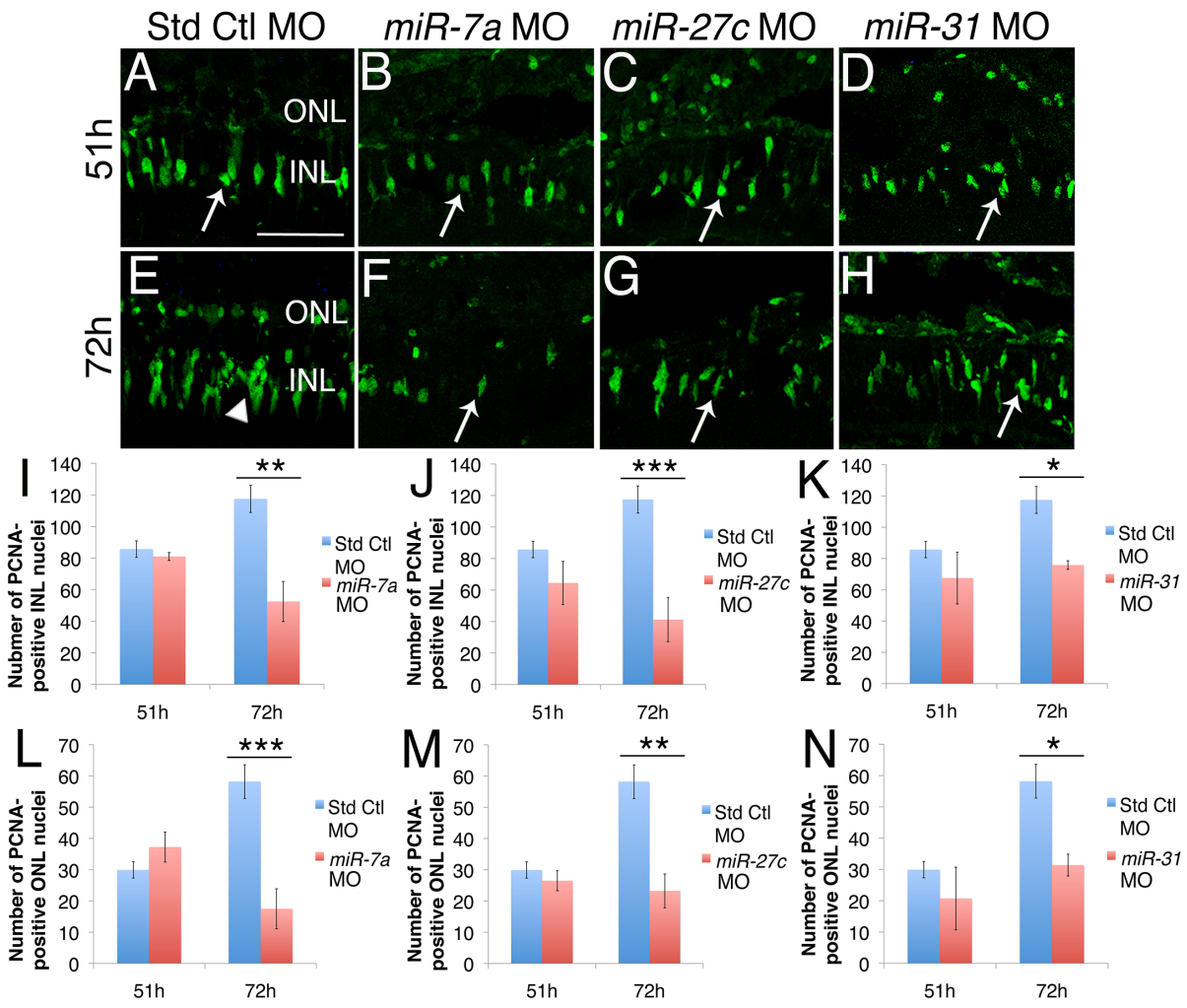

Figure 14. Knockdown of *miR-7a*, *miR-27c* and *miR-31* reduced proliferation at 72h.

(A-D) Standard control morpholino and *miR-7a*, *miR-27c* and *miR-31* morphant retinas labeled for PCNA contained INL doublet proliferating nuclei (arrows) at 51h. (E) Standard control morphant retinas contain columns of INL proliferating nuclei (arrowhead) at 72h. (F-H) At 72h, *miR-7a*, *miR-27c* and *miR-31* morphant retinas contained mainly doublet INL and single nuclei (arrows). (I-K) There were no significant differences in the number of PCNA-positive INL cells at 51h between the standard control morphant retina and the *miR-7a* (I), *miR-27c* (J), and *miR-31* (K) morphant retinas. In contrast, significantly fewer PCNA-positive INL cells were present in all three miRNA morphant retinas compared to standard control morphant retinas at 72h. (L-N) There were no significant differences in the number of PCNA-positive ONL cells at 51h between the standard control morphant retina and the *miR-7a* (L), *miR-27c* (M), and *miR-31* (N) morphant retinas. In contrast, significantly fewer PCNA-positive INL cells were present in all three miRNA morphant retinas compared to standard control morphant retinas at 72h. INL, inner nuclear layer; ONL, outer nuclear layer; scale bar in panel A is 50 mm and is the same for panels B-H; data represent mean +/- s.e.m. *, $p< 0.05$; **, $p< 0.01$; ***, $p<0.001$ using Tukey's post-hoc test following 2-way ANOVA. n=3.

miR-2190: No Regulation of Retina Regeneration

Finally, knockdown of *miR-2190* had no effect on the number of INL or ONL PCNA-positive cells during regeneration relative to the standard control morphant at either 51h (Figure 15A, B, E, F) or 72h (Figure 15C, D, E, F). This was a little surprising considering the large increase in *miR-2190* expression at 35h and 51h relative to the undamaged retina (Figure 11C). While this work was in progress, however, Wei et al (2012) discovered that *miR-2190* is likely not a true miRNA, but is a product of rRNA degradation (Wei et al., 2012), which could account for the lack of effect on retina regeneration upon *miR-2190* knockdown.

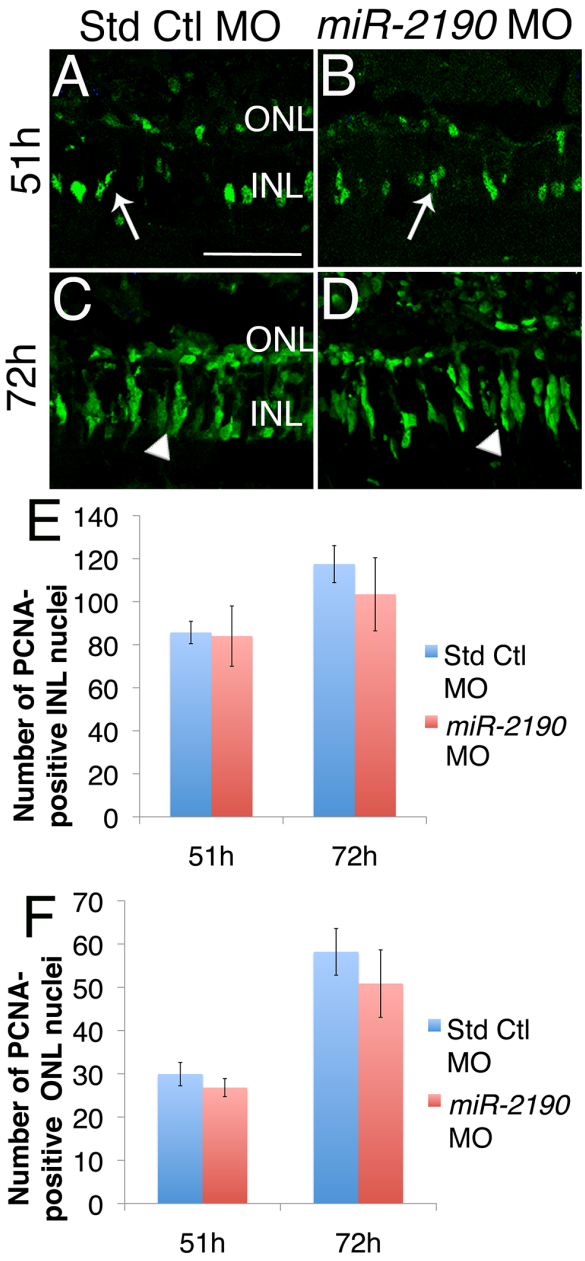

Figure 15. Knockdown of *miR-2190* does not affect proliferation.

(A-B) Standard control and *miR-2190* morphant retinas at 51h of light damage display PCNA-positive doublet INL proliferating nuclei (arrows). (C-D) Standard control and *miR-2190* morphant retinas display clusters of INL nuclei (arrowheads) at 72 hours of light damage. (E-F) Statistically equivalent numbers of INL and ONL PCNA-positive nuclei are present in standard control and *miR-2190* morphant retinas. INL, inner nuclear layer; ONL, outer nuclear layer; scale bar in panel A is 50 mm and is the same for panels B-D; data represent mean +/- s.e.m. *, p< 0.05. n=3.

Summary

We demonstrate that miRNA processing, through the expression of Dicer, is necessary for the proliferation of the MG-derived neuronal progenitor cells. This study also represents the first thorough examination of changes in miRNA expression during regeneration of the adult zebrafish retina. These miRNAs revealed dynamic expression patterns during retina regeneration with individual miRNAs functioning in either early MG-derived neuronal progenitor cell proliferation, late neuronal progenitor cell proliferation, or both. Together with previous reports of miRNAs functioning in tissue regeneration in other non-mammalian vertebrates (Ramachandran et al., 2010; Sehm et al., 2009; Thatcher et al., 2008; Yin et al., 2012; Yin et al., 2008; Yu et al., 2011), it is apparent that miRNAs play pivotal roles at multiple steps during the regeneration of diverse tissues in a range of animals .

Acknowledgements

We thank the technicians at the Freimann Life Science Center for their care and dedication to the zebrafish in the Center for Zebrafish Research at the University of Notre Dame. We thank Qiang Guan for expert zebrafish care at the Vanderbilt University Stevenson Center Fish Facility. We thank Travis Clark and John Gibbons for helpful discussions and suggestions about Illumina high-throughput sequencing. This study was supported in part by grants from the National Eye Institute–National Institutes of Health to J.G.P (R21 EY 019759) and D.R.H. (R01-EY018417) and the Center for Zebrafish Research at the University of Notre Dame. K.R. was supported in part by the Vanderbilt

International Scholar Program and by the Gisela Mosig Fund in the Department of Biological Sciences.

CHAPTER III

APPLICATION OF CONSTANT INTENSE LIGHT EXPOSURE TO LESION AND INITIATE REGENERATION IN NORMALLY PIGMENTED ZEBRAFISH*

Kamya Rajaram, Emily R. Summerbell and James G. Patton[a]

Department of Biological Sciences, Vanderbilt University, Nashville, TN

---

* This work has been accepted for publication in the journal Molecular Vision.
[a] KR and JGP conceived and designed the research. KR and ERS performed experiments. KR analyzed the data. KR, ERS and JGP wrote the paper.

Abstract

Zebrafish are capable of robust and spontaneous regeneration of injured retina. Constant intense light exposure of adult *albino* zebrafish specifically causes apoptosis of rod and cone photoreceptor cells, and is an excellent model to study the molecular mechanisms underlying photoreceptor regeneration. However, this paradigm has only been employed to lesion zebrafish of the non-pigmented *albino* genetic background, which precludes the use of numerous transgenic reporter lines that are widely used to study regeneration. Here, we explored the effectiveness of constant intense light exposure in causing photoreceptor apoptosis and stimulating regeneration in normally pigmented zebrafish retinas. We show that constant intense light exposure causes widespread photoreceptor damage in the dorsal-central retinas of pigmented zebrafish. Photoreceptor loss triggers dedifferentiation and proliferation of Müller glia, as well as progenitor cell proliferation. We also demonstrate that the timeline of regeneration response is comparable between the *albino* and the pigmented retinas.

Keywords: retina regeneration, constant intense light exposure, pigmented retinas

Introduction

Photoreceptor loss is the leading cause of many human retina degenerative diseases. Retinal cell loss is irreversible in mammals, but the non-mammalian vertebrate zebrafish can spontaneously regenerate any lost retinal cell type. A range of retinal damage models have been employed to study regeneration in zebrafish, including light induced damage (Bernardos et al., 2007; Vihtelic and Hyde, 2000; Weber et al., 2013), mechanical injury (Fausett and Goldman, 2006), chemical/ toxin treatment (Fimbel et al., 2007; Montgomery et al., 2010) and laser ablation (Wu et al., 2001). In all these cases, supportive retinal glial cells called Müller glia (MG) dedifferentiate and proliferate to generate progenitor cells (Nagashima et al., 2013). The progenitor cells rapidly proliferate and form progenitor clusters that migrate to the region of damage and differentiate into the lost retinal cell types (Fausett and Goldman, 2006; Thummel et al., 2010).

Amongst the damage models, light induced lesions are non-invasive and highly specific, in that they cause synchronous photoreceptor apoptosis while leaving the rest of the retina intact, thereby allowing study of the molecular mechanisms underlying photoreceptor regeneration (Wenzel et al., 2005). Light induced photoreceptor apoptosis was discovered in rats, and the mechanisms involved have been characterized in rodent retinas (Noell et al., 1966). Constant intense light exposure causes repetitive bleaching of the visual pigment rhodopsin, which results in accumulation of retinoid intermediates that ultimately induce apoptosis (Wenzel et al., 2005). Activation of pro-apoptotic transcription factor AP-1 is also necessary for light-induced apoptosis, although the exact mechanisms remain unclear (Karin and Chang, 2001; Wenzel et al., 2000).

In zebrafish, two main paradigms of light lesioning free-swimming fish have been described, although recently, combinatory models and a third light lesioning model that utilizes focused retinal lesioning of immobilized fish have also been described (Thomas et al., 2012; Thomas and Thummel, 2013; Weber et al., 2013). Amongst the models used to lesion free-swimming zebrafish, the constant intense light paradigm employs exposure of dark-adapted *albino* fish to ~10,000 lux light for 3-4 days (Vihtelic and Hyde, 2000). This causes extensive photoreceptor apoptosis in the dorsal and central retina, while leaving the ventral retina mostly undamaged. Although some rod photoreceptor loss was observed in the dorsal retinas of pigmented zebrafish, this light lesioning model does not elicit significant MG proliferation in pigmented zebrafish retinas (Thomas and Thummel, 2013). The second model involves exposing normally pigmented, free-swimming zebrafish to ultra high intensity UV light (~180,000 lux) for 30 min, and causes photoreceptor apoptosis in the central retina with sporadic damage in the dorsal and ventral regions (Bernardos et al., 2007; Thomas et al., 2012). Extensive studies exploring the efficacy of each model, including the types of cells damaged and the initiation of regeneration response have been undertaken (Thomas et al., 2012; Vihtelic et al., 2006; Weber et al., 2013). Recently, combining the high intensity UV light exposure with 48h of constant intense light exposure was shown to cause widespread photoreceptor apoptosis and trigger regeneration in pigmented zebrafish retinas (Thomas and Thummel, 2013). However, it remains unknown if the timeline of regeneration is identical between pigmented and *albino* zebrafish.

In this study we sought to evaluate the utility of a modified constant intense light exposure paradigm to damage normally pigmented, non-albino zebrafish retinas. We

developed a protocol in which constant intense light triggers photoreceptor apoptosis and MG-induced regeneration response in the central-dorsal regions of the pigmented retinas. By performing parallel light lesioning experiments with *albino* and normally pigmented zebrafish, we demonstrate that the timeline of photoreceptor apoptosis and regeneration response is largely identical. These results are significant as they allow the use of existing pigmented transgenic reporter lines in the constant intense light lesion model without having to breed new *albino* lines. Additionally, this paradigm does not require the use of expensive UV light source, is relatively simple and cheap to set up, and regeneration in the central-dorsal retina can be compared between different zebrafish lines, irrespective of their pigmentation status.

Materials and Methods

Fish maintenance

Zebrafish were maintained in 14h light and 10h dark cycles at 28.5°C. The following lines were used: *albino* (Vihtelic and Hyde, 2000), *tg:zop:nfsB:EGFP* (Montgomery et al., 2010), *tg:1016tuba1a:gfp* (Fausett and Goldman, 2006)and *tg:gfap:gfp* (Bernardos and Raymond, 2006)and AB (wildtype). All experiments were performed with the approval of the Vanderbilt University Institutional Animal Care and Use Committee (Protocol # M/09/398).

Constant intense light lesioning

Adult zebrafish between 6-9 months old were used for the constant intense light lesioning. Light lesioning was performed as previously described (Vihtelic and Hyde,

2000). Briefly, adult zebrafish were dark adapted for 14 days, transferred to clear tanks placed between two fluorescent lights with light intensity at ~20,000 lux for 16h-4 days. The distance from the tank to each light source was ~10cm. Each light treatment tank contained about 20 free-swimming zebrafish. An aquarium water heater (25W) and 1-2 air bubblers were introduced into each tank to maintain the water temperature at 30-33°C.

Immunohistochemistry and TUNEL assay

Adult zebrafish eyes were collected and fixed in 4% paraformaldehyde for 2-5h at room temperature followed by cryoprotection in 30% sucrose/1X PBS and embedding in Shandon cryomatrix (Thermo Scientific). Eyes were cryosectioned at 10-12 microns and collected on charged Histobond slides (VWR). For immunohistochemistry (IHC), slides were rehydrated in 1X PBS, blocked with serum before overnight primary antibody incubation. Primary antibodies used were mouse anti-PCNA monoclonal antibody (1:500, Sigma), rabbit anti-GFP polyclonal antiserum (1:1000, Torrey Pines Biolabs), mouse anti-glutamine synthetase monoclonal antibody (1:200, Chemicon) and mouse anti-zpr-1 monoclonal antibody (1:200, ZIRC). Following primary antibody incubation, sections were washed before secondary antibody and nuclear stain TOPRO 3 (1:1000, Invitrogen) application. Secondary antibodies used were donkey anti-mouse AF488 (1:200), donkey anti-mouse Cy3 (1:100), donkey anti-mouse Cy5 (1:100), Donkey anti-rabbit Cy3 (1:200) and donkey anti-rabbit AF488 (1:200)(Jackson Immuno). Slides were washed, dried and mounted with Vectashield (Vector labs). For PCNA IHC, antigen retrieval with 10mM sodium citrate buffer containing 0.05% Tween-20 (pH 6) was performed prior to blocking. For TUNEL assays, sections were processed as for IHC.

TUNEL assays were performed using the TMR red *in situ* cell death detection kit (Roche).

Cell counts, retina morphometry and statistical analyses

Confocal microscopy was performed using Zeiss LSM 510 META inverted confocal microscope at the Vanderbilt cell imaging shared resource (CISR). Only retina sections containing optic nerves were used for immunohistochemistry, retina morphometry and quantifications. Unless otherwise noted, all quantifications were done in the central-dorsal retina, at a linear distance of ~300 microns from the optic nerve. ImageJ (NIH) was used to measure the ONL thickness in the retina morphometric analyses. 5-7 retinas were used for each time point. For each retina, the average of three independent measurements of the ONL thickness across the central-dorsal retina was calculated. In all figures, data are represented as mean +/- standard deviation (S.D.). In Figure 4D, one-way ANOVA (StatPlus software, Analystsoft) followed by Tukey's HSD post-hoc test was used to calculate significance (p values). In all other figures, Student-t tests were used to calculate significance.

Results

Constant intense light exposure of pigmented zebrafish destroys both rod and cone photoreceptors

To assess the effects of constant intense light exposure on pigmented zebrafish retinas, we subjected normally pigmented adult wildtype zebrafish (AB background) to constant intense light. Following a 2-week dark adaptation period, AB fish were exposed

to intense light for varying periods of time, after which retinas were dissected and probed using the Zpr1 antibody that recognizes the red-green double cones. At the 0h time point, prior to intense light exposure, we detected an ordered arrangement of zpr1^{+} double cones in the ONL with outer segments (OS) projecting beyond the ONL (Figure 16; arrowheads). However, by 24h of intense light exposure we detected disorganization and hypertrophy of the zpr1^{+} double cones in addition to thinning of the ONL across the central-dorsal retina (compare brackets in 0h and 24h panels), with sporadic damage in the ventral retina (data not shown). By 48h in intense light, the cone photoreceptor OS begin to breakdown further and the cells appeared detached from the ONL. By 72h, the ONL is thinner and the cone cells have entirely lost their projections and appear clumped or condensed (arrows).

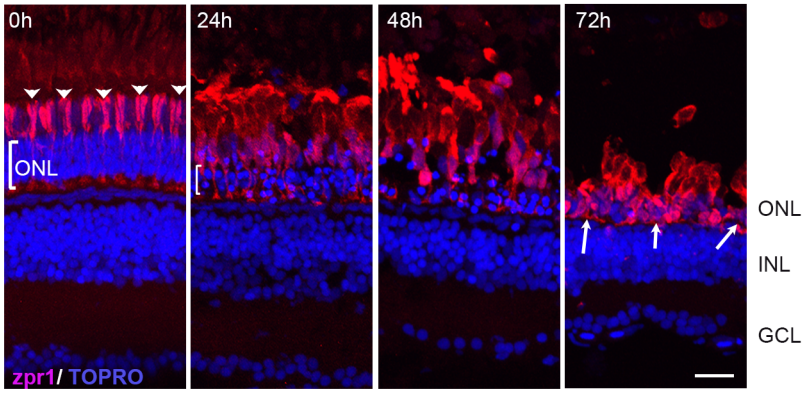

Figure 16. Effects of constant intense light exposure on cone cells of pigmented AB zebrafish.

Retinas were collected from zebrafish before (0h) and after different lengths of light exposure (24h, 48h and 72h). Retinas were processed for immunohistochemistry and stained with zpr1 antibody (red). Nuclei were counter-stained with TOPRO (blue). Dorsal retinas are shown. The arrowheads at 0h indicate the ordered arrangement of the double cones; the bracket indicates the ONL. White arrows show the condensed zpr^{+} cells at 72h of intense light. ONL, outer nuclear layer; INL, inner nuclear layer; GCL, ganglion cell layer. Scale bar, 50 um.

Intense light exposure induced thinning of the ONL indicated loss of rod photoreceptors in addition to cones. To confirm rod loss, we utilized the pigmented *zop:nfsB:EGFP* transgenic zebrafish, which express EGFP specifically in the rod photoreceptors (Montgomery et al., 2010) and subjected them to constant intense light lesioning. Retinas were collected at different time points before (0h) and during intense light treatment (16h, 35h, 48h, 72h), processed for immunohistochemistry and stained with zpr-1 and anti-GFP antibodies (Figure 17A). At 0h, an intact array of GFP^+ rod photoreceptors interspersed with zpr-1^+ cones were detected in *zop:nfsB:EGFP* retinas. Rod OS were clearly seen projecting beyond the ONL. Disorganization of GFP^+ rods and loss of rod OS was detected as early as 16h of light exposure. By 35h, there were fewer GFP^+ and zpr-1^+ cells in the ONL. By 72h of light exposure, the ONL is much thinner with very few GFP^+ rod cells remaining. These cells looked rounded up and had lost their outer segments (arrows). The few zpr-1^+ cones that persisted appeared condensed and had lost their projections.

Importantly, when we exposed *albino* zebrafish to light treatment in parallel with the *zop:nfsB:EGFP* transgenic zebrafish, we observed that photoreceptor destruction happened at comparable times in the pigmented and non-pigmented zebrafish retinas (Figure 17B). As in the pigmented retinas, by 35h, cone photoreceptor loss was observed in the *albino* retina (arrowheads) and by 72h most cone photoreceptors were destroyed. Taken together, these studies show that the intense light paradigm used to lesion non-pigmented *albino* zebrafish was efficient in lesioning normally pigmented retinas, and the time course of photoreceptor loss is identical between pigmented and non-pigmented retinas. Additionally, spatial loss of photoreceptors in the pigmented retinas is akin to the

albino retinas, with severe photoreceptor loss in the dorsal-central retina and patchy damage in the ventral retina.

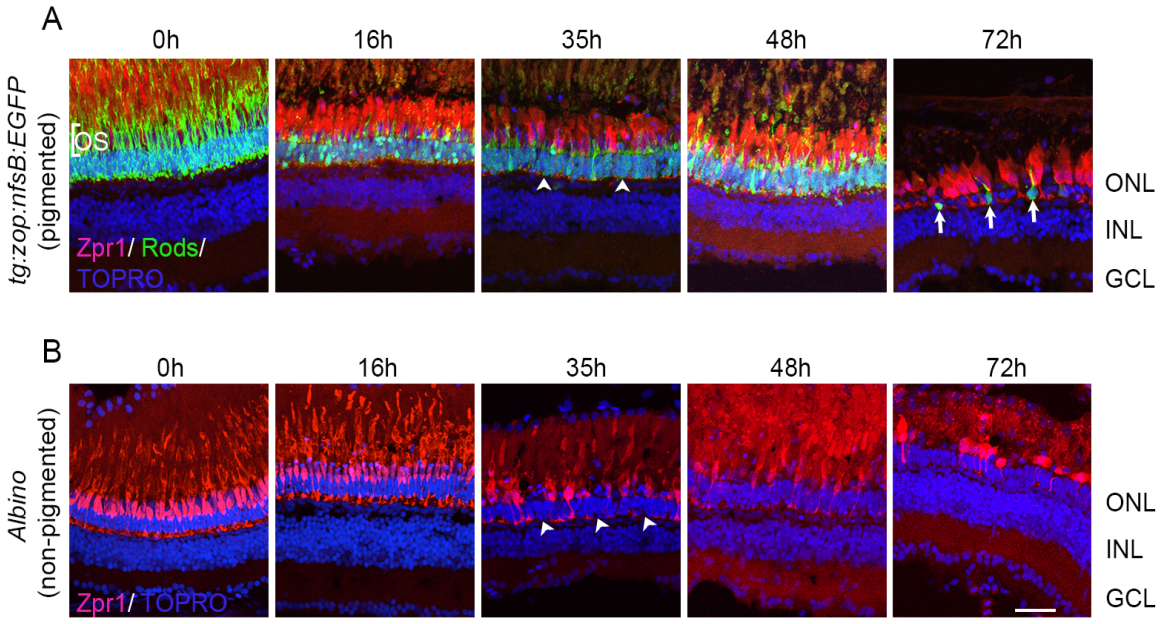

Figure 17. Comparison of photoreceptor loss in pigmented and non-pigmented retinas.

Pigmented *tg:zop:nfsB:EGFP* zebrafish (A) or non-pigmented *albino* zebrafish (B) were subjected to intense light damage and retinas were collected at the indicated time points and processed for immunohistochemistry. Retinas in (A) were stained with zpr-1 (red) and anti-GFP (green) antibodies, while retinas in (B) were stained with zpr-1 (red) antibody; nuclei were counter-stained with TOPRO (blue). Dorsal retinas are shown. Arrowheads indicate regions of photoreceptor loss. Arrows denote rods photoreceptors that have rounded up and lost their outer segments. ONL, outer nuclear layer; INL, inner nuclear layer; GCL, ganglion cell layer; OS, outer segments. Scale bar, 50 um.

Constant intense light exposure induces apoptosis of photoreceptors in pigmented zebrafish retinas

In *albino* retinas, intense light exposure induces photoreceptor apoptosis. The rounded and condensed photoreceptor morphology that we observed in the light treated pigmented retinas was highly indicative of photoreceptors dying by apoptosis. To verify this, we performed TUNEL on sections from AB retinas exposed to constant intense light for different lengths of time (Figure 18). No TUNEL staining was detected prior to light exposure (0h). However, as light treatment proceeded, a number of $TUNEL^{+}$ nuclei were observed in the ONL, with TUNEL staining peaking at 24h and attenuating at later time points.

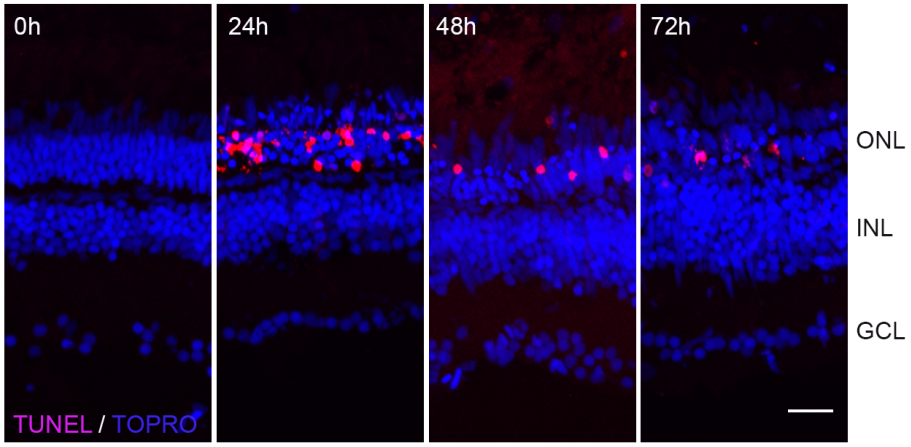

Figure 18. TUNEL labeling of light treated pigmented retinas.

Retinas from light treated AB fish were collected at different times during the light treatment and processed for TUNEL labeling (Red). Nuclei were counter stained with TOPRO (blue). Scale bar 50 um.

Previous studies in *albino* zebrafish established the peak of photoreceptor apoptosis around a day of intense light exposure (Vihtelic and Hyde, 2000). To directly compare the timeline of photoreceptor apoptosis in pigmented and non-pigmented retinas, we exposed *albino* zebrafish to light damage concurrent with *zop:nfsB:EGFP* transgenic fish and quantified the $TUNEL^+$ nuclei in the ONL. As shown in Figure 19A, few $TUNEL^+$ nuclei begin to appear in the ONL of the *tg:zop:nfsB:EGFP* by 16h of light exposure. Strikingly, the GFP^+ rod photoreceptors lose their OS and become shortened. TUNEL labeling increases at 35h of light exposure but is drastically reduced by 48h in light and continues to decrease at 72h and 96h. By 72h, very few rods remain and these cells look condensed and lack OS (arrowheads). When we compared the timeline of TUNEL labeling between the non-pigmented *albino* retinas and pigmented retinas, there were significantly fewer $TUNEL^+$ nuclei in the pigmented retina ONL at 16h compared to non-pigmented *albino* retinas ($p< 0.005$; n=5 retinas). However, by 35h TUNEL labeling is identical between the two groups and continues to taper off at later time points (Figure 19C). We also monitored changes in the thickness of the ONL across regeneration (Figure 19D). By 16h of light damage, the ONL thickness was significantly reduced in both pigmented and *albino* zebrafish retinas ($p< 0.005$; n=5-7 retinas). However, we did not observe any differences in the ONL thickness between the pigmented and *albino* groups, indicating that the rate of photoreceptor loss is identical between both groups.

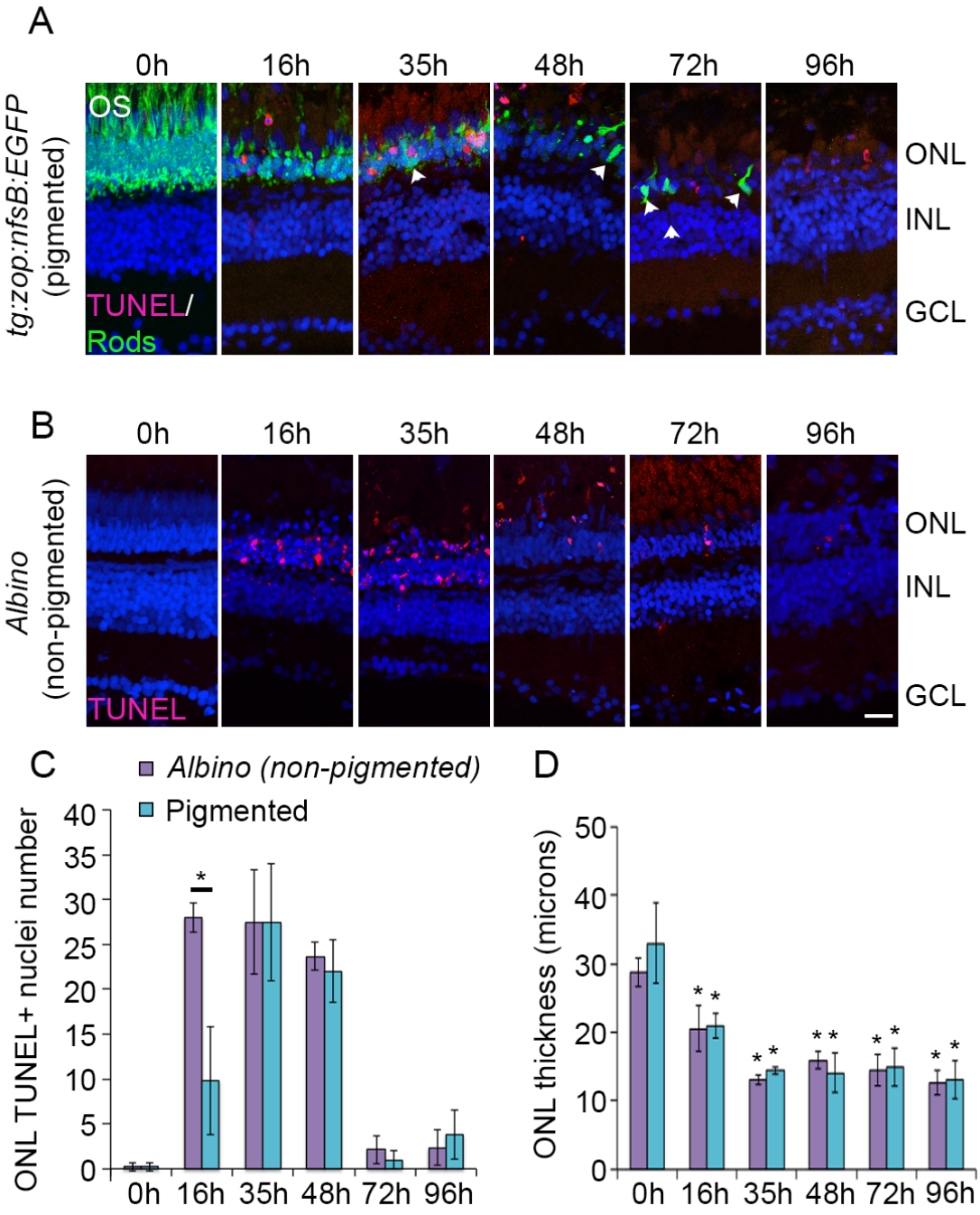

Figure 19. Time course of photoreceptor apoptosis in pigmented and non-pigmented zebrafish retinas

Pigmented *tg:zop:nfsB:EGFP* zebrafish (A) or non-pigmented *albino* zebrafish (B) were subjected to intense light damage and retinas were collected at the indicated time points and processed for TUNEL labeling. In (A), rods were stained with anti-GFP (green) antibody; nuclei

were counter-stained with TOPRO (blue). Dorsal retinas are shown. Arrowheads indicate rods that appear condensed and lack OS. (C) Quantification of TUNEL labeling for *albino* and pigmented zebrafish. Data represent mean ± S.D. *, $p<0.005$; *n*= 3-7 retinas for each time point. (D) Quantification of the ONL thickness for *albino* and pigmented zebrafish. All comparisons were made with 0h. Data represent mean ± S.D. *, $p<0.05$ using one-way ANOVA with Tukey's HSD post-hoc test; *n*= 5-7 retinas for each time point. ONL, outer nuclear layer; INL, inner nuclear layer; GCL, ganglion cell layer; OS, outer segments. Scale bar, 50 um.

Constant intense light exposure triggers MG cell cycle re-entry and progenitor cell proliferation in pigmented zebrafish retinas

In *albino* zebrafish, light induced photoreceptor apoptosis triggers MG proliferation, which generates $PCNA^+$ progenitor cells. These progenitors rapidly divide to form clusters of progenitors that migrate to the ONL and differentiate into photoreceptors (Kassen et al., 2007). We wanted to examine if light damage of pigmented zebrafish retinas stimulated the MG-induced regeneration response and if the timeline of the response corresponds to that in the *albinos*. For this, we exposed the *tg:zop:nfsB:EGFP* fish and *albino* fish to the intense light paradigm concurrently, collected retinas at various stages and monitored progenitor generation and proliferation using PCNA immunohistochemistry (Figure 20). We did not detect any statistically significant differences between the PCNA response in the pigmented *tg:zop:nfsB:EGFP* fish and the *albino* fish (Figure 20C). In both groups, $PCNA^+$ cells begin to appear in the INL around 35h of light exposure. By 72h, progenitor clusters have elaborated in the INL and the progenitor cells start migrating to the ONL. By 96h, most of the $PCNA^+$ progenitor cells have reached the ONL. In the *tg:zop:nfsB:EGFP* fish PCNA expression pattern was consistent across the dorsal-central retina but remained sporadic in the ventral retina.

To confirm that the PCNA^{+} cells in the INL at 35h of light are indeed MG, we utilized the pigmented *tg:GFAP:GFP* zebrafish (Bernardos and Raymond, 2006), which express GFP under the glial specific GFAP promoter. After 35h of light exposure, numerous GFP^{+} MG in the dorsal-central retina expressed PCNA (Figure 21A). By 51h of light exposure, ~85% of MG expression PCNA or were associated with PCNA^{+} progenitor cells (85±7% of MG were PCNA^{+}; *n*= 7 retinas) (Figure 21B; arrows). Some progenitors were migrating to the ONL.

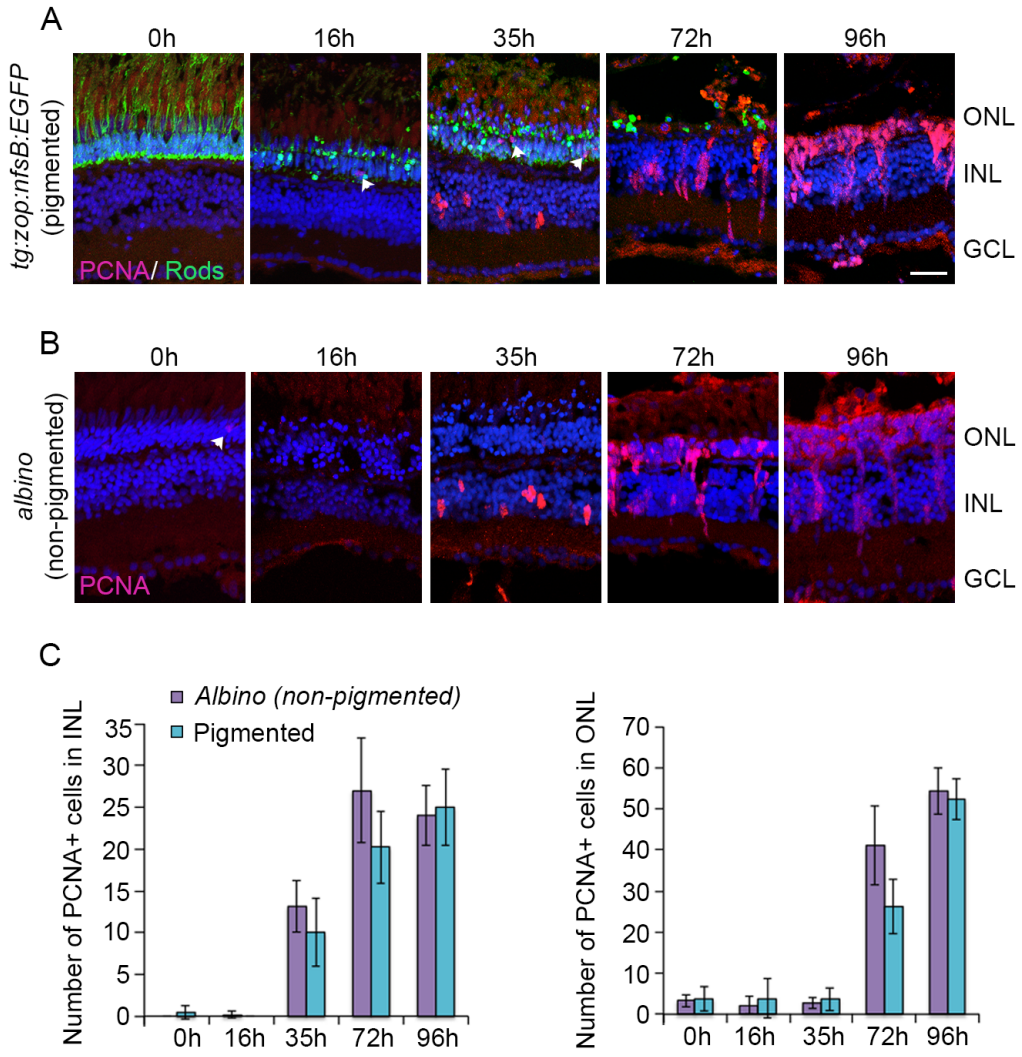

Figure 20. PCNA expression during intense light exposure.

Pigmented *tg:zop:nfsB:EGFP* zebrafish (A) or non-pigmented *albino* zebrafish (B) were subjected to intense light damage and retinas were collected at the indicated time points and processed for immunohistochemistry. Retina sections were stained with anti-GFP (green in panel A) and anti-PCNA (panels A and B) antibodies; nuclei were counter-stained with TOPRO (blue). Dorsal retinas are shown. Arrowheads indicate rod precursors in the ONL that label for PCNA. (C) Quantification of $PCNA^{+}$ cells in the INL and ONL. Data represent mean ± S.D. *n*=3-7 retinas/ time point. ONL, outer nuclear layer; INL, inner nuclear layer; GCL, ganglion cell layer. Scale bar, 50 um.

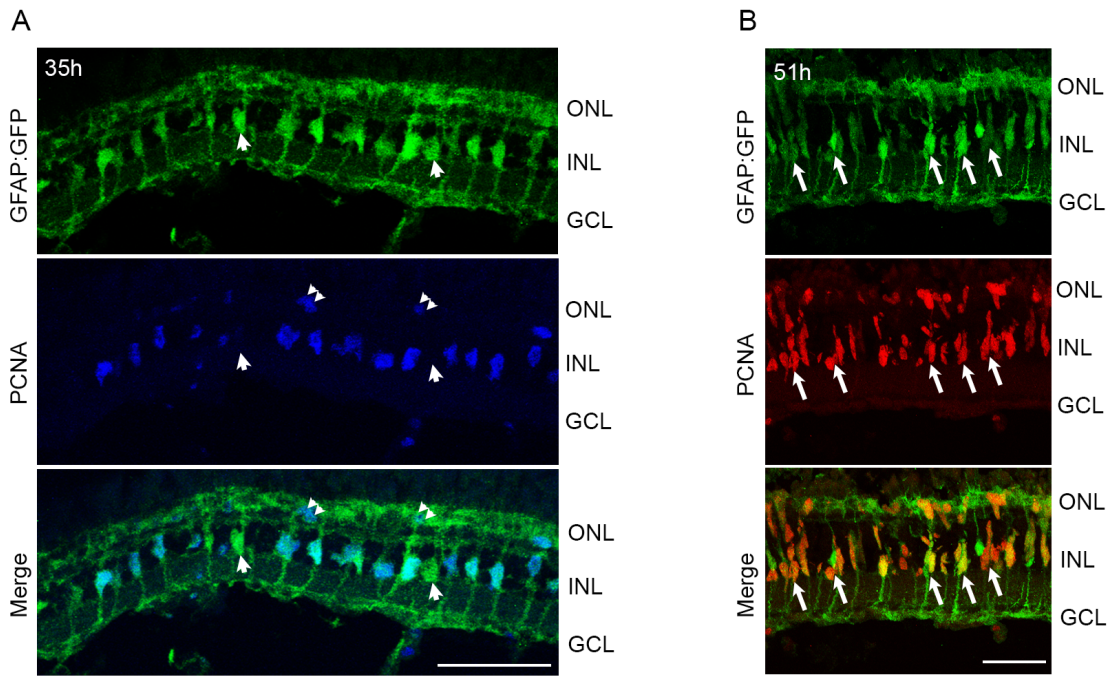

Figure 21. Light treatment of pigmented retinas stimulates proliferation of MG and progenitor cells.

tg:GFAP:GFP fish were exposed to intense light for 35h (A) or 51h (B) and retinas were processed for immunohistochemistry. (A) PCNA immunohistochemistry (blue) reveals co-staining with GFP^+ MG. Very few MG do not express PCNA (arrowheads in A). PCNA also labels rod precursors in the ONL (double arrowheads). (B), Most GFP^+ MG continue to express PCNA. Arrows indicate MG associated with small $PCNA^+$ progenitor clusters. Few $PCNA^+$ cells are migrating to the ONL. ONL, outer nuclear layer; INL, inner nuclear layer; GCL, ganglion cell layer. Scale bars, 50 um.

All together, these data demonstrate that intense light exposure triggers MG cell cycle re-entry, progenitor cell generation and proliferation in the pigmented zebrafish. Importantly, the time line of the regeneration response is consistent with that in *albino* zebrafish.

Constant intense light exposure triggers tuba1a:GFP transgene expression in dedifferentiated MG and progenitor cells.

MG dedifferentiation post retinal damage is one of the earliest steps in retina regeneration. In the transgenic pigmented zebrafish *1016:tuba1a:GFP* (Fausett and Goldman, 2006), GFP expression is specifically driven in the dedifferentiated MG by activation of a 1.7kb α1 Tubulin promoter, and GFP persists in the MG-derived progenitor cells. Previously, this transgenic line has been utilized in the poke model of retina regeneration to label dedifferentiated MG and progenitor cells (Fausett and Goldman, 2006; Ramachandran et al., 2010).

To evaluate the applicability of this transgenic line to study light damage induced retina regeneration, we exposed these fish to the constant intense light paradigm and monitored GFP expression using immunohistochemistry (Figure 22A). We did not detect any GFP expression prior to light damage (0h). However, after 24h of light exposure, we detected a few GFP^+ cells in the INL of the dorsal retina (arrowheads in A). By 51h, a number of GFP^+ cells occupied the INL of the central-dorsal retina and most of the ventral retina. GFP^+ processes extended into the IPL, morphologically resembling MG processes. We also detected few GFP^+ cells in the ONL. By 72h, GFP^+ cells existed in large cell clusters within the INL (double arrowheads) and staining persisted in the processes spanning the IPL, which was highly indicative of progenitor cell clusters associated with MG. We also detected a large number of GFP^+ cells in the ONL. To verify that the tuba1a:GFP expressing cells were indeed MG, we co-stained 51h sections with an antibody against MG specific glutamine synthetase (GS) (Figure 22B). ~80% of

the GS$^+$ cells expressed GFP, indicating that these are MG that have dedifferentiated post light damage (arrows) (81±8%; *n*=3 retinas).

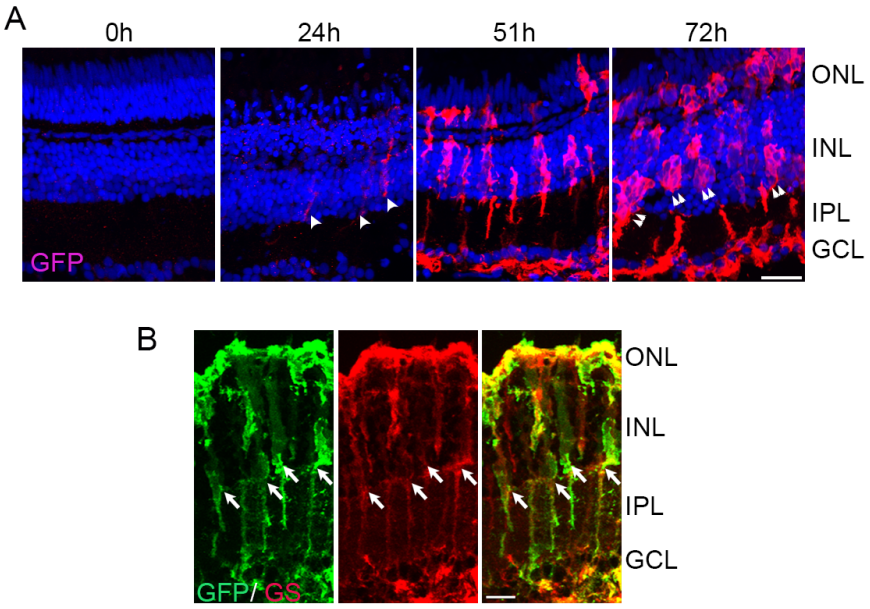

Figure 22. Light damage triggers tuba1a:GFP transgene expression in MG.

(A), *tg:1016tuba1a:GFP* zebrafish were exposed to the constant intense light paradigm and retinas were collected at the indicated time points and assessed for GFP expression (red) by immunohistochemistry. GFP$^+$ cells began to appear in the INL by 24h (arrowheads). By 72h, clusters of GFP$^+$ cells were detected in the INL and ONL (double arrowheads). (B) Immunohistochemistry for GFP and GS in 51h light exposed *1016tuba1a:GFP* retinas. Arrows indicate GS$^+$ and GFP$^+$ MG. ONL, outer nuclear layer; INL, inner nuclear layer; GCL, ganglion cell layer; IPL, inner plexiform layer. Scale bars, 50 um.

To confirm that the GFP$^+$ cell clusters we observed at 72h of light exposure were progenitor cell clusters that associate with MG, we co-stained the light damaged retina sections with PCNA (Figure 23). We detected few PCNA$^+$ rod precursors in the ONL of 0h retinas (arrowheads). By 51h, most of the INL was occupied by GFP$^+$/PCNA$^+$ cells and we detected small progenitor cell clusters containing 2-4 progenitor cells associating along a GFP$^+$ MG process (double arrowheads). The large clusters of GFP$^+$ cells at 72h

of light co-labeled with PCNA confirming that these are indeed clusters of progenitor cells that are migrating to the ONL (arrows).

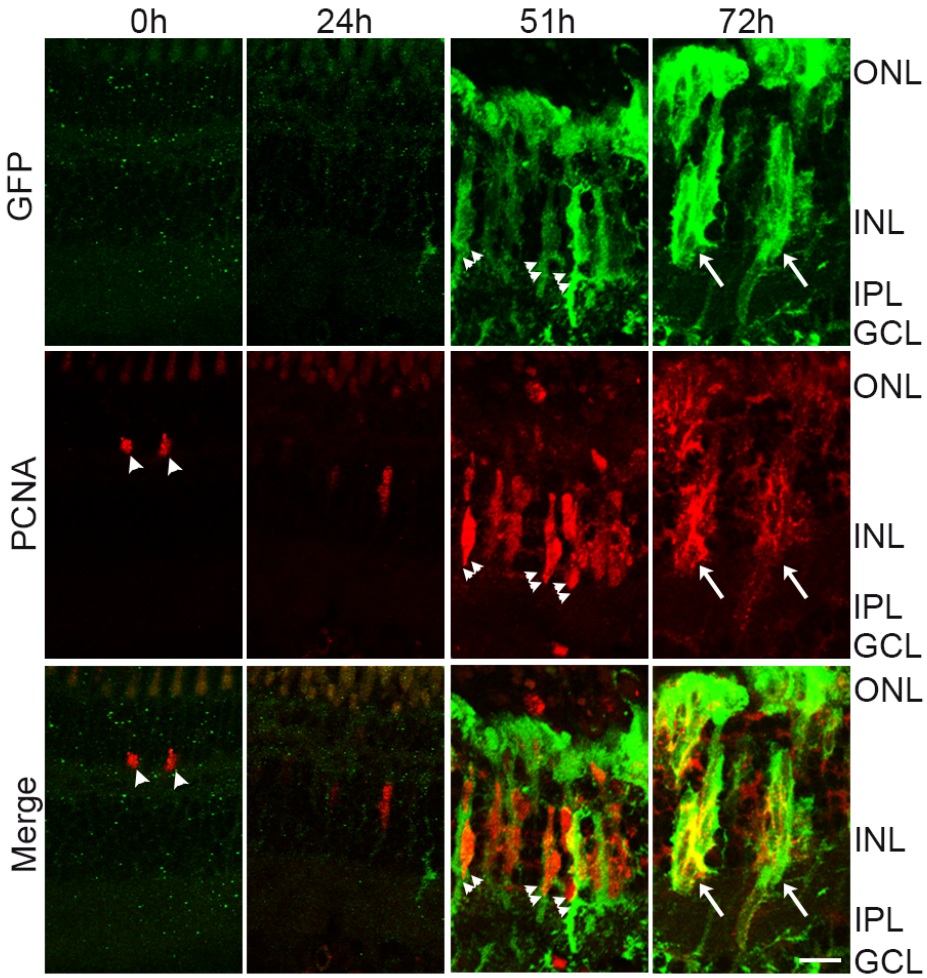

Figure 23. Proliferating progenitor cells express tuba1a:GFP transgene following light damage.

tg:1016tuba1a:GFP zebrafish were exposed to the constant intense light paradigm and retinas were collected at the indicated time points and assessed for GFP (green) and PCNA(red) expression by immunohistochemistry. Small clusters of $GFP^+/PCNA^+$ cells associate with MG processes at 51h (double arrowheads). Large clusters of $GFP^+/PCNA^+$ cells span in the INL at 72h (arrows). Arrowheads indicate rod precursors in the ONL. ONL, outer nuclear layer; INL, inner nuclear layer; GCL, ganglion cell layer; IPL, inner plexiform layer. Scale bar, 50 um.

Discussion

Here, we demonstrate that the constant intense light exposure model of lesioning retinal photoreceptors, which has been restricted to *albino* zebrafish, is also effective in lesioning pigmented retinas. Intense light exposure causes photoreceptor cell death within a day of exposure, prompts MG cell cycle re-entry, and induces progenitor cell production. The progenitor cells proliferate, form clusters associated with MG, and migrate to the ONL. Importantly, by performing simultaneous light lesioning we show that the timeline of initiation and progression of the regeneration response is identical in pigmented and *albino* fish.

There are two limitations to the extent of damage. First, photoreceptor apoptosis was extensive in the dorsal and central retinas, while damage was inconsistent and sparse in the ventral retina. However, this is also seen in *albino* zebrafish and rodents (Rapp and Williams, 1980; Vihtelic et al., 2006). Although the exact causes for the regional difference remain unknown, possible explanations could be presence of the retinal tapetum in the dorsal retina or the shorter rod outer segments found in the ventral retina. Ventral rod photoreceptors contain lesser amounts of rhodopsin, which limits constant intense light induced damage (Thomas et al., 2012). Second, quantification revealed an early delay in the initiation of ONL apoptosis, though by 35h apoptosis looks identical to *albino* retinas (Figure 19C). In our analyses, we detected almost complete loss of rods and a large number of double cones by 3 days of light exposure (Figure 17). It is possible that intense light does not completely destroy other cone types in the pigmented retina, or has a delayed effect on these cells. This, however, seems unlikely since others have reported that red-green double cones appear to be less susceptible to light induced

damage than uv and blue cones (Weber et al., 2013). Probing uv-cones and blue cones using specific antibodies will be important to address this issue. Melanin in the RPE of pigmented retinas also absorbs light, thus accounting for the delay in the onset of photoreceptor apoptosis compared to *albino* retinas. Reduced or delayed light induced photoreceptor damage has been observed in fish and rats with pigmented retinas (Rapp and Williams, 1980; Weber et al., 2013) (Noell et al., 1966). *Albino* retinas lack melanin, which allows for light to be scattered back to the photoreceptors, allowing more photoreceptor damage.

Regardless of these limitations, the extent of photoreceptor damage is sufficient to trigger a robust regeneration response in the dorsal-central retina of pigmented fish. By 51h in light, ~85% of $GFAP^+$ MG in the dorsal-central retina expressed PCNA and/or associated with $PCNA^+$ progenitor cells (Figure 21) and ~80% of GS^+ MG had dedifferentiated and expressed the tuba1a:GFP transgene (Figure 22). Additionally, progenitor cell proliferation and migration was identical to *albino* retinas (Figure 20), although it will be interesting to see if regeneration is completed at comparable times. Intriguingly, we detected tuba1a:GFP activation across most of the ventral retinas that we examined, although photoreceptor damage was sporadic in this region. Nevertheless, we rarely detected a proliferation response in the ventral retina. It is possible that extensive damage in the dorsal-central retina triggers MG dedifferentiation in ventral regions through a secreted or diffusible factor (Nelson et al., 2013; Wan et al., 2012). In the puncture model of retina damage, 4-6 'poke' lesions across the retina are sufficient to trigger MG dedifferentiation and proliferation response across the entire retina (Fausett

and Goldman, 2006; Ramachandran et al., 2010). In our model, damage of the dorsal-central retina is not sufficient to trigger a proliferation response in the ventral retina.

Though constant intense light exposure can lesion pigmented zebrafish retinas, the regional differences in damage admittedly limit some experimental procedures. Examination of specific retinal regions using immunohistochemistry or *in-situ* hybridization should be reliable whereas retina-wide gene, transcriptome or protein profiling might be challenging. Nevertheless, this study demonstrates that both normally pigmented and *albino* zebrafish can be damaged using the constant intense light paradigm and the timing of initiation and progression of regeneration is identical irrespective of the pigmentation status of the zebrafish used. In addition to expanding the tools available to study molecular mechanisms underlying photoreceptor regeneration, this study allows direct comparisons of regeneration between different zebrafish lines.

Acknowledgements

We thank D. Hyde (University of Notre Dame) and D. Goldman (University of Michigan) for sharing zebrafish lines. We thank Qiang Guan for excellent zebrafish care at the Vanderbilt University Stevenson Center Fish Facility. This study was supported by a grant from the National Eye Institute–National Institutes of Health to J.G.P (R21 EY 019759). K.R. was supported in part by the Vanderbilt International Scholar Program and by the Gisela Mosig Fund in the Department of Biological Sciences.

Conflict of Interests

The authors declare no financial or other conflicts of interests.

CHAPTER IV

miR-203 REGULATES PROGENITOR CELL PROLIFERATION DURING ADULT ZEBRAFISH RETINA REGENERATION[1]

Kamya Rajaram[a], Rachel Harding[b], David R. Hyde[b] and James G. Patton[a, 2]

[a]Department of Biological Sciences, Vanderbilt University, Nashville, TN, USA

[b]Department of Biological Sciences, University of Notre Dame, Notre Dame, IN, USA

---

[1] This work has been published online. Rajaram, K., Harding, R.L., Hyde, D.R., Patton, J.G. (2014). "*miR-203* regulates progenitor cell proliferation during adult zebrafish retina regeneration." Developmental Biology, 10.1016/j.ydbio.2014.05.005

[2] KR and JGP conceived and designed the experiments. KR and RLH performed the experiments. KR and JGP analyzed the data. KR, DRH and JGP wrote the paper.

Abstract

Damage of the zebrafish retina triggers a spontaneous regeneration response that is initiated by Müller Glia (MG) dedifferentiation and asymmetric cell division to produce multipotent progenitor cells. Subsequent expansion of the progenitor pool by proliferation is critical for retina regeneration. Pax6b expression in the progenitor cells is necessary for their proliferation, but exact regulation of its expression is unclear. Here, we show that *miR-203* is downregulated during regeneration in proliferating progenitor cells. Elevated *miR-203* levels inhibit progenitor cell expansion without affecting MG dedifferentiation or progenitor cell generation. Using GFP-reporter assays and gain and loss of function experiments in the retina, we show that *miR-203* expression must be suppressed to allow *pax6b* expression and subsequent progenitor cell proliferation.

Key words: *miR-203*, progenitor cell proliferation, *pax6b*, retina regeneration

Introduction

Retinal cell loss is the cause of many degenerative human diseases, including retinitis pigmentosa and age-related macular degeneration. In humans as well as other mammals, retinal cell loss is irreversible and ultimately leads to blindness. This is in stark contrast to the zebrafish retina, where damage by a variety of methods triggers a spontaneous regeneration response that restores not only lost retinal cell types, but also retina function (Fausett and Goldman, 2006; Vihtelic and Hyde, 2000; Yurco and Cameron, 2005). Intriguingly, Müller glia (MG), the cell type that initiates retina regeneration, are not specific to the zebrafish retina, but are common to all vertebrates (Lamba et al., 2008). However, mammalian MG normally respond to injury by undergoing reactive gliosis, which leads to scarring (Bringmann et al., 2009). Treatment of explants with transcription factors and select growth factors can induce mammalian MG to mount a regeneration response but the response is extremely limited (Karl et al., 2008; Ooto et al., 2004; Pollak et al., 2013). Understanding the mechanisms controlling retina regeneration in the zebrafish is a starting point to design strategies to trigger regeneration in the mammalian retina.

Recently, a number of genes and signaling pathways that control important steps in zebrafish retina regeneration have been identified. Ascl1a and Lin-28 activate MG dedifferentiation and cell cycle reentry (Ramachandran et al., 2010), while Pax6a and Pax6b are essential for proliferation of MG-derived progenitor cells (Thummel et al., 2010). Precise regulation of these genes is central to ensure efficient regeneration. miRNAs regulate gene expression by binding to recognition sites in the 3' untranslated regions (UTRs) of target mRNAs triggering both mRNA decay and repression of

translation (Kloosterman and Plasterk, 2006). Distinct subsets of miRNAs have been shown to regulate proliferation, maintenance of pluripotency, cell specification, and differentiation (Melton et al., 2010; Wang et al., 2008). miRNAs have also been implicated in regulating regeneration in a number of species (Sehm et al., 2009). In zebrafish, miRNAs regulate regeneration of a variety of tissues including the fin, heart, spinal cord and retina (Park et al., 2011; Ramachandran et al., 2010; Thatcher et al., 2008; Yin et al., 2012; Yin et al., 2008). In this study, RNA sequencing and analysis of specific cell types during zebrafish retina regeneration revealed that *miR-203* expression must be downregulated during retina regeneration to enable proliferation of MG-derived progenitor cells. Downregulation of *miR-203* allows upregulation of *pax6b,* which is required for increased progenitor cell proliferation and the formation of clusters of replicating progenitor cells associated with dedifferentiated MG. Our results demonstrate for the first time that miRNAs play a key role in the zebrafish retinal regeneration response after MG dedifferentiation and during the proliferation of MG-derived progenitor cells.

Materials and Methods

Fish maintenance

Zebrafish were maintained in 14h light and 10h dark cycles at 28.5°C. *Albino* fish were received from David Hyde (University of Notre Dame), *tg:1016tuba1a:gfp* were received from Daniel Goldman (University of Michigan) (Fausett and Goldman, 2006). Other fish lines used were *tg:gfap:gfp* (Bernardos and Raymond, 2006) and wild type AB. Embryos for microinjections were obtained from matings of AB fish. All experiments were

performed with the approval of the Vanderbilt University Institutional Animal Care and Use Committee (Protocol # M/09/398).

Adult zebrafish light lesioning

Constant instense light lesioning was performed as previously described (Vihtelic and Hyde, 2000). Briefly, adult fish were dark adapted for 14 days, transferred to clear tanks placed between two fluorescent lights with light intensity at ~20,000 lux and the temperature maintained at 30-33°C. Zebrafish were subjected to light lesioning from 16h–3 days.

RNA isolation, RT-PCR, Taqman realtime PCR

Total RNA was isolated from control and light damaged zebrafish retinas using TRI Reagent®. For semi quantitative PCR, oligo-dT primers (Life Technologies) were used to synthesize cDNA using MMLV reverse transcriptase (Promega). PCR was performed using Phusion DNA polymerase (NEB) on a MyCycler thermal cycler (Biorad). GAPDH was used as a loading control. For quantitative real time PCR (qPCR), RNA was DNase treated (Rapid Out, Thermo Scientific), converted to cDNA using Maxima first strand cDNA synthesis kit (Thermo Scientific) and qPCR was performed using SYBR Green (Biorad). All qPCR primers spanned exon-exon junctions (IDT). miRNA realtime PCR was perfomed using Taqman probes as per the manufacturer's instructions (Life Technologies). Relative RNA expression during regeneration was determined using the ΔΔCt method and normalized to 18s rRNA levels and U6 snRNA levels for mRNAs and miRNAs respectively. Real time PCR was performed on a Biorad CFX 96 Real time system. Primer sequences are listed in Table 2.

Table 2. Primer sequences used in the *miR-203* study.

Primer Name	Sequence (5'- 3')
qpcr-fp-pax6b	tccgggaatttccttccaga
qpcr-rp-pax6b	cgtgggttggttatggtattcttt
qpcr-fp-ascl1a	tgagcgttcgtaaaaggaaact
qpcr-rp-ascl1a	cgtggtttgccggtttgtat
qpcr-fp-gs	ttctgttggtgtcaaggtgtt
qpcr-rp-gs	ctccctgaggcagttccata
qpcr-fp-18s	acgcgagatggagcaataac
qpcr-rp-18s	cctcgttgatgggaaacagt
rtpcr-fp-pax6b	atggccacttctggcaccgcttccacaggac
rtpcr-rp-pax6b	agttctgggagtgtgaaaagagctcgcgcctc
rtpcr-fp-ascl1a	atccgcgcgctgcagcaacttc
rtpcr-rp-ascl1a	cgagtgctgatatttttaagtt
rtpcr-fp-gapdh	attgatggtcatgcaatcacag
rtpcr-rp-gapdh	cattgatgacctttgccaaag

Morpholino and miRNA injection and electroporation

Lissamine tagged morpholinos (MOs) (Gene Tools) were injected and electroporated into adult zebrafish eyes prior to light lesioning as described (Thummel et al., 2008b). The following 3'-Lissamine-tagged MOs were used:

Gene Tools standard control MO: 5'-CCTCTTACCTCAGTTACAATTTATA-3'

pax6b MO: 5'-CTGAGCCCTTCCGAGCAAAACAGTG-3'

miR-203a MO: 5'-CAAGTGGTCCTAAACATTTCAC-3'

Duplex mature miRNAs (Thermo scientific) were injected and electroporated into eyes either prior to start of light lesioning (Figure 2, 3, 5), or 51h after light lesioning (Figure

4) using the same procedure as the MOs but with reversed electrode polarity. For initial experiments, we used RNAs that contained a Dy-547 fluorescent tag at the 3' end. Double stranded mature miRNAs were synthesized with 3'- UU overhangs for the following target sequences:

miR-203: 5'-GUGAAAUGUUUAGGACCACUUG-3'

control: 5'-AAAAACAUGCAGAAAAUGCUG-3'

Electroporation was performed using the Gene Pulser Xcell™ Electroporation Systems (Biorad).

Immunohistochemistry, BrdU labeling, TUNEL assay and in situ hybridization

Adult zebrafish eyes were collected and fixed in 4% paraformaldehyde for 2-5h at room temperature. Following fixation, eyes were cryoprotected overnight in 30% sucrose/1X PBS at 4°C, before embedding in Shandon cryomatrix (Thermo Scientific) for sectioning. Embedded samples were kept at -80°C until sectioning. 10-12 micron sections were obtained using a cryostat (Leica), collected on charged Histobond slides (VWR), dried and stored at -80°C until used. For immunohistochemistry (IHC), slides were thawed for 30 min on a slide warmer, rehydrated in 1X PBS and blocked (3% Donkey serum, 0.1% TritonX-100 in 1X PBS) for 1-2h at room temperature before incubating with primary antibodies overnight at 4°C. Primary antibodies were mouse anti-PCNA monoclonal antibody (1:500, Sigma), mouse anti-glutamine synthetase monoclonal antibody-clone GS8 (1:200, Millipore), rat anti-BrdU monoclonal antibody (1:500, Abcam), rabbit anti-GFP polyclonal antiserum (1:1000, Torrey Pines Biolabs) and mouse anti-β-catenin antibody (1:500, BD Bioscience). After primary antibody incubation, sections were washed 3 times in 1X PBS/0.1% Tween-20 for 10 min each followed by 1-2h incubation

in secondary antibody and nuclear stain TOPRO 3 (1:1000, Invitrogen) at room temperature. Secondary antibodies were donkey anti-mouse AF488 (1:200), donkey anti-mouse AF647 (1:200), donkey anti-rat Cy3 (1:100) and donkey anti-rabbit AF488 (1:200)(Jackson Immuno). Slides were washed in 1X PBS/0.1% Tween-20, 3 times for 10 mins, followed by a 5 min PBS wash before drying and coverslipping with Vectashield (Vector labs). Nuclear β-catenin was detected following citrate buffer antigen retrieval, as previously described (Ramachandran et al., 2011). For PCNA IHC, slides were boiled in 10mM sodium citrate buffer containing 0.05% Tween-20 (pH 6) for 20 mins, cooled at room temperature for 20 min and then quickly washed in 1X PBS prior to blocking. After IHC, slides were examined using an LSM 510 Meta inverted confocal microscope (Zeiss). For BrdU labeling, adult fish received a 25ul (20mM) IP injection of BrdU (Sigma) 3h prior to sacrifice. For BrdU IHC, sections were pretreated with 2N HCl for 20 min at 37°C and then quenched in 100mM sodium borate 2 times for 5 min each. For TUNEL assays, sections were processed as for IHC. TUNEL assays were performed using the TMR red *in situ* cell death detection kit (Roche). Digoxigenin labeled LNA probes (Exiqon) were used for *miR-203 in situ* hybridizations. A final probe concentration of 500nM and hybridization temperature of 42°C was used. Hybridization and wash conditions were previously described (Ramachandran et al., 2010). Slides were examined using a Leica DM6000B microscope.

Western blots

Protein lysates from 1dpf embryos were prepared as described previously (Flynt et al., 2007). Briefly, 1dpf embryos were dechorionated, deyolked and sonicated in lysis buffer supplemented with PMSF. For adult retinas, dorsal retinas were dissected from 7 fish per

treatment group and sonicated in lysis buffer. Insoluble debris was removed by centrifugation and 20ug and 40ug of protein was separated on 12% polyacrylamide gels, for embryo lysates and adult retina lysates respectively. Proteins were transferred to PVDF membranes and probed with antibodies against GFP (1:1000, Torrey Pines), Pax6 (1:4000, Covance), Actin (1:100, Santa Cruz) and α-tubulin (1:1000, Abcam). For visualization, HRP-conjugated secondary antibodies (1:5000, GE Healthcare) were used followed by detection with ECL (Perkin Elmer). Imaging was performed on an LAS4000 Chemiluminescent CCD Imager (GE Healthcare) and blots were quantified using LAS4000 ImageQuant software (GE healthcare). GFP levels were normalized to α-tubulin levels and the GFP/tubulin ratio was determined for different injection conditions. Actin served as loading control for Pax6 Western blots.

Fluorescence activated cell sorting (FACS)

FACS was used to purify GFP^+ cells from the retinas of undamaged *tg:gfap:gfp* fish and *tg:1016tuba1a:gfp* fish that were exposed to 72h of light damage following a procedure adapted from Qin et al. (Qin and Raymond, 2012). Briefly, retinas were pooled from 15 undamaged *tg:gfap:gfp* fish and 20, 72h light treated *tg:1016tuba1a:gfp* fish. Dissected retinas were treated with activated papain/dispase (Worthington) and incubated at 28°C for 30 min on a nutator for dissociation. Dissociated cells were pelleted by centrifugation, resuspended in DNaseI solution (Sigma) and gently tapped to complete tissue dissociation. Cells were triturated briefly, filtered through 35-micron filters and then sorted **using** BD FACSAria III (BD Biosciences). Approximately 27,000 GFP^+ cells were obtained from 15 undamaged *tg:gfap:gfp* fish and 28,000 GFP^+ cells were obtained from 20 light-damaged *tg:1016tuba1a:gfp* fish. As quality control for FACS, qPCR was

used to confirm MG specific glutamine synthetase and progenitor cell specific *ascl1a* expression (Figure 25). FACS was performed in the VUMC Flow Cytometry Shared Resource.

Molecular cloning and embryo microinjections

The *pax6b* 3'UTR was amplified from cDNA by PCR with the following primers:

pax6b-3'utr-fp: 5'-ACTAGTAAGGAACAACAGCCATTGTG-3'

pax6b-3'utr-rp: 5' CTGTCTTGCAGATATTTCAATTTAACCTCGAG-3'

The 3' UTR was cloned into the $pCS2^{+}$ plasmid downstream of the GFP coding sequence. Capped RNA was transcribed from these reporter constructs using SP6 mMessage mMachine (Life Technologies). Zebrafish embryos at the single-cell stage were injected with 50pg of mRNA with or without 100pg of synthetic duplex *miR-203a* (Thermo Scientific). Titrations were performed to determine the lowest effective injection concentrations.

Cell counts and statistical analyses

For confocal microscopy, only retina sections that comprised optic nerves were used. All cell counts were done in the central-dorsal retina, at a linear distance of ~300 microns from the optic nerve. 3-8 retinas were used in every experiment. In Figures 29, 31 and 33, progenitor clusters were defined as groups of more than 3 closely adherent $PCNA^{+}$ cells. In Figures 27, 28, 29, 31 and 33O-P data are represented as mean +/- standard error of the mean (s.e.m) and significance was calculated using the non-parametric Mann-Whitney U test. Student-t tests were used to calculate significance for qPCR data and Western blots.

Results

miR-203 is downregulated in proliferating progenitor cells during retina regeneration

To identify differentially expressed miRNAs during regeneration of the light-damaged zebrafish retina, we performed a high-throughput sequencing screen. We identified 35 miRNAs that showed altered expression during regeneration (Harding, R., Rajaram, K., Bailey, T.J., Hyde, D.R., and Patton, J.G., manuscript in preparation). Among these, the *miR-203* family was found to be downregulated (Figure 24A), a finding that intrigued us because we previously showed that *miR-203* downregulation is necessary for zebrafish caudal fin regeneration (Thatcher et al., 2008). Similarly, *miR-203* is downregulated in proliferating progenitor cells during mouse skin development and regeneration (Lena et al., 2008; Viticchie et al., 2012; Yi et al., 2008). To determine the role of *miR-203* in retina regeneration, we examined its spatial expression pattern in undamaged and regenerating retinas using *in situ* hybridization with an LNA probe targeting mature *miR-203* (Figure 24B, C). Sections from undamaged retinas showed *miR-203* expression in the Ganglion Cell Layer (GCL), most of the Inner Nuclear Layer (INL) and the photoreceptor outer segments; with slightly lower expression in the Outer Nuclear Layer (ONL) (Figure 24B). In contrast, *miR-203* expression was markedly reduced in light-damaged retinas that were actively regenerating (Figure 24C). The reduction was most striking in the INL, whereas the relative *miR-203* levels in the GCL were overall similar or only slightly reduced between damaged and undamaged retinas.

Following light-induced injury, Müller glia respond by dedifferentiating and undergoing a single asymmetric division to produce progenitor cells that then continue to divide (Nagashima et al., 2013). As regeneration proceeds, clusters of proliferating

progenitor cells occupy the INL along the processes of dedifferentiated MG (Fausett and Goldman, 2006; Nagashima et al., 2013; Thummel et al., 2008a). We sought to determine whether *miR-203* levels are reduced in proliferating progenitor cells. To test this, we used fluorescence activated cell sorting (FACS) to isolate specific retinal cell types from two different transgenic lines: one expressing GFP in post-mitotic MG from undamaged retinas (*tg:gfap:gfp)* (Bernardos and Raymond, 2006), and the other expressing GFP in dedifferentiated MG and proliferating progenitor cells from actively regenerating retinas (*tg:1016tuba1a:gfp*) (Fausett and Goldman, 2006) (Figure 25). Quantitative real-time PCR (qPCR) for *miR-203* in these FACS-purified cell types revealed a ~70% reduction in *miR-203* expression levels in proliferating progenitor cells relative to undamaged MG (Figure 24D). Together, these experiments indicate that *miR-203* expression is downregulated in proliferating progenitor cells in the regenerating retina.

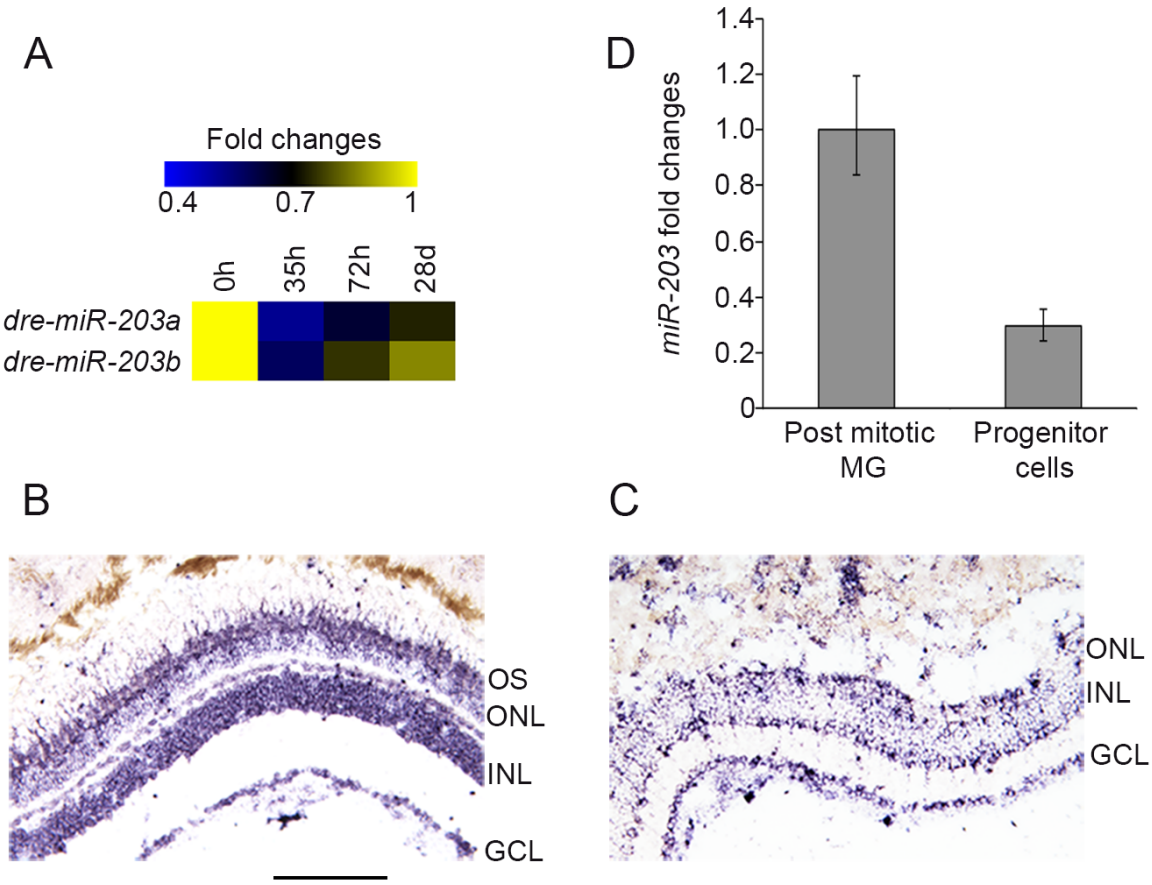

Figure 24. *miR-203* is downregulated in proliferating progenitor cells during retina regeneration.

(A) Heat map showing fold changes in deep sequencing reads for *miR-203a* and *b* during retina regeneration. Fold changes relative to 0h read number are shown. (B-C) LNA *in situ* hybridization for *miR-203*. Sections from undamaged retinas show strong *miR-203* signals in the INL, GCL and photoreceptor outer segments (B). Staining is reduced in the INL of light damaged retinas (60h), but persists in the GCL (C). (D) qPCR for *miR-203* in FACS purified post mitotic Müller glia (MG) and dedifferentiated MG-derived progenitor cells from 72h light treated fish. Data represent mean +/- s.e.m from 15 undamaged fish and progenitor cells were purified from 20 light damaged fish. OS, outer segments; ONL, outer nuclear layer; INL, inner nuclear layer; GCL, ganglion cell layer. Scale bar 100um

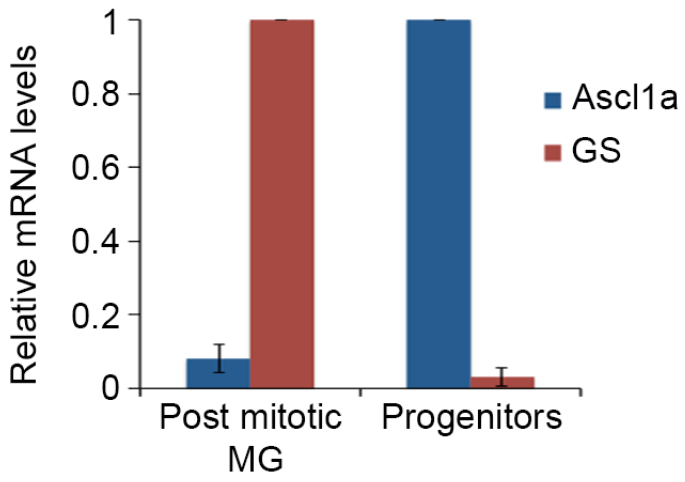

Figure 25. Verification of FACS.

FACS isolated post-mitotic MG and proliferating progenitor cells were analyzed by qPCR. Relative mRNA levels of MG-specific glutamine synthetase (GS) and progenitor cell-specific Ascl1a are shown. Data represent mean +/- s.e.m. (n=3 independent FACS).

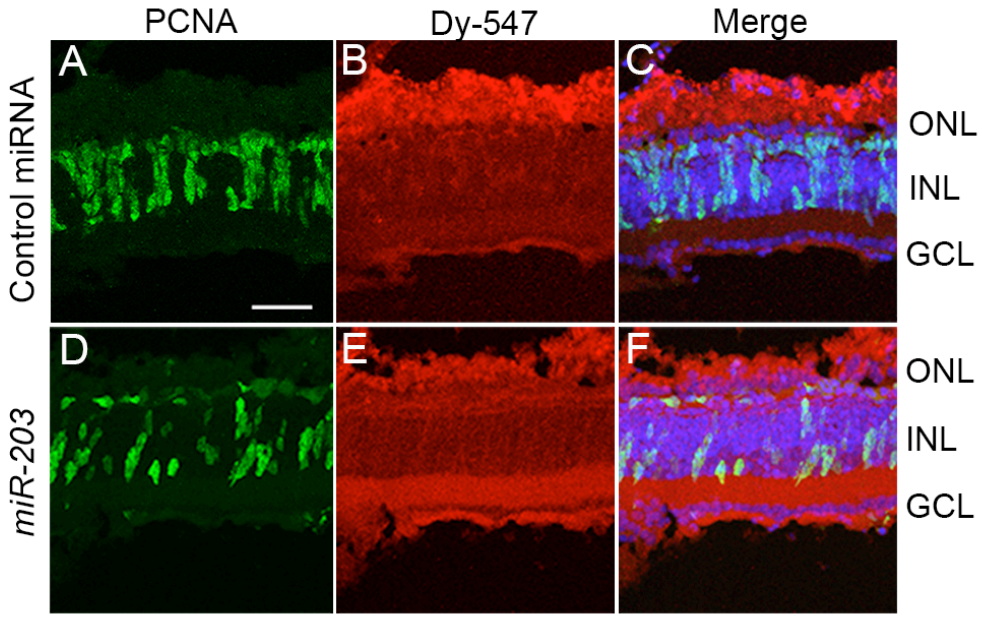

Figure 26. miRNA gain-of-function.

Albino fish retinas were injected and electroporated with Dy-547 tagged control miRNA (A-C) or *miR-203* (D-F) prior to the start of light exposure (0h). After 72h, retinas were assessed for PCNA expression (green) and Dy-547 fluorescent tag localization (red). Nuclei were counterstained with TOPRO (blue). ONL, outer nuclear layer; INL, inner nuclear layer; GCL, ganglion cell layer. Scale bar 50um.

miR-203 overexpression affects proliferation during regeneration.

Next, we examined if downregulation of *miR-203* was necessary for retina regeneration. We performed gain-of-function studies (Figure 26) by experimentally increasing the levels of *miR-203* or a control miRNA prior to the onset of light damage. In our hands, 51h of light exposure in *albino* fish corresponds to the peak of dedifferentiated MG cell cycle reentry and the generation of progenitor cells, while 72h of light exposure corresponds to progenitor cell proliferation in the regenerating retina (unpublished). Thus, we overexpressed *miR-203* or a control miRNA in dark-adapted *albino* fish retinas prior to the start of intense light damage (0h light exposure) and then assessed their effects on PCNA expression at 51h and 72h (Figure 27A). Compared to the control, *miR-203* overexpression resulted in a significant decrease ($p<0.001$; $n=8$) in the number of $PCNA^+$ proliferating progenitor cells at 72h, but not at 51h (Figure 27B,C). Additionally, ONL rod progenitor proliferation was unaffected by *miR-203* gain-of-function (Figure 27D). These data suggested that *miR-203* overexpression affects progenitor cell proliferation but not MG proliferation. To verify this, we injected zebrafish that were overexpressing either control miRNA or *miR-203* with BrdU to specifically label proliferating cells at 51h. We labeled MG processes using an antibody against glutamine synthetase (GS). Immunohistochemistry revealed GS^+ MG incorporating BrdU (Figure 28A, arrows). *miR-203* gain-of-function did not affect MG proliferation (Figure 28B) or rod progenitor proliferation (Figure 28A, arrowheads; Figure 28C). Taken together, these data indicate *miR-203* overexpression does not delay MG cell dedifferentiation or proliferation during retina regeneration, but specifically affects progenitor cell proliferation.

To test if suppression of *miR-203* was sufficient to trigger retina regeneration, we injected and electroporated either control morpholinos (MOs) or MOs targeting mature *miR-203* into undamaged *1016tuba1a:gfp* transgenic fish eyes. This transgenic line specifically expresses GFP in dedifferentiated MG and progenitor cells. Compared to control MO treatment, loss of *miR-203* did not cause significant changes in MG dedifferentiation or overall retinal proliferation (data not shown). Based on these results, we hypothesize that *miR-203* downregulation is necessary for progenitor cell proliferation, but is not sufficient for initiation of MG dedifferentiation or for progenitor cell generation.

Figure 27. *miR-203* overexpression affects proliferation during regeneration.

(A) Experimental scheme. (B) Control miRNA or *miR-203* was injected and electroporated into the left eyes of *albino* zebrafish before intense light exposure. Retinas were collected after 51h and 72h of light exposure, sectioned and immunostained using an antibody against PCNA (green). Nuclei were counterstained with TOPRO (blue). (C) Quantification of INL $PCNA^+$ cells. (D) Quantification of ONL $PCNA^+$ cells at 51h. Data represent mean +/- s.e.m (n= 8 fish); *, $p< 0.001$ by Mann-Whitney U test. ONL, outer nuclear layer; INL, inner nuclear layer; GCL, ganglion cell layer. Scale bar 50um.

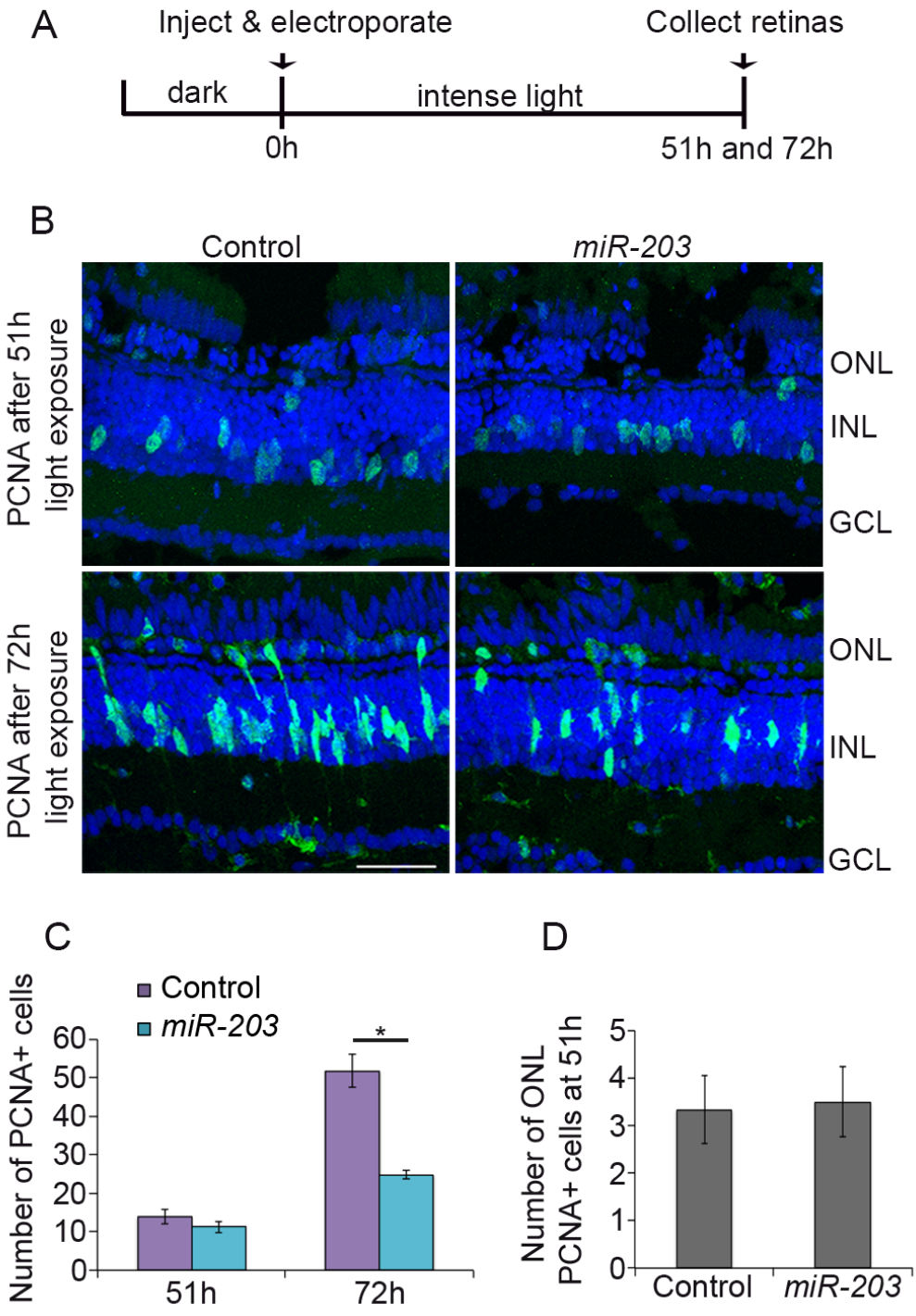
A
Inject & electroporate
Collect retinas
dark
intense light
0h
51h and 72h
B
Control
miR-203
PCNA after 51h light exposure
PCNA after 72h light exposure
ONL
INL
GCL
ONL
INL
GCL
C
Control
miR-203
Number of PCNA+ cells
60
50
40
30
20
10
0
*
51h
72h
D
Number of ONL PCNA+ cells at 51h
5
4
3
2
1
0
Control
miR-203

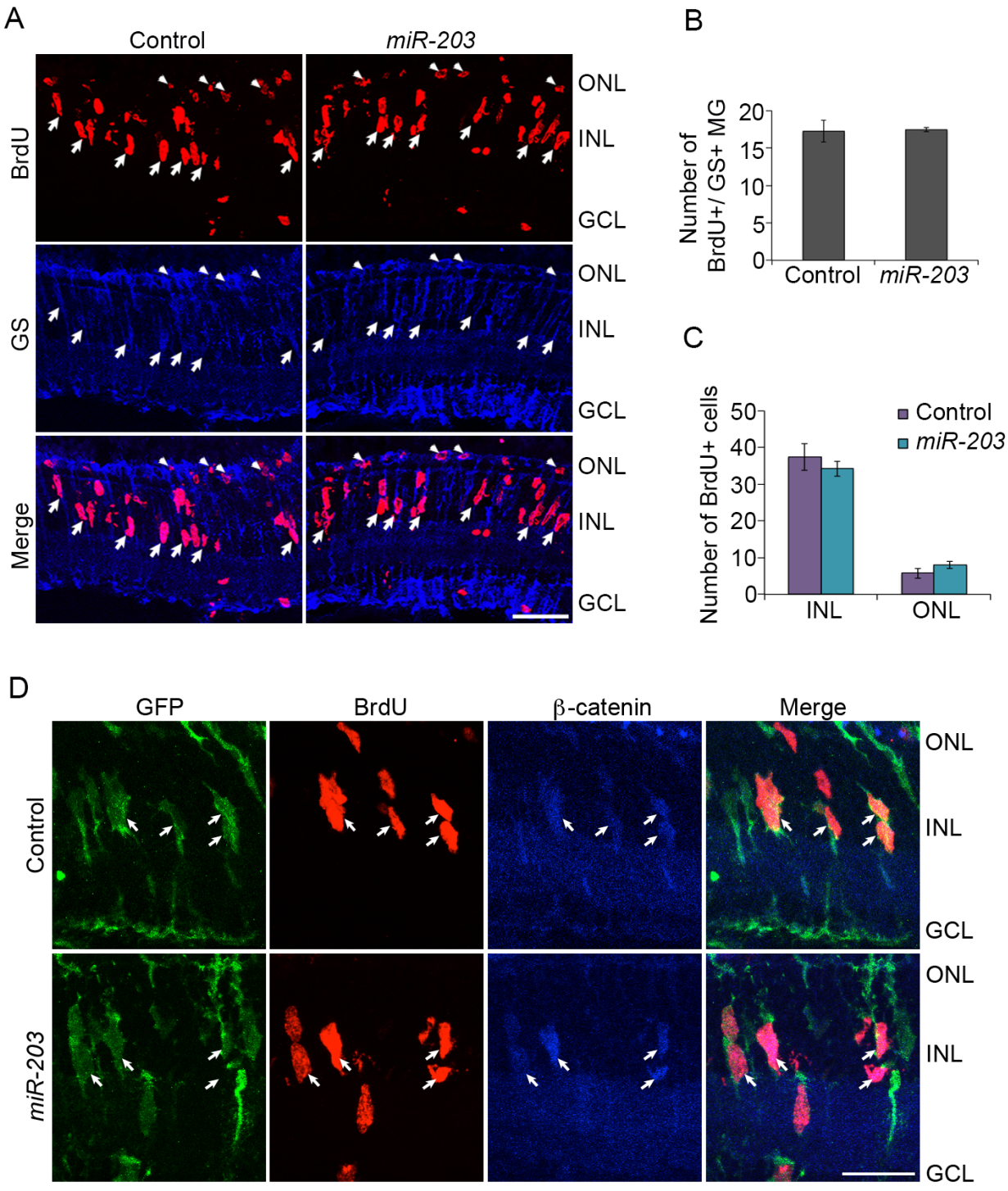

Figure 28. *miR-203* gain-of-function does not affect MG dedifferentiation or proliferation.

Control miRNA or *miR-203* was injected and electroporated into the left eyes of *albino* (A) or *tg:1016tuba1a:gfp* (D) zebrafish before intense light exposure. BrdU was injected intraperitoneally after 48h of light exposure and retinas were collected at 51h of light exposure, sectioned and immunostained with antibodies against BrdU and GS in (A) and BrdU, GFP and β-catenin in (D). In (A), $BrdU^+$ nuclei (red) colabel with MG specific anti-glutamine synthetase (GS; blue) antibody (arrows). ONL rod precursors also incorporate BrdU (arrowheads). (B) Quantification of $BrdU^+/GS^+$ MG. (C) Quantification of total $BrdU^+$ cells in INL and ONL. Data represent mean +/- s.e.m (n= 4 fish). No statistical significance was detected using Mann-Whitney U test. In (D), $BrdU^+$ nuclei (red; arrows) colabel with β-catenin (blue) and GFP (green). ONL, outer nuclear layer; INL, inner nuclear layer; GCL, ganglion cell layer. Scale bar 50um.

---

miR-203 inhibits progenitor cluster formation

To further test the hypothesis that progenitor cell proliferation and not progenitor cell generation is regulated by *miR-203*, we utilized the *1016tuba1a:gfp* transgenic line that specifically expresses GFP in dedifferentiated MG and progenitor cells. Constant intense light exposure elicited a regeneration response in these fish that followed a timeline consistent with that observed in *albino* zebrafish (unpublished). Overexpression of *miR-203* in these fish did not alter *tuba1a:GFP* transgene expression or BrdU incorporation at 51h (Figure 28D). We also detected β-catenin accumulation in GFP^+/ $BrdU^+$ MG in both control and *miR-203* overexpressing retinas (Figure 28D, arrows). β-catenin stabilization is required for MG proliferation and progenitor cell generation (Ramachandran et al., 2011). Thus MG proliferation and progenitor cell generation is unperturbed by *miR-203* gain-of-function.

In contrast, *miR-203* overexpression resulted in a significant reduction in the total number of $PCNA^+$ progenitor cells at 72h ($p<0.03$; *n=4*) (Figure 29C, G, J). We also observed a striking reduction in the number of dedifferentiated MG associated with clusters of at least four $PCNA^+$ progenitor cells ($p< 0.03$; *n=4;* Figure 29K; arrows in

Figure 29B-I; nuclei in higher magnification Figure 29C', G'). With increased *miR-203*, we found that most dedifferentiated MG were associated with only 1-3 $PCNA^{+}$ progenitor cells (arrowheads in Figure 29F-I; nuclei in higher magnification Figure 29 G''). These data are consistent with the hypothesis that *miR-203* inhibits progenitor cell proliferation and the formation of large progenitor clusters. TUNEL staining demonstrated that these effects were not simply due to toxicity associated with *miR-203* overexpression (Figure 30).

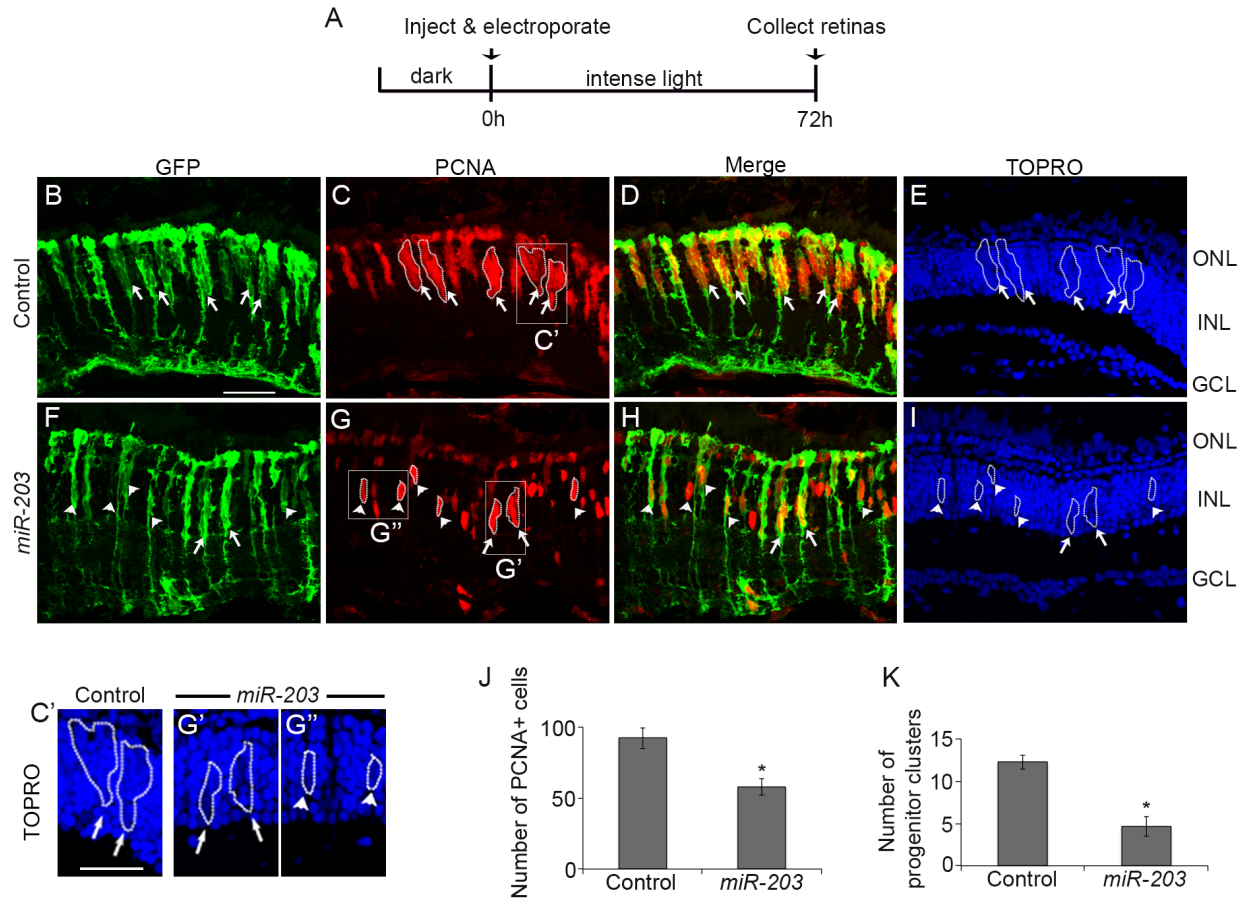

Figure 29. *miR-203* gain-of-function reduces the number of progenitor clusters.

(A) Experimental scheme. (B-I) Control miRNA or *miR-203* was injected and electroporated into the left eyes of *tg:1016tuba1a:gfp* fish prior to intense light exposure. Following 72h of light exposure, retinas were sectioned and stained with antibodies against GFP (green; panels B, F) and PCNA (red; panels C, G); nuclei are counterstained with TOPRO (blue; panels E, I). *1016tuba1a:gfp* transgene expression was unchanged after *miR-203* overexpression (B, F). In the control miRNA treated retinas, large clusters of $PCNA^+$ cells associated along the processes of dedifferentiated MG (arrows in B-E). *miR-203* overexpression reduced the number of dedifferentiated MG associated with large progenitor clusters (arrows in F-I) but increased the number of dedifferentiated MG associated with 1-3 $PCNA^+$ cells (arrowheads in F-I). (C' and G') Higher magnification view of the progenitor clusters boxed in C and G respectively. (G'') Higher magnification view of boxed progenitors in G. (J) Quantification of $PCNA^+$ cells. (K) Quantification of number of dedifferentiated MG associated with progenitor clusters. Data represent mean +/- s.e.m (n= 4 fish); *, $p< 0.03$ by Mann-Whitney U test. ONL, outer nuclear layer; INL, inner nuclear layer; GCL, ganglion cell layer. Scale bar (panels B-I) 50um; (panels C', G' and G'') 30um.

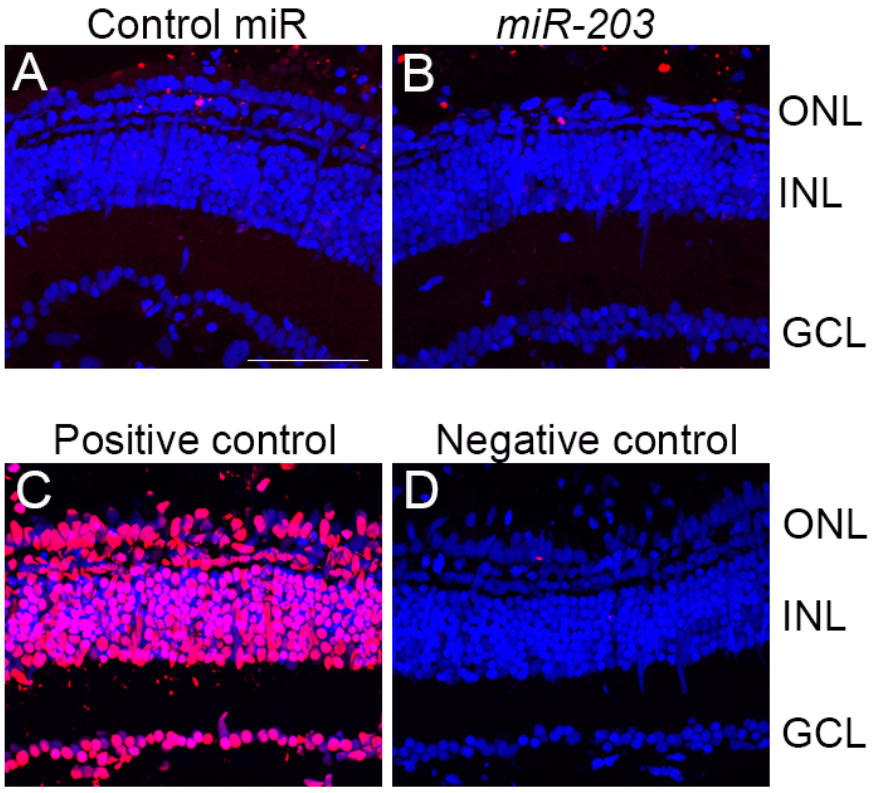

Figure 30. *miR-203* gain-of-function does not cause INL cell death.

TUNEL staining was performed on 72h light treated retina sections from control miRNA (A) or *miR-203* (B) gain-of-function. Some TUNEL^{+} nuclei (red) were detected in the ONL. DNaseI treated retinas were used as positive controls for the TUNEL assay and showed TUNEL^{+} nuclei in all retinal layers (C). No cell death was detected in the negative control retina sections, which were subjected to the TUNEL protocol in the absence of terminal transferase (D). ONL, outer nuclear layer; INL, inner nuclear layer; GCL, ganglion cell layer. Scale bar 50um.

Since MG dedifferentiation precedes progenitor cell proliferation during regeneration, we altered the timing of *miR-203* overexpression to more precisely define its role. Thus, we overexpressed *miR-203* at 51h, a time point after most MG have dedifferentiated and asymmetrically divided to generate progenitor cells (Figure 31A). Under these conditions, *miR-203* overexpression resulted in a significant reduction ($p<0.03$; *n=3-5* retinas; Figure 31C) in the number of $PCNA^+$ progenitor cells compared to control miRNA injections (Figure 31B). Large clusters (>3) of $PCNA^+$ progenitor cells with elongated cell bodies were almost undetectable in *miR-203* overexpressing retinas ($p<0.03$; *n=3-5*; Figure 31D; Figure 31B). Taken together, these results support the hypothesis that *miR-203* inhibits progenitor cell proliferation, and that downregulation of *miR-203* is necessary to generate large clusters of progenitor cells during retina regeneration.

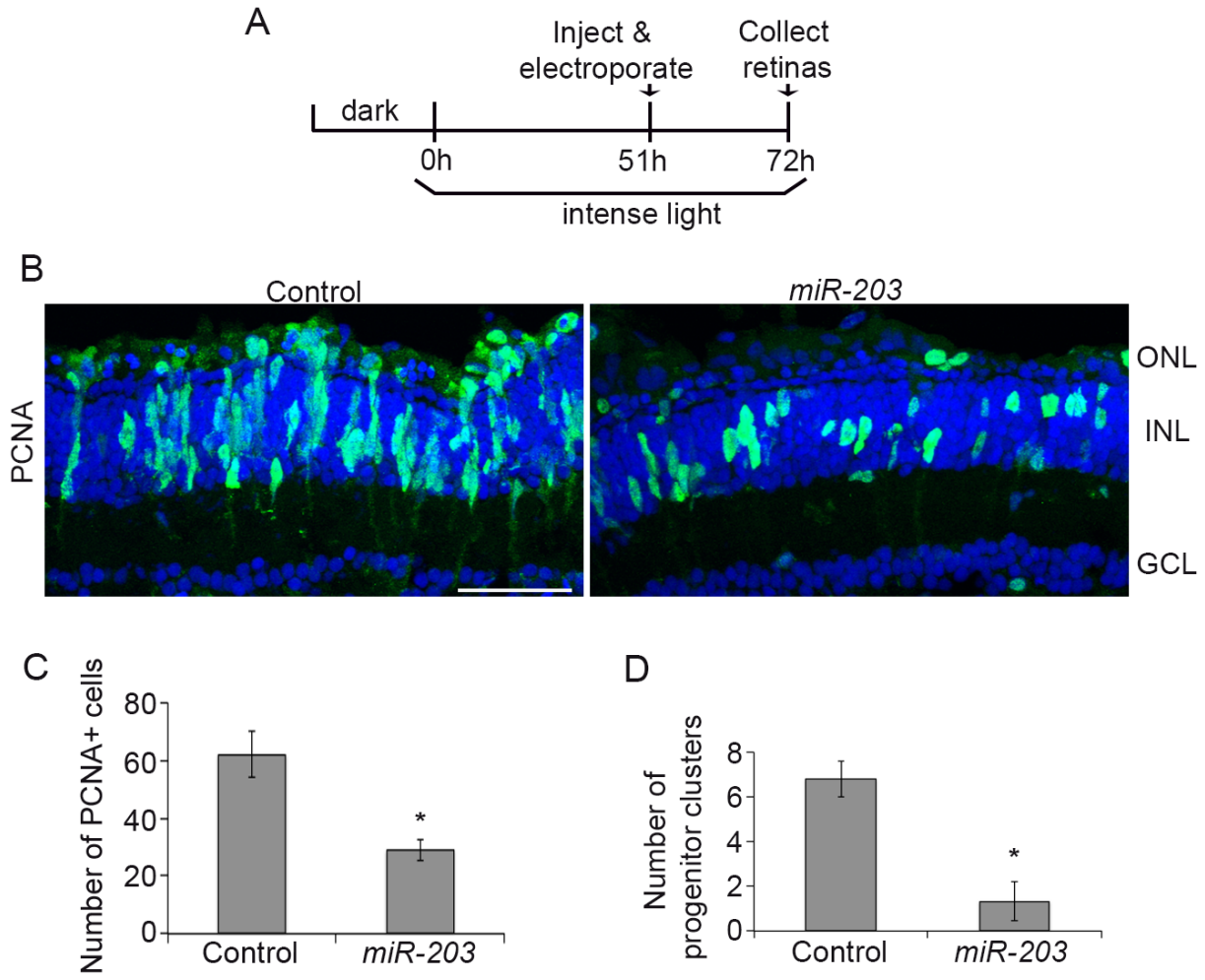

Figure 31. Excess *miR-203* during progenitor cell proliferation phase impairs progenitor cluster formation.

(A) Experimental scheme. (B) Control miRNA or *miR-203* was injected and electroporated into the left eyes of *albino* zebrafish after MG dedifferentiation and progenitor cell generation (51h of light). After 72h, retinas were collected, sectioned and immunostained with antibodies against PCNA (green). Nuclei were counterstained with TOPRO (blue). (C) Quantification of $PCNA^{+}$ cells. (D) Quantification of progenitor clusters. Data represent mean +/- s.e.m (n= 3-5 fish); *, $p< 0.03$ by Mann-Whitney U test. ONL, outer nuclear layer; INL, inner nuclear layer; GCL, ganglion cell layer. Scale bar 50um.

miR-203 regulates retina regeneration through pax6b

To determine what mRNA targets are regulated by *miR-203* during progenitor cell proliferation, we used target prediction algorithms including Targetscan (Lewis et al., 2005). Several potential *miR-203* targets were identified and tested for direct targeting (see Discussion; Table 3). Among these, *pax6b* emerged as a likely target (Figure 32B). Previous studies showed that Pax6b is expressed in proliferating progenitor cells during retina regeneration and is required for the formation of large clusters of progenitor cells (Thummel et al., 2008a). To determine if *miR-203* can directly regulate *pax6b*, we performed GFP reporter assays in zebrafish embryos (Flynt et al., 2007) (Figure 33A-C, Figure 32B). The 3'UTR of *pax6b* was cloned downstream of the GFP coding sequence and *in vitro* transcribed mRNAs from these reporter constructs were injected into single-cell stage zebrafish embryos in the presence or absence of exogenous *miR-203*. At 1dpf, co-injection with *miR-203* reduced GFP levels by ~40% relative to the control injections (Figure 33B,C) ($p<0.008$, n=3). Consistent with previous studies (Thummel et al., 2010; Thummel et al., 2008a) and consistent with our finding that *miR-203* levels decrease during regeneration, we detected upregulation of *pax6b* transcripts in RNA isolated from whole retinas during regeneration (Figure 33D and Figure 34). More precisely, we determined the levels of *pax6b* in FACS-purified cells and observed significant enrichment of *pax6b* mRNA in proliferating progenitor cells compared to post-mitotic MG from undamaged retinas ($p < 0.008$; n=3) (Figure 33E). These data are consistent with the hypothesis that *miR-203* regulates *pax6b*.

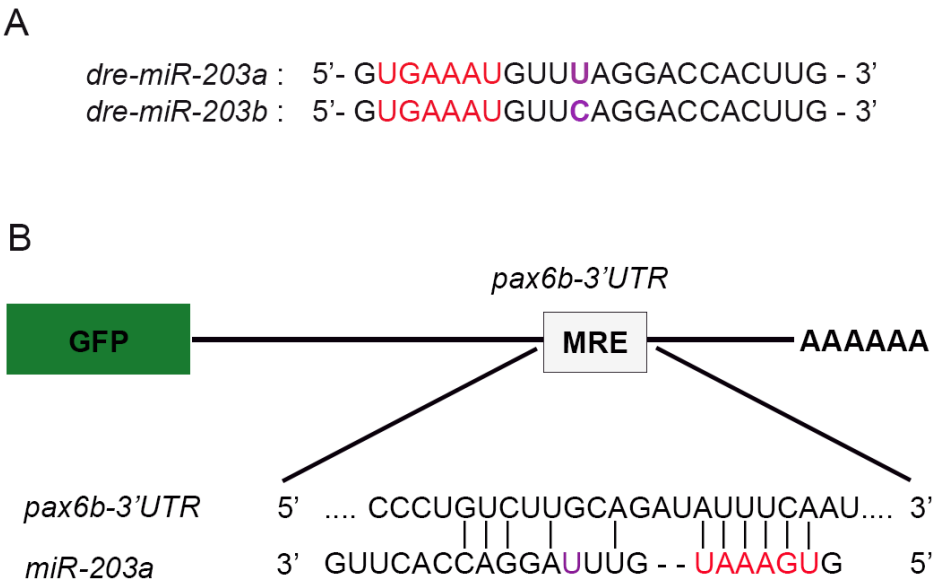

Figure 32. Pairing between *miR-203* and *pax6b 3'-UTR*.

(A) Mature miRNA sequences for *miR-203a* and *miR-203b*. The miRNA 'seed' is highlighted in red. The single nucleotide that differs between the two family members is highlighted in magenta. (B) The *pax6b 3' UTR* was cloned downstream of GFP. Pairing between *miR-203a* and its miRNA recognition element (MRE) in the *pax6b 3' UTR* is shown.

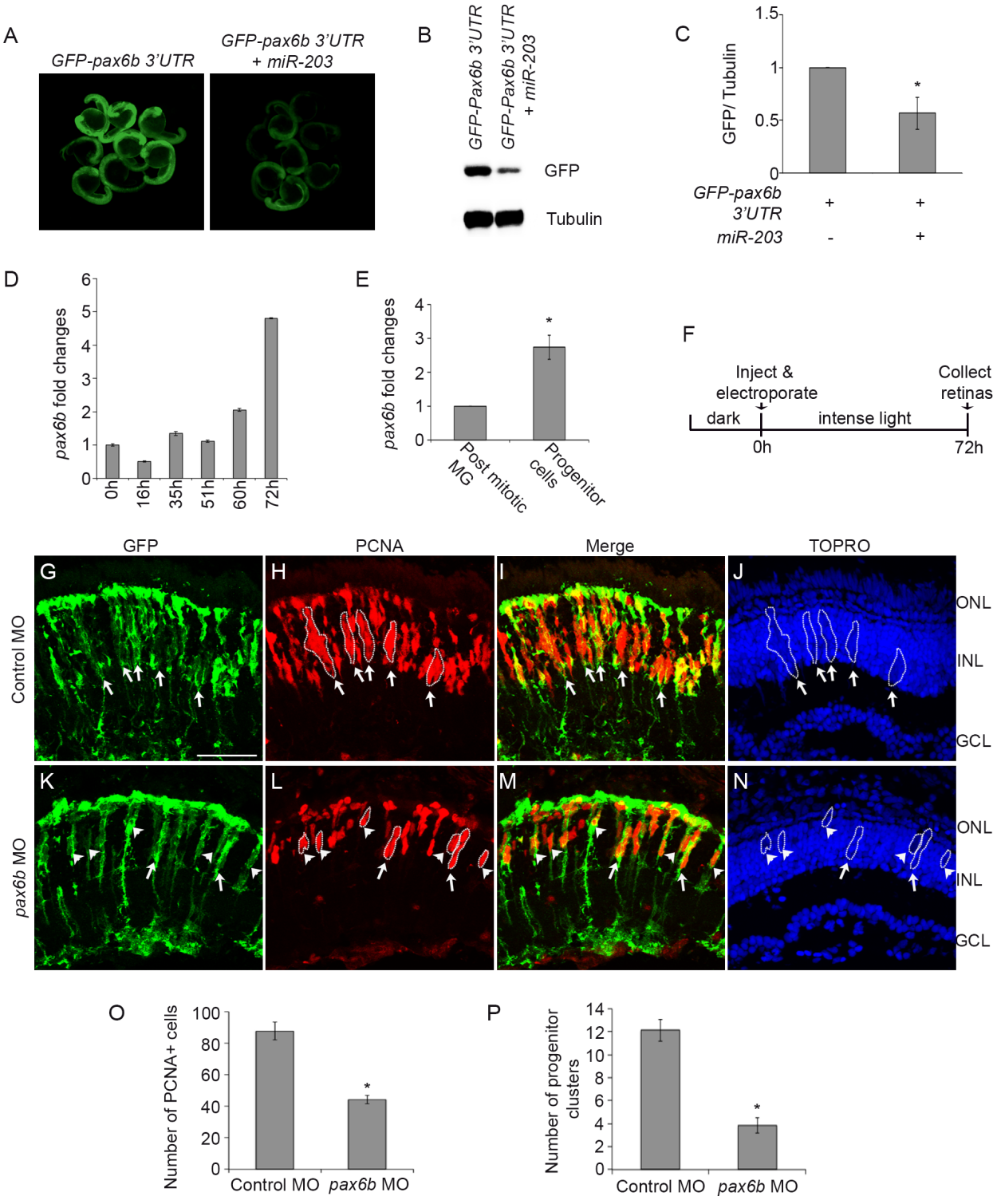
A
GFP-pax6b 3'UTR
GFP-pax6b 3'UTR + miR-203
B
GFP-Pax6b 3'UTR
GFP-Pax6b 3'UTR + miR-203
GFP
Tubulin
C
GFP/ Tubulin
1.5
1
0.5
0
*
GFP-pax6b 3'UTR
miR-203
+
+
-
+
D
pax6b fold changes
6
5
4
3
2
1
0
0h
16h
35h
51h
60h
72h
E
pax6b fold changes
4
3
2
1
0
*
Post mitotic MG
Progenitor cells
F
Inject & electroporate
Collect retinas
dark
intense light
0h
72h
GFP
PCNA
Merge
TOPRO
G
H
I
J
Control MO
ONL
INL
GCL
K
L
M
N
pax6b MO
ONL
INL
GCL
O
Number of PCNA+ cells
100
80
60
40
20
0
*
Control MO
pax6b MO
P
Number of progenitor clusters
14
12
10
8
6
4
2
0
*
Control MO
pax6b MO

Figure 33. *miR-203* regulates retina regeneration through *pax6b.*

(A-C) *miR-203* targets the 3' UTR of *pax6b*. The *pax6b* 3'UTR was fused to the GFP coding sequence. Single-cell zebrafish embryos were injected with *in vitro* transcribed mRNA from the GFP fusion construct in the presence or absence of *miR-203*. (A) Representative fluorescent images of injected embryos at 1dpf. (B) Western blot for GFP and α-tubulin control was performed on lysates prepared from the injected embryos in (A). (C) Quantification of GFP/tubulin ratios from multiple western blots as in (B). Data represent mean +/- s.d. (n=3 separate injection experiments); *, $p< 0.008$ by Student t-test. (D-E) *pax6b* mRNA is upregulated during retina regeneration. (D) qPCR was performed to quantitate *pax6b* levels from whole retina RNA. (E) qPCR for *pax6b* in FACS purified post mitotic MG and progenitor cells from 72h light treated fish. Data represent relative *pax6b* mRNA levels and show mean +/- s.e.m from 3 separate FACS experiments (n=3); *, $p< 0.008$ by Student t-test. For each FACS experiment post mitotic MG were purified from 15 undamaged fish and progenitor cells were purified from 20 light damaged fish. Samples were assayed in triplicate. 18s rRNA served as endogenous RNA control. (F) Experimental scheme for morpholino (MO) knockdown experiments in panels G-P. (G-N) Control MOs or *pax6b* MOs were injected and electroporated into the left eyes of *tg:1016tuba1a:gfp* fish prior to intense light exposure. Following 72h of light exposure, retinas were sectioned and stained with antibodies against GFP (green; panels G, K) and PCNA (red; panels H, L); nuclei were counterstained with TOPRO (blue; panels J, N). In the control MO treated retinas, large clusters of $PCNA^+$ cells associated along the processes of dedifferentiated MG (arrows in G-J). *pax6b* MO treatment reduced the number of dedifferentiated MG associated with progenitor clusters (arrows in K-N) but increased the number of dedifferentiated MG associated with 1-3 $PCNA^+$ cells (arrow heads in K-N). (O) Quantification of $PCNA^+$ cells. (P) Quantification of number of dedifferentiated MG associated with progenitor clusters. Data represent mean +/- s.e.m (n= 6-7 fish); *, $p< 0.002$ by Mann-Whitney U test. ONL, outer nuclear layer; INL, inner nuclear layer; GCL, ganglion cell layer. Scale bar 50um.

If *miR-203* regulates *pax6b*, then overexpression of *miR-203* should mimic morpholino knockdown of *pax6b*. Previously, Thummel et al. (2010) showed that loss of *pax6b* reduced the number of $PCNA^+$ and $BrdU^+$ cells in *albino* fish subject to intense light damage (Thummel et al., 2010). To test whether overexpression of *miR-203* only affects progenitor cell proliferation by regulating *pax6b*, we injected and electroporated either standard control MOs or *pax6b* MOs into the eyes of *1016tuba1a:gfp* transgenic zebrafish prior to the start of light lesioning (Figure 33F). Under these conditions, MG dedifferentiation was unaffected (Figure 33G, K), and consistent with previous results, there were fewer $PCNA^+$ progenitor cells in the *pax6b* MO-treated retinas at 72h compared to controls ($p<0.002$; n=6-7; Figure 33H, L, O). Interestingly, there was a significant decrease in the number of progenitor clusters (arrows in Figure 33I, M) associated along the processes of dedifferentiated MG in *pax6b* MO-injected retinas ($p<0.002$; n=6-7; Figure 33P). Additionally, knockdown of *pax6b* yielded clusters with only 1-3 progenitor cells per dedifferentiated MG (arrowheads in Figure 33M) relative to the larger clusters observed in standard control morphants. This indicates that loss of Pax6b significantly reduces progenitor cell proliferation and phenocopies the *miR-203* gain-of-expression result.

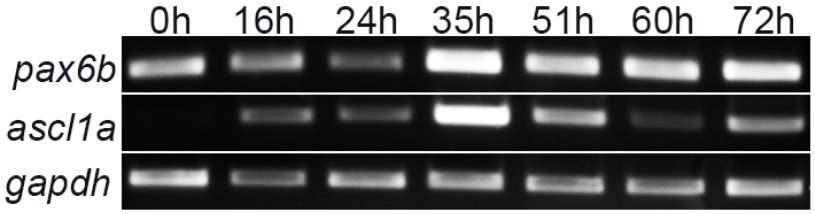

Figure 34. Semi-quantitative PCR for *pax6b.*

RT-PCR was performed for *pax6b*, *ascl1a* and *gapdh* from whole retinas during retina regeneration. *pax6b* is upregulated during regeneration. *ascl1a* served as a positive control for the progression of retina regeneration. *gapdh* served as loading control.

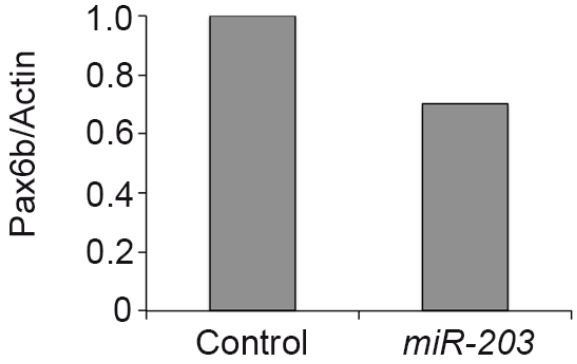

Figure 35. *miR-203* gain-of-function reduced Pax6b protein during regeneration.

Control miRNA or *miR-203* was injected and electroporated into the left eyes of *albino* zebrafish after MG dedifferentiation and progenitor cell generation (51h of light). After 72h, dorsal retinas were collected from control miRNA and *miR-203* injected fish and protein lysates were prepared for Western blots. Pax6b protein levels were probed and Actin served as loading control.

The reporter experiments and the Pax6b loss-of-function experiments indicate the *miR-203* regulates *pax6b*. To test whether overexpression of *miR-203* would decrease Pax6b levels *in vivo*, we analyzed Pax6b protein levels in the dorsal retina after *miR-203* or control miRNA gain-of-function. Consistent with the hypothesis that *miR-203* regulates Pax6b, we observed a ~30% reduction in Pax6b protein levels (Figure 35). We attempted to directly rescue the *miR-203* gain-of-function phenotype by injection and electroporation of *pax6b* mRNA but unfortunately we could not achieve mRNA delivery.

Discussion

Here, we identify *miR-203* as a novel regulator of zebrafish retina regeneration. We demonstrate that *miR-203* represses *pax6b,* which is necessary for progenitor cell expansion. During retina regeneration, *miR-203* levels must be reduced to allow progenitor cell amplification and cluster formation via *pax6b* expression. Elevated *miR-203* or loss of *pax6b* expression during retina regeneration inhibits progenitor cell proliferation and significantly impairs progenitor cluster formation. This reveals a novel regulatory mechanism that controls progenitor cell proliferation, a key step in retina regeneration.

miR-203 inhibits proliferation

miR-203 functions as negative regulator of proliferation and stem cell properties in a number of cancers (Viticchie et al., 2011; Wang et al., 2013; Wang et al., 2012; Yu et al., 2013), as well as in mouse skin development and regeneration (Jackson et al., 2013; Lena et al., 2008; Viticchie et al., 2012; Yi et al., 2008). *miR-203* is also important for zebrafish regeneration. We previously showed that downregulation of *miR-203* is

necessary to initiate blastema formation following caudal fin amputation (Thatcher et al., 2008). During retina regeneration, *in situ* localization showed that *miR-203* levels are significantly reduced in the INL upon light damage and qPCR revealed a nearly 70% reduction in *miR-203* levels in progenitor cells compared to undamaged post-mitotic MG (Figure 24). This is highly reminiscent of the role of *miR-203* in mouse skin development, where *miR-203* expression is restricted to the differentiated and basal layers of newly stratified skin epithelium, but conspicuously absent in the proliferating progenitor compartment (Yi et al., 2008). Overexpression of *miR-203* induced skin progenitors to exit the cell cycle, which severely reduced the pool of proliferating progenitors (Yi et al., 2008). During zebrafish retina regeneration, *miR-203* downregulation in progenitor cells is also necessary for their proliferation (Figures 27, 29, 31). We restricted our analysis of the effects of *miR-203* to the first 72h post injury. It will be interesting to determine the fate of the proliferating progenitor cells in retinas overexpressing *miR-203,* as well as the effects of long-term suppression of *miR-203* on regeneration.

miR-203 inhibits progenitor expansion by targeting pax6b

Intense light treatment causes dying photoreceptors to express TNFα, which induces MG dedifferentiation (Nelson et al., 2013). Dedifferentiated MG express *ascl1a*, activate Wnt signaling, and undergo asymmetric cell division to produce progenitor cells (Nagashima et al., 2013; Ramachandran et al., 2011). These progenitors undergo multiple rounds of cell division and form clusters, which associate along the processes of the dedifferentiated MG and span the length of the INL (Thummel et al., 2010). Ectopic expression of *miR-203* before starting intense light exposure in the transgenic

1016:tuba1a:gfp line did not affect overall MG dedifferentiation or the first cell divisions needed to generate progenitor cells (Figures 28, 30). However, relative to control retinas, we detected a significant reduction in the number of dedifferentiated MG associated with progenitor clusters that had >3 associated progenitor cells (Figure 29). Instead, most of the dedifferentiated MG were associated with only 1-3 progenitor cells. This reduction was apparent when *miR-203* was overexpressed specifically during the progenitor expansion phase in the regenerating retina (Figure 31).

Progenitor cell proliferation during retina regeneration is under the control of *pax6* genes. While *pax6b* controls the first cell division of the MG-derived progenitor cells to generate 4 cell clusters, *pax6a* is required for further amplification of these 4 cell clusters (Thummel et al., 2010). It was previously reported that MO-mediated loss of *pax6b* prevents cluster formation by inhibiting the first cell division of the MG-derived progenitor cells. This is similar to the inhibition of progenitor cell proliferation and cluster formation phenotype we observed with *miR-203* gain-of-function (Figures 29, 31), and consistent with *miR-203* targeting of *pax6b* using reporter and qPCR assays (Figure 33). Similar to *miR-203* gain-of-function, we detected a reduction in progenitor cluster number upon MO-mediated reduction of *pax6b* (Figure 33). Moreover, overexpression of *miR-203* during the progenitor cell proliferation phase resulted in a ~30% reduction in Pax6b protein levels in dorsal retinas (Figure 35). A more elegant approach would be to rescue the *miR-203* overexpression phenotype by co-injection of *pax6b* mRNA. Unfortunately the ability to achieve delivery and expression of mRNAs by injection and electroporation into retinas has not been reported and proved technically challenging in our hands.

Regulation of Pax6b

Although the role of Pax6b in progenitor cell expansion is well established, the exact mechanism that regulates its expression is not clear. Knockdown of HB-EGF and *ascl1a* reduced the total amount of *pax6b* mRNA in the retina (Ramachandran et al., 2011; Wan et al., 2012) and stabilization of β-catenin upregulated *pax6b* levels (Ramachandran et al., 2011). Since *pax6b* is upregulated in proliferating progenitor cells, regulatory mechanisms must exist to precisely control its expression in these MG-derived progenitors. An intriguing hypothesis is that Wnt activation in asymmetrically derived progenitor cells suppresses *miR-203* leading to upregulation of *pax6b* and subsequent progenitor cell expansion.

Regulation of miR-203

While *miR-203* must be downregulated to allow progenitor cell proliferation, the mechanism of its downregulation remains unknown. In human keratinocytes, *miR-203* expression is activated by PKC and inhibited by EGF treatment (Sonkoly et al., 2010). We previously showed that during zebrafish development, *miR-203* expression is activated by suppressing hedgehog signaling (Thatcher et al., 2007). Studies in cancer also suggest epigenetic control of *miR-203* expression via promoter DNA methylation (Bueno et al., 2008; Diao et al., 2013; Taube et al., 2013). In zebrafish, both *miR-203* genes (*miR-203a* and *miR-203b;* Figure 32A) are monocistronic, contain their own promoters and reside on separate chromosomes, suggesting possible transcriptional and epigenetic control of *miR-203* gene expression. A recent study detected the existence of dynamic DNA methylation in MG and progenitor cells during zebrafish retina regeneration (Powell et al., 2013). Inhibition of DNA methylation during progenitor cell

expansion inhibited proliferation, suggesting that genes that inhibit progenitor cell proliferation might be epigenetically suppressed. Moreover, HB-EGF induction in the dedifferentiated MG is necessary for progenitor cell production and retina regeneration (Wan et al., 2012). It is tempting to speculate that *miR-203* expression in progenitor cells could be negatively regulated via both HB-EGF and promoter methylation, thus allowing progenitor cell proliferation and cluster formation.

Targets of miR-203

Several genes that are critical for retina regeneration are predicted to be *miR-203* targets, including HB-EGF, Lin-28, and Insm1a (Table 3). We found that *pcna* and *lef1*, which are both important for regeneration, are *bona fide miR-203* targets (unpublished data) (Thatcher et al., 2008). Interestingly, *miR-203* gain-of-function prior to retina damage does not inhibit PCNA expression early (51h of light), but does reduce PCNA expression at later stages (72h of light). This suggests that PCNA may not be a primary *miR-203* target during retina regeneration, but rather is a consequence of *miR-203* repressing DNA replication through its inhibition of the progenitor cell cycle. During zebrafish caudal fin regeneration, targeting of *lef1* by *miR-203* was central to both initiation and termination of regeneration (Thatcher et al., 2008). However, we have not found that targeting of *lef1* by *miR-203* affects retina regeneration (data not shown). In mouse skin development, the main target for *miR-203* is ΔNp63, a member of the p53 family and a regulator of proliferation in epithelial cells and various cancers (Dotto, 2012; Lee and Kimelman, 2002; Parsa et al., 1999; Rivetti di Val Cervo et al., 2012; Senoo et al., 2007; Truong et al., 2006; Yang et al., 1999). In zebrafish, *p63* expression is upregulated during optic nerve regeneration (Saul et al., 2010). However, we detected

very low levels of *p63* expression in FACS-purified post mitotic MG and progenitor cells from undamaged and regenerating retinas, respectively, suggesting that *p63* is not an important target for *miR-203* in the retina.

Table 3. *miR-203* targets tested by GFP-reporter assays.

Predicted targets	MRE position	Pairing	Valid targets
hbegfa	743-749	…GUCACGAAAAGUCAUAUUUCAAG… | | |||||| GUUCACCAGGAUUUGUAAAGUG	No
lin-28a	2636-2642 3398-3405	…AAAAGAAACGGAAAACAUUUCAU… ||| ||||||||||| GUUCACCAGGAUUUGUAAAGUG …UUUGUAUCCCAUUAUCAUUUCAA… ||| | ||||||| GUUCACCAGGAUUU--GUAAAGUG	No
insm1a	717-723	…UAUUAUUAUUUAUUUAUUUCAAA… | || ||||| GUUCACCAGGAUUUGUAAAGUG	No
pcna	313-319	…UUGUCCUCUUGUGUGUCCAUUUCAG… | ||||| ||||||| GUUCACCAGGAUUU-------GUAAAGUG	Yes
pax6b	3328-3334	…CCCUGUCUUGCAGAUAUUUCAAU… ||| | | |||||| GUUCACCAGGAUUUG--UAAAGUG	Yes

Limitations and implications of miRNA gain-of-function experiments

A caveat of our *miR-203* overexpression studies is that all retinal cells, not just MG, take up the miRNA (Figure 26). Hence, it is formally possible that inhibition of progenitor cell proliferation is a result of gain of *miR-203* in cell types other than the

MG-derived progenitor cells, that the effects we observe may not be cell autonomous. Since *miR-203* can regulate many targets and Pax6 proteins are also expressed in amacrine and bipolar cells, it is possible that *miR-203* inhibition of Pax6b or additional targets in these retinal neurons feeds back and inhibits progenitor cell proliferation by additional secondary mechanisms. It is therefore possible that the loss of progenitor cell proliferation due to excess *miR-203* could be the result of the function of *miR-203* in progenitor cells, retinal neurons or both.

miRNAs and regeneration

Early zebrafish retina regeneration can be divided into distinct steps requiring precise gene expression changes as MG dedifferentiate, undergo asymmetric division, and generate progenitor cells (Fausett and Goldman, 2006; Nagashima et al., 2013; Thummel et al., 2008a). We show for the first time that *miR-203* must be downregulated to derepress *pax6b* and allow progenitor cell proliferation. Coupled with previous work showing that *let-7* plays a key role regulating MG dedifferentiation (Ramachandran et al., 2010), it seems likely that additional miRNAs will be identified that regulate not only early steps during regeneration, but also migration and re-differentiation as lost cell types are replaced. *miR-203* is an especially interesting case as it has now been demonstrated to play a key regulatory role in progenitor proliferation during development (Jackson et al., 2013; Lena et al., 2008; Yi et al., 2008), regeneration (Thatcher et al., 2008), and possibly adult neurogenesis.

Acknowledgements

We thank Qiang Guan for zebrafish maintenance at the Vanderbilt University Stevenson Center Fish Facility. This study was supported in part by grants from the National Eye

Institute–National Institutes of Health to J.G.P (R21 EY 019759) and D.R.H. (R01-EY018417) and the Center for Zebrafish Research, University of Notre Dame. K.R. was supported in part by the Vanderbilt International Scholar Program and by the Gisela Mosig fund in the Department of Biological Sciences.

Competing Interests

The authors declare no financial or non-financial competing interests.

CHAPTER V

miR-216 REGULATES EARLY STAGES OF ADULT ZEBRAFISH RETINA REGENERATION

Kamya Rajaram, Emily R Summerbell and James G. Patton*

---

* KR and JGP conceived and designed the research. KR and ERS performed experiments and analyzed the data.

Introduction

Despite conservation in the structure and function of the retina, mammalian and non-mammalian vertebrates have contrasting responses to retinal injury (Lamba et al., 2008). Retinal damage in the non-mammalian vertebrate zebrafish triggers a spontaneous regeneration response that restores both retinal structure and function (Fausett and Goldman, 2006; Vihtelic and Hyde, 2000; Yurco and Cameron, 2005). This response is initiated by resident retinal glia called Müller glia (MG), which revert to a less differentiated state and generate progenitor cells that can differentiate into any of the lost retinal cell types in the zebrafish retina. In contrast, damage to the mammalian retina stimulates reactive gliosis of the MG, and spontaneous regeneration of retinal neurons is very rare (Bringmann et al., 2009; Dyer and Cepko, 2000). However, recent *in vitro* studies demonstrated that mammalian MG can be induced to enter the regeneration pathway by treatment with various growth factors and transcription factors, which suggests that initiation of MG-mediated retinal regeneration is blocked in mammalian retinas (Close et al., 2006; Del Debbio et al., 2010; Karl et al., 2008; Ooto et al., 2004; Pollak et al., 2013). Thus, understanding the molecular mechanisms underlying initiation of the MG-mediated regeneration response in the zebrafish retina is key to triggering regeneration in mammalian retinas.

Small non-coding RNAs called microRNAs (miRNAs) have been shown to be important regulators of tissue regeneration in a number of animals (Thatcher and Patton, 2010). miRNAs are derived from endogenously produced hairpin precursors that are processed sequentially by the RNaseIII-like enzymes Drosha and Dicer, to generate a ~22nt, mature miRNA duplex (Bartel, 2004, 2009; Olena and Patton, 2010). One strand

of the duplex is incorporated into a complex of proteins called the RNA induced silencing complex (RISC) and is guided by the RISC to the 3' untranslated regions (3'-UTRs) of target mRNAs (Chendrimada et al., 2005; Gregory et al., 2005). miRNAs function by base-pairing with partial complementarity in the target mRNA 3'-UTRs where they regulate gene expression by causing mRNA destabilization and/ or repression of protein production (Kloosterman and Plasterk, 2006). In zebrafish, miRNAs regulate regeneration of the heart, retina, spinal cord and caudal fin (Rajaram, 2014b; Ramachandran et al., 2010; Thatcher et al., 2008; Yin et al., 2012; Yin et al., 2008; Yu et al., 2011). We previously showed that an intact miRNA biogenesis pathway is necessary for zebrafish retina regeneration and we elucidated the role of one miRNA, *miR-203* in regulating proliferation of MG-derived progenitor cells (Rajaram, 2014a, b).

In this study, we focus on *miR-216* and its role in the initiation of retina regeneration. We show that *miR-216* is suppressed in dedifferentiated MG early in retina regeneration. Using gain-of-function studies, we demonstrate that suppression of *miR-216* is necessary for MG dedifferentiation and proliferation. We identify the histone methyl transferase *dot1l* as a *bona fide* target of *miR-216*, and using loss-of-function studies in the retina, we demonstrate the requirement for *dot1l* in the initiation of retina regeneration. Our results demonstrate key roles for *miR-216* and *dot1l* in initiating the MG-mediated regeneration response.

Materials and methods

Zebrafish husbandry and adult zebrafish light lesioning

Zebrafish were maintained in 14h light and 10h dark cycles at 28.5°C. The following

zebrafish lines were used: *tg:1016tuba1a:gfp* (Fausett and Goldman, 2006), *tg:gfap:gfp* (Bernardos and Raymond, 2006), *albino* (Vihtelic and Hyde, 2000) and wildtype AB. Embryos for microinjections were obtained from matings of AB fish. All experiments were performed with the approval of the Vanderbilt University Institutional Animal Care and Use Committee (Protocol # M/09/398). Constant instense light lesioning was performed as previously described (Rajaram, 2014b). Briefly, adult fish were dark adapted for 14 days, transferred to clear tanks placed between two fluorescent lights with light intensity at ~20,000 lux for 16h-3days. The tank temperature was maintained at 30-33°C.

Fluorescence activated cell sorting (FACS), RNA isolation, Taqman realtime PCR

FACS was used to purify GFP^+ and GFP^- cells from the retinas of undamaged *tg:gfap:gfp* fish and *tg:1016tuba1a:gfp* fish that were exposed to 45h or 72h of light damage. Retina dissociation protocol for FACS is published elsewhere (Rajaram, 2014b). Cells were sorted using BD FACSAria III (BD Biosciences) at the VUMC Flow Cytometry Shared Resource. Sorted cells were collected in Trizol LS (Ambion) and total RNA was isolated following the manufacturer's protocol. For mRNA quantitative real time PCR (qPCR), RNA was DNase treated (Rapid Out, Thermo Scientific), converted to cDNA using Maxima first strand cDNA synthesis kit (Thermo Scientific) and qPCR was performed using SYBR Green (Biorad). All qPCR primers spanned exon-exon junctions (IDT). miRNA realtime PCR was perfomed using Taqman probes as per the manufacturer's instructions (Life Technologies). Relative RNA expression during regeneration was determined using the ΔΔCt method and normalized to 18s rRNA levels and U6 snRNA

levels for mRNAs and miRNAs respectively. Real time PCR was performed on a Biorad CFX 96 Real time system. The following primer sequences were used:

dot1l-qpcr-fp: 5’- CATGATGCTGCACACGAAAT-3’

dot1l-qpcr-rp: 5’-TCTCGAAGCTCTTGGTGTCA-3’

18srRNA-qpcr-fp: 5’- ACGCGAGATGGAGCAATAAC-3’

18srRNA-qpcr-rp: 5’- CCTCGTTCATGGGAAACAGT-3’

Morpholino and miRNA injection and electroporation

Lissamine tagged morpholinos (MOs) (Gene Tools) were injected and electroporated into adult zebrafish eyes prior to light lesioning as described (Thummel et al., 2008b). The following 3'-Lissamine-tagged MOs were used:

Gene Tools standard control MO: 5’-CCTCTTACCTCAGTTACAATTTATA-3’

Dot1 MO: 5’-CCCAGCTATACACACAAAAAGCAGC-3’

miR-216a MO: 5’- TCACAGTTGCCAGCTGAGATTA-3’

Duplex mature miRNAs (Thermo scientific) were injected and electroporated into eyes prior to start of light lesioning as previously described (Rajaram, 2014b). Double stranded mature miRNAs were synthesized with 3’- UU overhangs for the following target sequences:

miR-216: 5’-UAAUCUCAGCUGGCAACUGUGAUU-3’

control: 5’-AAAAACAUGCAGAAAAUGCUG-3’

Electroporation was performed using the Gene Pulser Xcell™ Electroporation Systems (Biorad).

Immunohistochemistry

Adult zebrafish eyes were processed for immunohistochemistry (IHC) as previously described (Rajaram, 2014b). Briefly, eyes were fixed in 4% paraformaldehyde or a fixant containing 9 parts 95% ethanol: 1 part 37% formaldehyde (for dot1l IHC), followed by cryoprotection in 30% sucrose/1X PBS before embedding. 10-12 micron sections were obtained using a cryostat (Leica), collected on charged Histobond slides (VWR), dried and stored at -80°C until used. For IHC, slides were warmed to room temperature, blocked with serum before incubating with primary antibodies overnight at 4°C. Primary antibodies were mouse anti-PCNA monoclonal antibody (1:500, Sigma), anti-PCNA polyclonal antibody (1:500, Abcam), rabbit anti-GFP polyclonal antiserum (1:1000, Torrey Pines Biolabs), mouse anti-β-catenin antibody (1:500, BD Bioscience) and rabbit anti-dot1l polyclonal antibody (1:200, Bethyl labs). After primary antibody incubation, sections were washed and incubated with secondary antibody and nuclear stain TOPRO 3 (1:1000, Invitrogen) at room temperature. Secondary antibodies were donkey anti-mouse AF488 (1:200), donkey anti-mouse AF647 (1:200), donkey anti-mouse Cy-3 (1:100), donkey anti-rabbit Cy3 (1:100) and donkey anti-rabbit AF488 (1:200)(Jackson Immuno). Slides were washed, dried and coverslipped with Vectashield (Vector labs). Antigen retrieval was performed for β-catenin and PCNA IHC as previously described (Rajaram, 2014b).

Molecular cloning and embryo microinjections

The *dot1l* 3'UTR was amplified from cDNA by PCR with the following primers:

dot1l-3'utr-fp: 5'-AGACTTGAATTCCCTTCCAGGAACTGAGTTTAACC-3'

dot1l-3'utr-rp: 5'- AGTCTGCTCGAGCAGCTCCACAGGTAAATGATCC-3'

The 3' UTR was cloned into the pCS2^{+} plasmid downstream of the GFP coding sequence. Capped RNA was transcribed from these reporter constructs using SP6 mMessage mMachine (Life Technologies). Zebrafish embryos at the single-cell stage were injected with 100pg of mRNA with or without 100pg of synthetic duplex *miR-216* (Thermo Scientific). Titrations were performed to determine the lowest effective injection concentrations.

Cell counts and statistical analyses

For confocal microscopy, only retina sections that comprised optic nerves were used. All cell counts were done in the central-dorsal retina, at a linear distance of ~300 microns from the optic nerve. In all figures data are represented as mean +/- standard error of the mean (s.e.m) and significance was calculated using the Student-t tests.

Results and Discussion

miR-216 is downregulated in dedifferentiated MG early in retina regeneration.

We had earlier identified *miR-216* as an important regulator of MG cell identity in the developing zebrafish retina (Olena, 2014). To elucidate the roles of *miR-216* in zebrafish retina regeneration, we began by examining its expression in the adult retina. Specifically, we focused on MG and tested whether *miR-216* levels change in these cells during regeneration. We purified GFP^{+} and GFP^{-} cells from two different transgenic zebrafish lines: undamaged *tg:gfap:gfp*, in which only post-mitotic MG express GFP, and light damaged *tg:1016tuba1a:gfp,* in which dedifferentiated MG and progenitor cells express GFP. From the *tg:1016tuba1a:gfp* fish, we collected retinas at 2 different time

points during regeneration, 45h of light damage, when MG have dedifferentiated and are starting to generate progenitor cells and 72h of light damage, when progenitor cells are rapidly proliferating and forming large progenitor clusters. From the FACS-purified cells, we extracted RNA and performed qPCR for *miR-216*.

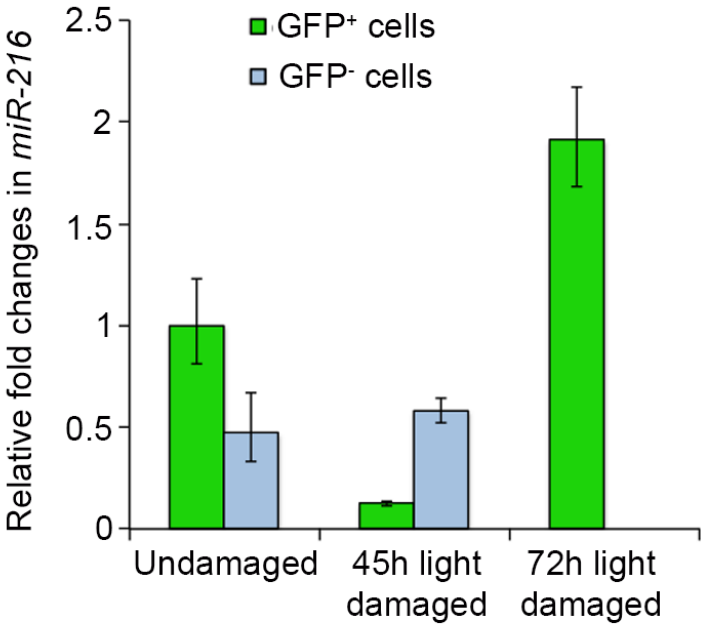

Figure 36. *miR-216* is downregulated in dedifferentiated MG early in retina regeneration.

Relative fold changes in *miR-216* levels in FACS-purified cell types were determined by qPCR. *miR-216* is enriched in post-mitotic MG (GFP^+) in undamaged retinas. After 45h of light exposure, *miR-216* is downregulated ~10 fold in dedifferentiated MG (GFP^+), but its levels increase in the proliferating progenitor cells (GFP^+) at 72h of light exposure. *miR-216* expression did not change in non-MG cells (GFP^-) during regeneration. Data represent mean +/- s.e.m from 15 undamaged fish, dedifferentiated MG and progenitor cells were purified from 18 and 20 light damaged fish respectively.

In undamaged retinas, *miR-216* was enriched in the post-mitotic MG (GFP^+), compared to the other retinal cells (GFP^-) (Figure 36- 'undamaged' bar graph). However, by 45h of light damage, we detected a ~10-fold reduction in *miR-216* in the dedifferentiated MG compared to post-mitotic MG (Figure 36). By 72h of light damage, *miR-216* levels were elevated in the GFP^+ proliferating progenitor cells. *miR-216* expression did not change in the rest of the retina (GFP^-). These data indicate that *miR-216* is suppressed in dedifferentiated MG early during retina regeneration; however, its levels increase in the progenitor cells as they proliferate and form clusters.

Suppression of miR-216 is necessary for MG dedifferentiation and proliferation during retina regeneration.

Next, we focused on the function of *miR-216* during retina regeneration. Since this miRNA was downregulated in dedifferentiated MG, we first examined the effects of excess *miR-216* on early stages of retina regeneration. We injected and electroporated *miR-216* or a control miRNA into zebrafish retinas before light damage (0h) and assessed the effects on MG dedifferentiation and proliferation at 45h of light exposure (Figure 37A). Using the *tg:1016tuba1a:gfp* zebrafish, we observed numerous GFP^+ dedifferentiated MG in control miRNA-overexpressing retinas. In contrast, GFP^+ cells were completely absent in all the *miR-216* overexpressing retinas that we examined (n= 5-6 fish) (Figure 37B). This result suggests that excess *miR-216* affects MG dedifferentiation and tuba1a promoter activation. We also probed retinal proliferation using PCNA as a marker (Figure 37C). Compared to the control miRNA overexpressing retinas, which contained small clusters of INL $PCNA^+$ cells, *miR-216* overexpression

significantly reduced the number of proliferating cells in the INL ($p<0.01$, n= 5-6 fish) (Figure 37C, D). Next we assessed β-catenin staining in the INL, as β-catenin accumulation in MG has been previously shown to be necessary for MG dedifferentiation and proliferation (Ramachandran et al., 2011). Compared to control miRNA-overexpressing retinas which contained a single β-catenin^{+} MG associated with each PCNA cell cluster (5/5 retinas examined), we observed complete loss of β-catenin staining upon *miR-216* gain-of-function (3/5 retinas examined) (Figure 37E). These results demonstrate that suppression of *miR-216* in the MG is necessary for their dedifferentiation and proliferation.

Figure 37. *miR-216* gain-of-function impairs MG dedifferentiation and proliferation.

(A) Experimental scheme. Control miRNA or *miR-216* was injected and electroporated into the left eyes of zebrafish before intense light exposure (0h). After 45h, retinas were collected, sectioned and immunostained using antibodies against GFP (B), PCNA(C, E) or β-catenin (E). Nuclei were counterstained with TOPRO (blue). (B, C, E) *miR-216* gain-of-function abolished tuba1a:GFP transgene expression (B), significantly reduced the number of INL PCNA^{+} proliferating cells (C and E) and abolished β-catenin expression in MG (E). (D) Quantification of PCNA^{+} cells in the INL and ONL. Data represent mean +/- s.e.m (n= 5-6 fish); *, $p<0.01$. ONL, outer nuclear layer; INL, inner nuclear layer; GCL, ganglion cell layer. Scale bar 50um.

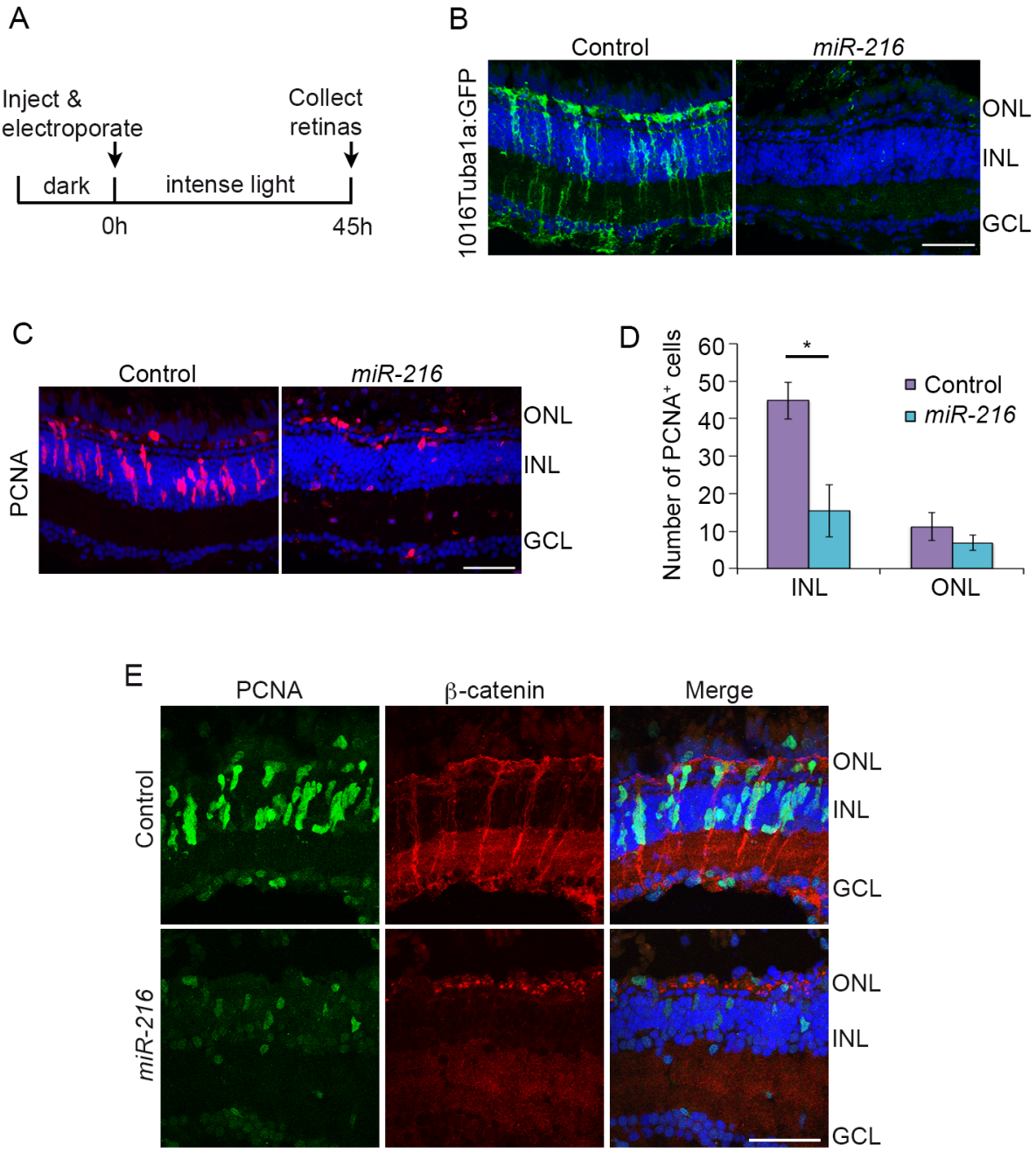
A
Inject &
electroporate
Collect
retinas
dark
intense light
0h
45h
B
Control
miR-216
1016Tuba1a:GFP
ONL
INL
GCL
C
Control
miR-216
PCNA
ONL
INL
GCL
D
Number of PCNA+ cells
60
50
40
30
20
10
0
*
Control
miR-216
INL
ONL
E
PCNA
β-catenin
Merge
Control
miR-216
ONL
INL
GCL
ONL
INL
GCL

We also examined the effects of *miR-216* gain-of-function on later stages of regeneration. *miR-216* overexpression significantly reduced MG dedifferentiation compared to control miRNA overexpression at 60h of light exposure (Figure 38B, C) ($p<0.03$, n=5-8 fish). We detected a significant reduction in INL proliferation compared to control miRNA overexpression (Figure 38B, D) ($p<0.003$, n=10 fish). However, *miR-216* gain-of-function did not affect PCNA cell numbers or tuba1a:GFP transgene expression after 72h of light exposure (data not shown). It is highly likely that suppression of *miR-216* is not the only mechanism controlling the important step of MG differentiation and proliferation. The regenerating retina may employ additional mechanisms that can sidestep the initial repression caused by excess *miR-216*. Nevertheless, it is apparent that suppression of *miR-216* is a critical step in the initiation of MG-mediated regeneration response.

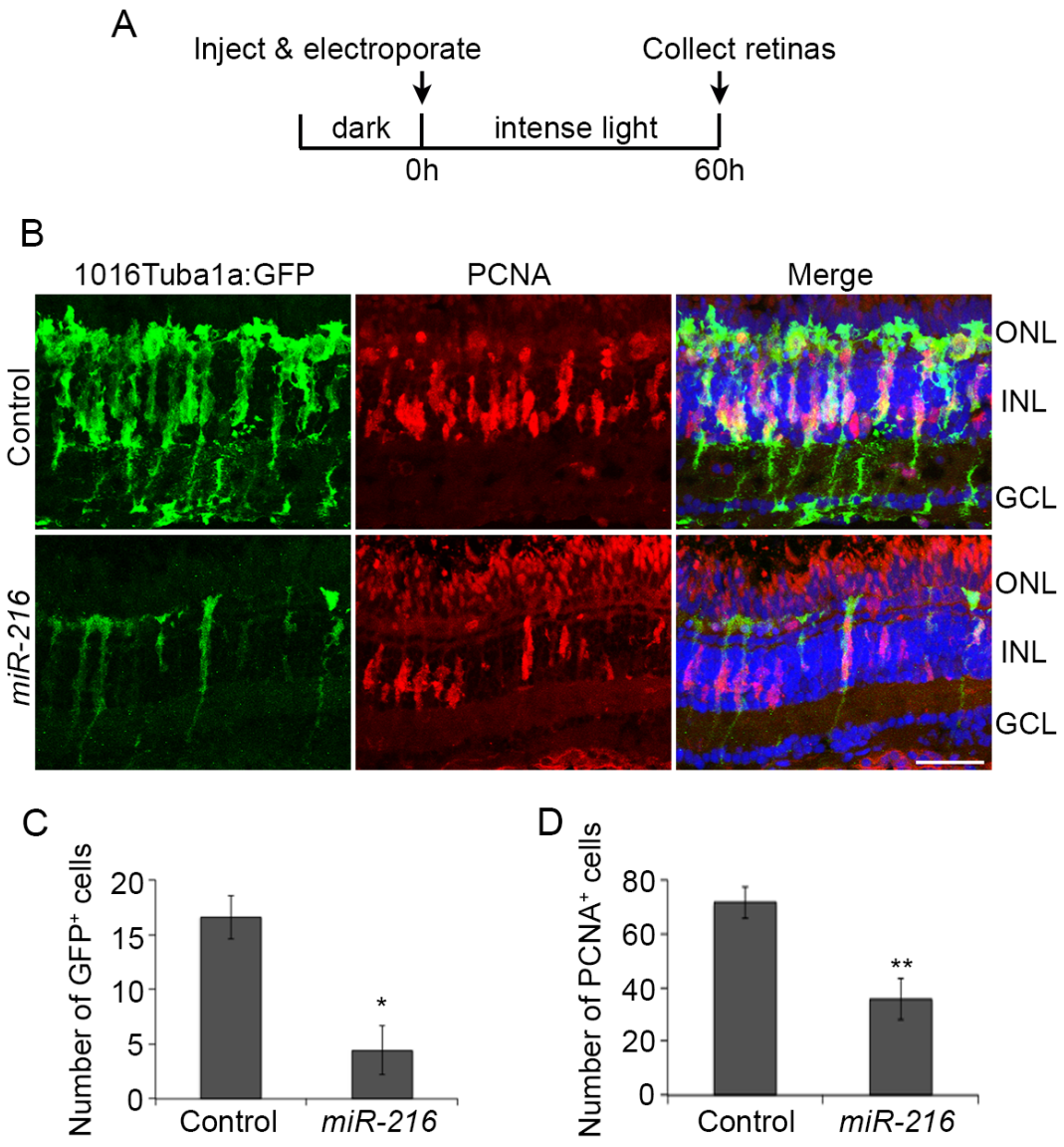

Figure 38. *miR-216* gain-of-function weakens the regeneration response at later stages of retina regeneration.

(A) Experimental scheme. Control miRNA or *miR-216* was injected and electroporated into the left eyes of tg:1016tuba1a:gfp zebrafish before intense light exposure (0h). After 60h, retinas were collected, sectioned and immunostained using antibodies against GFP (green) and PCNA (red). Nuclei were counterstained with TOPRO (blue). (B) Excess *miR-216* impairs MG dedifferentiation (green) and progenitor production (red). (C) Quantification of total GFP^+ cells. Data represent mean +/- s.e.m (n= 5-8 fish); *, $p<0.03$ (D) Quantification of total $PCNA^+$ cells. Data represent mean +/- s.e.m (n= 10 fish); **, $p<0.003$. ONL, outer nuclear layer; INL, inner nuclear layer; GCL, ganglion cell layer. Scale bar 50um.

Suppression of miR-216 is not sufficient to trigger retina regeneration.

Next, we tested if downregulation of *miR-216* is sufficient to trigger MG dedifferentiation and proliferation. For this, we injected and electroporated either control morpholinos (MOs) or MOs targeting the mature sequence of *miR-216* into the retinas of undamaged *tg:1016tuba1a:gfp* zebrafish and assessed the effects on MG dedifferentiation (via GFP expression) and proliferation. At 51h after MO injections, we detected few GFP^+ dedifferentiated MG in both control and *miR-216* MO injected fish (Figure 39A). Although we surprisingly observed GFP^+ dedifferentiated MG in the control MO injected and electroporated retinas, it is possible that subjecting the retina to electroporation triggers some damage and induces some MG dedifferentiation. Nevertheless, compared to control morphant retinas, *miR-216* morphant retinas contained more GFP^+ cells. However, this difference was not statistically significant (n= 6-7 fish; Figure 39B). To ascertain if the regeneration response persists and proliferating progenitor cells are generated from MG, we assessed GFP and PCNA expression in the INL of these retinas 72h after MO injections. We did not detect any significant differences in GFP^+ or $PCNA^+$ cell numbers between the two treatment groups (n= 5 fish; Figure 39C-E). Based on these results, we hypothesize that suppression of *miR-216* is necessary but not sufficient to stimulate MG dedifferentiation and proliferation.

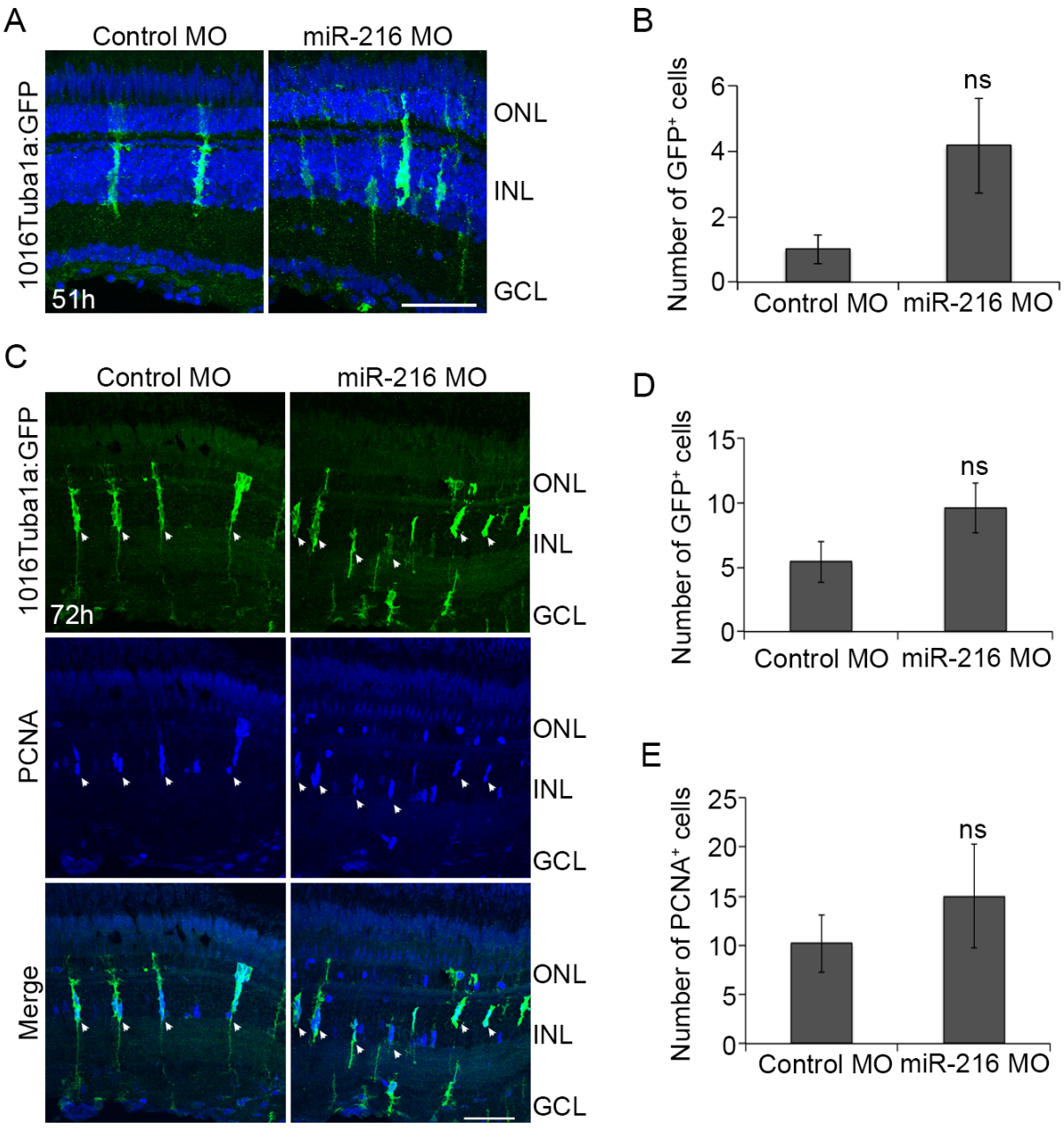

Figure 39. Suppression of *miR-216* is not sufficient to trigger retina regeneration.

Control MO or miR-216 MO was injected and electroporated into the left eyes of undamaged *tg:1016tuba1a:gfp* zebrafish. Retinas were collected 51h (A), or 72h (C) post MO injection, sectioned and immunostained using antibodies against GFP (green) and PCNA (blue in C). In (A) nuclei were counterstained with TOPRO (blue). (B, D, E) Quantification of total GFP^+ cells at 51h (B) and 72h (D). Quantification of total $PCNA^+$ cells at 72h (E). Data represent mean +/- s.e.m; n= 6-7 fish in (B); n= 5 fish in (D, E). ONL, outer nuclear layer; INL, inner nuclear layer; GCL, ganglion cell layer. Scale bar 50um.

miR-216 can target the histone methyl transferase dot1l.

To better characterize the mode of action of *miR-216* during retina regeneration, we focused on determining its targets. Using the online target prediction algorithm Targetscan (www.targetscan.org), we predicted potential targets. Since *miR-216* is suppressed early in dedifferentiated MG and because miRNAs function by repressing their target mRNAs, we concentrated on predicted targets that are upregulated early in dedifferentiated MG, but not in other retinal cells. We further filtered this list of targets and centered on epigenetic regulators. This seemed logical as dynamic changes in the DNA methylation profile of dedifferentiated MG have been previously reported (Powell et al., 2013). One predicted target that met the above criteria was the histone 3 lysine 79 methyl transferase called dot1l. Dot1l was an attractive target to pursue, since previous reports demonstrated its function as an activator of canonical Wnt dependent transcription in zebrafish (Mahmoudi et al., 2010), and canonical Wnt activation is necessary for MG dedifferentiation and proliferation during retina regeneration (Ramachandran et al., 2011). Analyses of FACS-purified cells revealed ~2-fold upregulation in *dot1l* transcripts in the dedifferentiated MG compared to post-mitotic MG. We did not detect changes in *dot1l* expression in other retinal cells (Figure 40B).

The 3' UTR of *dot1l* contains 3 MREs (miRNA recognition elements) for *miR-216* (Figure 40A). We verified the physical interaction between the miRNA and the *dot1l 3'-UTR* by performing GFP reporter assays in embryos. For this, we cloned the *dot1l 3'-UTR* downstream of the GFP coding sequence, *in vitro* transcribed reporter mRNAs, and injected them with or without exogenous *miR-216* into zebrafish embryos at the 1-cell stage. We assessed GFP expression in the injected embryos one day later. Compared to

embryos injected with the GFP reporter alone, those co-injected with *miR-216* had lesser GFP expression (Figure 40C), indicating direct interaction between *miR-216* and the *dot1l* 3'UTR.

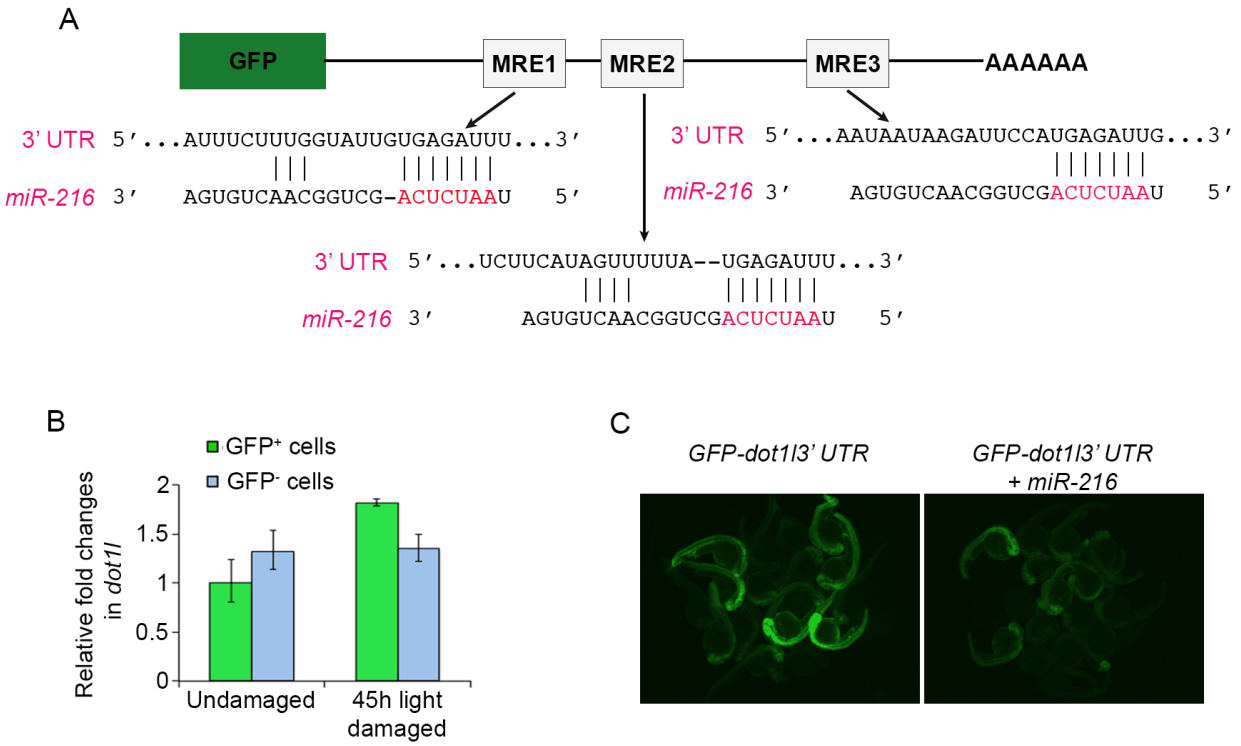

Figure 40. *miR-216* can target *dot1l 3'-UTR*.

(A) For GFP-reporter assays, *dot1l 3'-UTR* was cloned downstream of the GFP coding sequence. *dot1l 3'-UTR* contains 3 miRNA recognition elements (MREs) for *miR-216*. Pairing between *miR-216* and the MREs is shown, with the *miR-216* seed region highlighted in red. (B) *dot1l* mRNA is upregulated ~2 fold in dedifferentiated MG (GFP^+) after 45h of light exposure compared to post-mitotic MG (GFP^+) from undamaged retinas. Data represent mean +/- s.e.m from 15 undamaged fish and dedifferentiated MG were purified from 18 light damaged fish. (C) Results of GFP reporter assays in zebrafish embryos. 1-cell stage zebrafish embryos were injected with 100pg of *GFP-dot1l 3'-UTR*, with or without 100pg of *miR-216*. At 1dpf, GFP expression was apparent in embryos injected with *GFP-dot1l 3'-UTR* but was reduced in embryos co-injected with *miR-216*.

Dot1l is expressed in proliferating MG and progenitor cells during retina regeneration.

Next, we explored the expression pattern of Dot1l during retina regeneration. Immunohistochemistry revealed punctate localization of Dot1l protein in tuba1a:GFP$^+$/ PCNA$^+$ cells after 51h of light exposure (Figure 41). We also probed Dot1l protein expression across different time points during regeneration (Figure 42). Dot1l was not detected in undamaged retinas (0h). However, by 24h of light exposure, we began to observe Dot1l expression in INL cells. Many of these cells also expressed PCNA, indicating that these are MG that have re-entered the cell cycle (arrows). In addition, we also detected Dot1l$^+$/PCNA$^-$ cells within the INL (double arrowheads). By 51h of light, we observed MG proliferation in the INL, and all PCNA$^+$ proliferating cells also expressed Dot1l. Interestingly, we also noted Dot1l expression in PCNA$^-$ non-proliferating cells that morphologically looked like MG (double arrowheads). Based on this expression pattern, we hypothesize that Dot1l expression precedes PCNA expression in MG. Our hypothesis is supported by the finding that when we analyzed retinas exposed to 60h of light, punctate Dot1l localization was observed in all PCNA$^+$ cells (arrows). By 72h, PCNA$^+$ cells had migrated to the ONL, and Dot1l staining perfectly localized to proliferating progenitor cells (arrowheads). These data indicate that Dot1l expression begins early in the dedifferentiated MG, continues in the MG derived progenitor cells, and persists as they proliferate and migrate to the ONL.

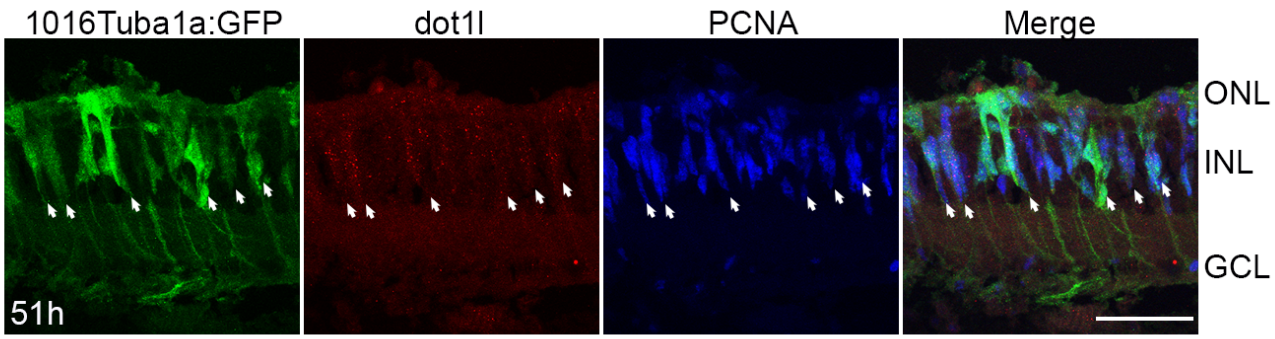

Figure 41. Dot1l is expressed in proliferating MG.

Retinas were collected from *tg:1016tuba1a:gfp* zebrafish that were light damaged for 51h, sectioned and stained with antibodies against GFP (green), Dot1l (red) and PCNA (blue). Arrows indicate some $GFP^{+}/PCNA^{+}$ dedifferentiated MG that express Dot1l. ONL, outer nuclear layer; INL, inner nuclear layer; GCL, ganglion cell layer. Scale bar 50um.

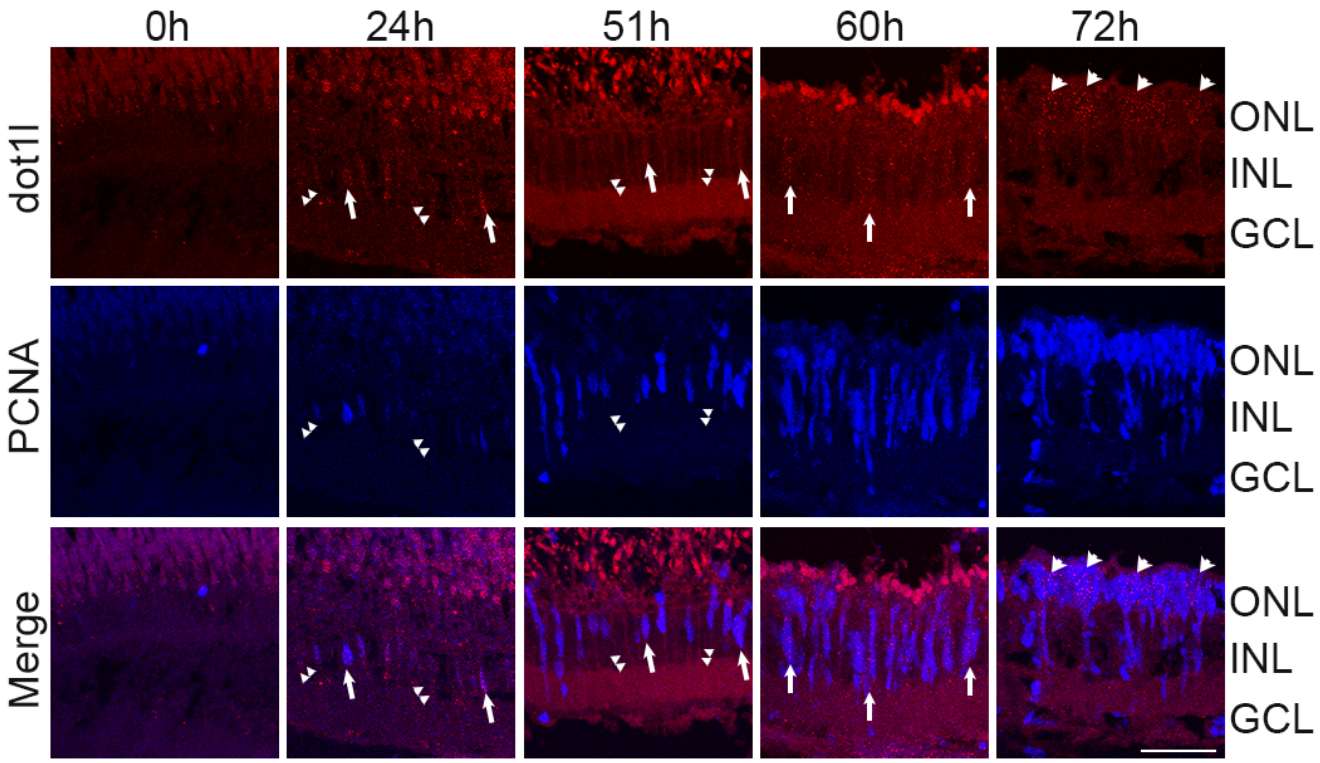

Figure 42. Time course of Dot1l expression during retina regeneration.

Retinas were collected from zebrafish before light exposure (0h) or at different time points during light exposure (24h, 51h, 60h, 72h), sectioned and stained with antibodies against Dot1l (red) or PCNA (blue). Dot1l expression was undetectable at 0h. By 24h, dot1l expression began in the INL. Many $Dot1l^{+}$ cells also expressed PCNA (arrows). Some $Dot1l^{+}$/ $PCNA^{-}$ cells were also detected (double arrowheads) at 24h and 51h. By 60h, all $PCNA^{+}$ cells expressed Dot1l. By 72h, Dot1l expression colabeled with the $PCNA^{+}$ cells that had migrated to the ONL (arrowheads). ONL, outer nuclear layer; INL, inner nuclear layer; GCL, ganglion cell layer. Scale bar 50um.

Dot1l is necessary for proliferation during retina regeneration

Analysis of the expression pattern of Dot1l indicated that Dot1l expression precedes PCNA and tuba1a:GFP expression in dedifferentiating MG (Figure 42 and data not shown). Based on this, we hypothesized that Dot1l expression in MG is necessary for cell cycle re-entry. To test this, we knocked down Dot1l by injecting and electroporating MOs into the zebrafish retina prior to light exposure, and assessed the effects on PCNA accumulation after 51h of light exposure (Figure 43A). Compared to control MO injections and electroporations, loss of Dot1l reduced the number of INL proliferating cells ($p<0.0001$, n= 5-9 fish) (Figure 43B, C). We detected few doublet $PCNA^+$ cells in Dot1l MO injected retinas (double arrowheads in Figure 43B). These data demonstrate that loss of Dot1l expression impairs MG proliferation and that Dot1l is necessary for initiation of retina regeneration.

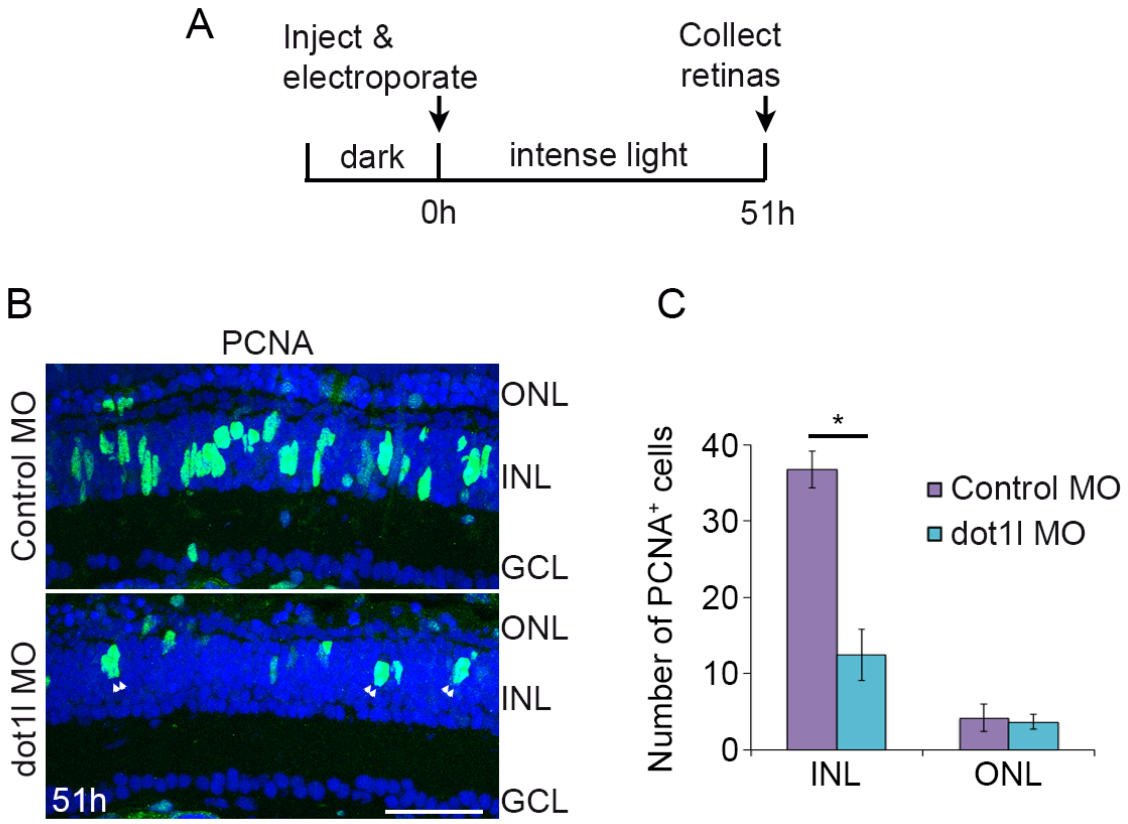

Figure 43. Dot1l loss-of-function impairs proliferation.

(A) Experimental scheme. Control MO or Dot1l MO was injected and electroporated into the left eyes of zebrafish before intense light exposure (0h). After 51h, retinas were collected, sectioned and immunostained using antibodies against PCNA (green). Nuclei were counterstained with TOPRO (blue). (B) Loss of Dot1l impaired proliferation in the INL. Few single or doublet (arrowheads) $PCNA^+$ cells were detected in the INL. (C) Quantification of $PCNA^+$ cells in the INL and ONL. Data represent mean +/- s.e.m (n= 5-9 fish); *, $p<0.0001$. ONL, outer nuclear layer; INL, inner nuclear layer; GCL, ganglion cell layer. Scale bar 50um.

Currently, we are investigating the effects of Dot1l loss-of-function on MG dedifferentiation by determining tuba1a:GFP transgene expression, as well as immunohistochemistry for other markers including β-catenin. Simultaneously, we are assessing the effects of *miR-216* gain-of-function on Dot1l protein and mRNA expression in the regenerating retina. We have identified binding sites for Insm1a, a transcriptional repressor that is induced early in dedifferentiated MG (Ramachandran et al., 2012), in the promoter region of *miR-216*. Using CHIP (chromatin immunoprecipitation), we are now testing the hypothesis that Insm1a suppresses *miR-216* expression in dedifferentiated MG.

CHAPTER VI

SUMMARY AND CONCLUSIONS

Significance

In humans, both systemic (diabetic retinopathy) and eye-specific (retinitis pigmentosa, age-related macular degeneration) diseases compromise vision by triggering photoreceptor cell loss. Retina degeneration is a pertinent health issue and the National Eye Institute estimates the economic impact of eye diseases to be nearly $22 billion. Interestingly, the structure, development and function of vertebrate retinas are highly similar, but retinal cell loss in mammals is degenerative, while in zebrafish, cell loss triggers a spontaneous and highly regulated regeneration response (Bernardos et al., 2007; Fimbel et al., 2007; Vihtelic and Hyde, 2000). Interestingly, the cell type responsible for regeneration in the zebrafish retina, the Müller glia (MG), is found in all vertebrate retinas, yet retina damage triggers opposing responses from the MG in mammalian vs. non-mammalian retinas. In the former, retina damage induces reactive gliosis of the MG resulting in scarring (Bringmann et al., 2006). In contrast, MG in damaged zebrafish retinas function as stem cells that initiate a regeneration response. It remains unclear why MG respond in opposing ways in different vertebrates, and why the ability of MG to function as stem cells has been lost during the evolution of vertebrates.

Two lines of research have emphasized the limited, yet promising potential of mammalian MG to function as progenitor cells: (1) gene expression profiling revealed that mammalian MG and retinal progenitor cells during development shared remarkable

similarities (Jadhav et al., 2009; Roesch et al., 2008; Trimarchi et al., 2008); (2) *in vitro* studies demonstrated that growth factor treatment or forced expression of transcription factors can induce mammalian MG to produce some neurons (Close et al., 2006; Karl et al., 2008; Ooto et al., 2004; Pollak et al., 2013; Takeda et al., 2008). Thus, understanding the molecular mechanisms underlying spontaneous MG-mediated retina regeneration in the teleost zebrafish could be key to designing strategies to stimulate a robust regeneration response in mammalian retinas.

Studies of zebrafish retina regeneration have mainly focused on identifying genes and signaling pathways controlling important steps of the regeneration process (Lenkowski et al., 2013; Nelson et al., 2013; Ramachandran et al., 2011, 2012; Thummel et al., 2010; Wan et al., 2012). Recently, the focus has shifted to understanding regulation of these genes and several regulatory mechanisms including DNA methylation (Powell et al., 2013), transcriptional activation (Ramachandran et al., 2011) and repression (Ramachandran et al., 2012) have been identified. Gene expression can also be regulated post transcriptionally by miRNAs, however, very little is known about the roles of miRNA-mediated gene regulation during retina regeneration.

miRNAs have previously been shown to regulate tissue regeneration in a number of non-mammalian vertebrates including urodele amphibians and zebrafish (Ramachandran et al., 2010; Sehm et al., 2009; Thatcher et al., 2008; Tsonis et al., 2007; Yin et al., 2012; Yin et al., 2008; Yu et al., 2011). Recently, Goldman and colleagues (Ramachandran et al., 2010) identified suppression of the *let-7* family of miRNAs in progenitor cells during zebrafish retina regeneration. However, functional studies in the retina were lacking. In the work presented in this thesis, I (1) determined the global

requirement of miRNAs for zebrafish retina regeneration, (2) discovered the identity and expression patterns all retinal miRNAs and (3) determined the function of specific miRNAs during zebrafish retina regeneration. To facilitate these studies, I also developed and characterized a retinal photoreceptor lesioning model that overcomes several limitations of previously used damage models.

Summary of Results

Research presented in this dissertation demonstrates that miRNAs are required for retina regeneration. Using HTS, I discovered that miRNAs are differentially expressed during active regeneration, but return to their basal expression levels once regeneration is completed. *In vivo* loss-of-function studies demonstrated that distinct miRNAs function in specific steps of retina regeneration. Using whole retina HTS and cell type-specific RNA analyses, I identified that *miR-203* is suppressed in progenitor cells during retina regeneration. Functional studies in the retina demonstrated that suppression of *miR-203* enabled *pax6b* expression, which is necessary for progenitor cell proliferation. Cell type-specific RNA analyses and *in vivo* functional studies, established that downregulation of *miR-216* is required for MG dedifferentiation during retina regeneration. Preliminary studies suggest that the H3K79 methyl transferase *dot1l* is a valid target of *miR-216* and that expression of Dot1l is required for proliferation during retina regeneration. Altogether, these studies emphasize the importance of miRNA-mediated regulation for initiation and progression of zebrafish retina regeneration. Additionally, I also developed and characterized a modified lesioning paradigm that induces identical photoreceptor apoptosis and regeneration in pigmented and *albino* zebrafish.

Discussion and Future Directions

Global requirement of miRNAs for retina regeneration

To evaluate the overall requirement of miRNAs during retina regeneration, we knocked down the miRNA-processing enzyme Dicer and assessed the effects on regeneration. Loss of canonical miRNAs significantly reduced progenitor cell proliferation and migration. However, we did not detect statistically significant effects on PCNA labeling of MG. Although this result suggested that Dicer-dependent canonical miRNAs were not required for MG cell cycle re-entry, it is essential to assess additional markers like β-catenin and Ascl1a to verify that miRNA loss has no effect on MG dedifferentiation. It is also possible that MO-mediated knockdowns only caused partial Dicer loss-of-function, which allowed low levels of miRNA biogenesis in the retina. Studies in development have demonstrated that only a subset of miRNAs are expressed in stem cells, and more miRNAs are expressed as cells begin to differentiate (Thatcher et al., 2007; Wienholds et al., 2003). Additionally, conditional Dicer loss-of-function studies in developing mice retinas demonstrated functions for miRNAs in promoting shifts of the retinal progenitors from early to late competence states. Loss of miRNAs resulted in progenitors being stuck in early competence states, leading to excess production of early-born RGC and loss of later-born cell types (Georgi and Reh, 2010; La Torre et al., 2013). Based on these results, it is likely that in the regenerating retina, reversion of MG to a less differentiated, stem cell-like state may require expression of only a small subset of miRNAs; however, as more committed progenitor cells are produced from the MG, expression of larger numbers of miRNAs becomes necessary. This could explain the robust effect of Dicer loss-of-function on progenitor cell

proliferation and migration, and the mild effect on MG dedifferentiation. It will be interesting to follow the fate of the progenitor cells in the Dicer loss-of-function retinas and assess if they retain the ability to differentiate into functional retinal neurons.

Dynamic expression profile of miRNAs during retina regeneration

High throughput sequencing (HTS) of zebrafish retinas before, during, and after regeneration identified subsets of miRNAs that are differentially expressed during retina regeneration. Importantly, almost all the differentially expressed miRNAs returned to their basal expression levels once regeneration was completed, suggesting that they function during regeneration. This dynamic miRNA expression profile was reminiscent of our identical finding during zebrafish caudal fin regeneration (Thatcher et al., 2008), which emphasizes the importance of miRNAs for regeneration of diverse tissues. To test if differential expression of miRNAs is an essential requirement or a secondary outcome of retina regeneration, we performed loss-of-function studies of six upregulated miRNAs and assessed their effects on regeneration. Loss of different miRNAs affected distinct steps in regeneration, including MG proliferation, progenitor cell proliferation, and progenitor cell migration.

Although we do not as yet know all the targets and the molecular pathways through which these miRNAs function in retina regeneration, it is important to note that some of these miRNAs have similar functions in other tissues. For instance, *miR-142b* has been shown to control mesenchymal stem cell proliferation via regulation of canonical Wnt signaling during lung development (Carraro et al., 2014). In the regenerating retina, canonical Wnt signaling is required for MG proliferation and we

observed significant reduction in MG proliferation upon *miR-142b* loss-of-function (Ramachandran et al., 2011). Loss of *miR-27c* and *miR-7a* impaired proliferation of the progenitor cells during retina regeneration. The *miR-27* miRNA family also functions in muscle regeneration, where it regulates satellite cell activation by promoting proliferation and delaying differentiation (Lozano-Velasco et al., 2011) (Crist et al., 2009). It will be interesting to examine the effects of *miR-27c* loss on progenitor cell differentiation during retina regeneration. Similarly, *miR-7* has also been implicated in maintaining the neural stem cell (NSC) pool in the brain (de Chevigny et al., 2012). In contrast, the other miRNAs we tested by loss-of-function studies have been barely investigated in additional tissues, or have contradicting roles in different tissues (Cekaite et al., 2012; Valastyan and Weinberg, 2011). It is apparent that in addition to transcription factor networks and signaling pathways, miRNAs constitute an essential network of regulators of retina regeneration.

Role of miR-203 in progenitor cell proliferation

miR-203 is downregulated during active retina regeneration. I chose to investigate the role of *miR-203* during retina regeneration due to previous research that demonstrated its functions as an 'anti-proliferation' or 'anti-stemness' factor in cancers, development and regeneration of multiple tissues (Lena et al., 2008; Thatcher et al., 2008; Viticchie et al., 2012; Viticchie et al., 2011; Wang et al., 2013; Wang et al., 2012; Yi et al., 2008). Expression of *miR-203* is widespread in the undamaged retina, with strong expression observed in the GCL, INL and photoreceptor OS. However, its expression is widely suppressed in the INL during regeneration. Specifically, using qPCR

of FACS-purified retinal cells, I discovered that *miR-203* expression is downregulated in proliferating progenitor cells. This finding is significant since suppression of *miR-203* has also been observed in proliferating progenitor cells in the developing and regenerating mouse skin, and overexpression of *miR-203* in the progenitor cells induced their differentiation (Lena et al., 2008; Viticchie et al., 2012; Yi et al., 2008).

Using miRNA gain-of-function studies in the regenerating retina I discovered that excess *miR-203* does not impair MG dedifferentiation or progenitor cell generation, but affected proliferation of MG-derived progenitor cells by targeting Pax6b. While no INL apoptosis was observed, the fate of the MG-derived progenitors in *miR-203* overexpressing retinas remains unclear. Pulse labeling the MG-derived progenitors with a thymidine analog and following them over time could provide insight regarding their fate. Interestingly, suppression of *miR-203* alone was not sufficient to trigger a regeneration response in undamaged retinas. Possibly, downregulation of *miR-203* is necessary in cell types that are not present in the undamaged retina (like the MG-derived progenitor cells), or suppression of *miR-203* may not be the only mechanism necessary to initiate regeneration, as noted by other studies (Nelson et al., 2013).

Work from the Hyde lab established the requirement of *pax6b* for progenitor cell proliferation (Thummel et al., 2010), but regulation of *pax6b* expression was unclear prior to this work. Additionally, we still do not know how *miR-203* expression is suppressed in the progenitor cells. Epigenetic modulation of *miR-203* expression has been reported in cancer models (Bueno et al., 2008; Taube et al., 2013), while Hedgehog signaling has been shown to suppress *miR-203* expression in zebrafish embryos during development (Thatcher et al., 2007). Analyzing the promoter regions of the *miR-203*

genes for epigenetic marks could help understand its regulation during retina regeneration.

Its important to note that *pax6b* may not be the only target of *miR-203* during retina regeneration. Studies of *miR-203* in other systems have identified distinct targets, including *lef1* in the zebrafish caudal fin and *p63* in mouse skin and several cancer models (Thatcher et al., 2008; Yi et al., 2008). I did not detect any interaction of *miR-203* with *lef1* or *p63* during retina regeneration. Additionally, *in situ* hybridizations revealed suppression of *miR-203* expression in not just the MG, but also other INL retinal neurons, suggesting regulatory roles for this miRNA in these cell types. Cell type specific overexpression of *miR-203* could potentially help dissect out its roles in distinct retinal cells.

Role of miR-216 in MG dedifferentiation

Analysis of miRNA expression in MG before and during regeneration identified *miR-216* as a miRNA that is enriched in post-mitotic MG in undamaged retinas, but is suppressed in dedifferentiated MG in regenerating retinas. *miR-216* gain-of-function during regeneration reduced expression of dedifferentiated MG-specific markers β-catenin and the tuba1a:GFP transgene. MG proliferation was drastically reduced, with the effects being highly significant during early stages of regeneration, but less apparent during later stages of regeneration. Possibly, the regenerating retina employs other mechanisms to overcome the repression mediated by excess *miR-216*. Loss of *miR-216* was not sufficient to trigger a statistically significant MG dedifferentiation response in undamaged retinas. However, we consistently detected more dedifferentiated MG in

retinas treated with miR-216 MOs, compared to control MOs, suggesting that effects of *miR-216* suppression on MG dedifferentiation might be biologically relevant. Notably, loss of *miR-216* in undamaged retinas did not reduce MG cell numbers, suggesting that *miR-216* may not be necessary for MG maintenance. This is a crucial finding, since post-mitotic MG in undamaged retinas are enriched for *miR-216* compared to other retinal neurons. Taken together, these results suggest that enrichment of *miR-216* in post-mitotic MG suppresses expression of dedifferentiation related genes.

I analyzed various predicted targets for *miR-216*, focused on those with roles in dedifferentiation and identified the histone methyl transferase *dot1l.* Recent reports in zebrafish intestinal stem cells revealed direct interaction between Dot1l and β-catenin, as well as a role for Dot1l in activating transcription of canonical Wnt targets (Mahmoudi et al., 2010). This is promising since accumulation of β-catenin is necessary for MG dedifferentiation and proliferation (Ramachandran et al., 2011). Our preliminary studies indicate that *miR-216* can target the *dot1l-3'UTR*, ongoing experiments seek to verify direct targeting. Dot1l expression is absent in the undamaged retinas, but begins as early as 24h in what appears to be MG. Analysis of additional MG markers like GFAP and GS will be necessary to verify this, although PCNA labeling suggests that the cells expressing Dot1l are MG. Dot1l loss-of-function during regeneration significantly reduces proliferation, thus emphasizing its importance for regeneration. In the future, we plan to analyze the effects of Dot1l loss on MG dedifferentiation, by assessing β-catenin localization and the tuba1a:GFP transgene expression.

Additionally, we are also trying to understand regulation of *miR-216* expression during regeneration. Analysis of the *miR-216* promoter regions identified binding sites

for the transcriptional repressor Insm1a. Previous work demonstrated expression of Insm1a very early in dedifferentiated MG and the requirement of Insm1a for MG dedifferentiation (Ramachandran et al., 2012). We are performing CHIP experiments to verify Insm1a binding to the *miR-216* promoter regions.

Work from Abby Olena and Mahesh Rao in our lab identified *miR-216* as a regulator of Notch signaling during zebrafish retina development (Olena, 2014). In that model, *miR-216* targets *snx5* (sorting nexin 5), which associates with the Notch ligand Delta and enables Delta endocytosis. This model predicts that *miR-216* functions in cells containing the Notch ligand Delta. My preliminary studies indicate activation of Notch signaling in MG that are associated with progenitor cell clusters around 51h of light damage. *In situ* hybridization studies from the Goldman lab agree with these results, in that they observe expression of Notch ligands in cells adjacent to proliferating $BrdU^+$ cells and expression of Notch receptors in $BrdU^+$ cells (Wan et al., 2012). Additionally, using qPCR of FACS-purified cells, I detected no changes in *snx5* mRNA levels in post-mitotic MG, dedifferentiated MG or progenitor cells during regeneration. However, *snx5* mRNA levels increased in the other retinal neurons as regeneration proceeded. Importantly, the increase in *snx5* mRNA starts around 51h of light damage, which is when I detect notch reporter activity in MG. It is, therefore possible that *miR-216* functions in different pathways in different retinal cells. My data suggest that in the MG, suppression of *miR-216* mediates Dot1l expression and MG dedifferentiation, possibly via canonical Wnt activation. It is possible that in other retinal cells, suppression of *miR-216* allows expression of Snx5, which via its interaction with Delta activates Notch signaling in MG. We are currently performing *in situ* hybridization for *miR-216* across

regeneration to determine the temporal expression of *miR-216* in different retinal cells. Additional experiments are necessary to dissect out the myriad targets of *miR-216* in retina regeneration.

A light lesioning paradigm to damage pigmented zebrafish

Since its development in the Hyde lab, constant intense light exposure has been routinely used to lesion and study regeneration of photoreceptors (Vihtelic and Hyde, 2000). However, this paradigm has been restricted to zebrafish of the *albino* genetic background, which precludes use of transgenic zebrafish lines of the pigmented background. We modified the light lesioning model to permit photoreceptor lesioning in both pigmented and non-pigmented (*albino*) zebrafish. Additionally, we characterized the timing and robustness of the regeneration response and found that initiation and progression of retina regeneration were comparable, irrespective of the pigmentation status of the zebrafish. It will be interesting to test if retina regeneration is completed at similar times in the pigmented and *albino* zebrafish.

Conclusion

In conclusion, work discussed in this thesis emphasizes the overall importance of miRNAs for retina regeneration. Expression of these small RNAs is critical for control of distinct steps during retina regeneration. Taken together with research in other animals, it is apparent that miRNAs are important regulators of tissue regeneration.

REFERENCES

Abou-Khalil, R., and Brack, A.S. (2010). Muscle stem cells and reversible quiescence: the role of sprouty. Cell Cycle *9*, 2575-2580.

Ambros, V. (2003). MicroRNA pathways in flies and worms: growth, death, fat, stress, and timing. Cell *113*, 673-676.

Anokye-Danso, F., Trivedi, C.M., Juhr, D., Gupta, M., Cui, Z., Tian, Y., Zhang, Y., Yang, W., Gruber, P.J., Epstein, J.A.*, et al.* (2011). Highly efficient miRNA-mediated reprogramming of mouse and human somatic cells to pluripotency. Cell Stem Cell *8*, 376-388.

Bar, M., Wyman, S.K., Fritz, B.R., Qi, J., Garg, K.S., Parkin, R.K., Kroh, E.M., Bendoraite, A., Mitchell, P.S., Nelson, A.M.*, et al.* (2008). MicroRNA discovery and profiling in human embryonic stem cells by deep sequencing of small RNA libraries. Stem Cells *26*, 2496-2505.

Bartel, D.P. (2004). MicroRNAs: genomics, biogenesis, mechanism, and function. Cell *116*, 281-297.

Bartel, D.P. (2009). MicroRNAs: target recognition and regulatory functions. Cell *136*, 215-233.

Bartel, D.P., and Chen, C.Z. (2004). Micromanagers of gene expression: the potentially widespread influence of metazoan microRNAs. Nat Rev Genet *5*, 396-400.

Baye, L.M., and Link, B.A. (2008). Nuclear migration during retinal development. Brain Res *1192*, 29-36.

Bentley, D.R., Balasubramanian, S., Swerdlow, H.P., Smith, G.P., Milton, J., Brown, C.G., Hall, K.P., Evers, D.J., Barnes, C.L., Bignell, H.R.*, et al.* (2008). Accurate whole human genome sequencing using reversible terminator chemistry. Nature *456*, 53-59.

Bernardos, R.L., Barthel, L.K., Meyers, J.R., and Raymond, P.A. (2007). Late-stage neuronal progenitors in the retina are radial Muller glia that function as retinal stem cells. J Neurosci *27*, 7028-7040.

Bernardos, R.L., and Raymond, P.A. (2006). GFAP transgenic zebrafish. Gene Expr Patterns *6*, 1007-1013.

Boucher, S.E., and Hitchcock, P.F. (1998). Insulin-like growth factor-I binds in the inner plexiform layer and circumferential germinal zone in the retina of the goldfish. J Comp Neurol *394*, 395-401.

Brennecke, J., Hipfner, D.R., Stark, A., Russell, R.B., and Cohen, S.M. (2003). bantam encodes a developmentally regulated microRNA that controls cell proliferation and regulates the proapoptotic gene hid in Drosophila. Cell *113*, 25-36.

Bringmann, A., Iandiev, I., Pannicke, T., Wurm, A., Hollborn, M., Wiedemann, P., Osborne, N.N., and Reichenbach, A. (2009). Cellular signaling and factors involved in Muller cell gliosis: neuroprotective and detrimental effects. Progress in Retinal and Eye Research *28*, 423-451.

Bringmann, A., Pannicke, T., Grosche, J., Francke, M., Wiedemann, P., Skatchkov, S.N., Osborne, N.N., and Reichenbach, A. (2006). Muller cells in the healthy and diseased retina. Progress in Retinal and Eye Research *25*, 397-424.

Bueno, M.J., Perez de Castro, I., Gomez de Cedron, M., Santos, J., Calin, G.A., Cigudosa, J.C., Croce, C.M., Fernandez-Piqueras, J., and Malumbres, M. (2008). Genetic and epigenetic silencing of microRNA-203 enhances ABL1 and BCR-ABL1 oncogene expression. Cancer Cell *13*, 496-506.

Cai, X., Hagedorn, C.H., and Cullen, B.R. (2004). Human microRNAs are processed from capped, polyadenylated transcripts that can also function as mRNAs. Rna *10*, 1957-1966.

Cameron, D.A. (2000). Cellular proliferation and neurogenesis in the injured retina of adult zebrafish. Visual Neuroscience *17*, 789-797.

Carraro, G., Shrestha, A., Rostkovius, J., Contreras, A., Chao, C.M., El Agha, E., Mackenzie, B., Dilai, S., Guidolin, D., Taketo, M.M.*, et al.* (2014). miR-142-3p balances proliferation and differentiation of mesenchymal cells during lung development. Development *141*, 1272-1281.

Cekaite, L., Rantala, J.K., Bruun, J., Guriby, M., Agesen, T.H., Danielsen, S.A., Lind, G.E., Nesbakken, A., Kallioniemi, O., Lothe, R.A.*, et al.* (2012). MiR-9, -31, and -182 deregulation promote proliferation and tumor cell survival in colon cancer. Neoplasia *14*, 868-879.

Centanin, L., and Wittbrodt, J. (2014). Retinal neurogenesis. Development *141*, 241-244.

Cepko, C.L., Austin, C.P., Yang, X., Alexiades, M., and Ezzeddine, D. (1996). Cell fate determination in the vertebrate retina. Proc Natl Acad Sci U S A *93*, 589-595.

Chen, C.Z., Li, L., Lodish, H.F., and Bartel, D.P. (2004). MicroRNAs modulate hematopoietic lineage differentiation. Science *303*, 83-86.

Chen, J.F., Tao, Y., Li, J., Deng, Z., Yan, Z., Xiao, X., and Wang, D.Z. (2010). microRNA-1 and microRNA-206 regulate skeletal muscle satellite cell proliferation and differentiation by repressing Pax7. J Cell Biol *190*, 867-879.

Chen, P.Y., Manninga, H., Slanchev, K., Chien, M., Russo, J.J., Ju, J., Sheridan, R., John, B., Marks, D.S., Gaidatzis, D.*, et al.* (2005). The developmental miRNA profiles of zebrafish as determined by small RNA cloning. Genes Dev. *19*, 1288-1293.

Chendrimada, T.P., Gregory, R.I., Kumaraswamy, E., Norman, J., Cooch, N., Nishikura, K., and Shiekhattar, R. (2005). TRBP recruits the Dicer complex to Ago2 for microRNA processing and gene silencing. Nature *436*, 740-744.

Cheng, L.C., Pastrana, E., Tavazoie, M., and Doetsch, F. (2009). miR-124 regulates adult neurogenesis in the subventricular zone stem cell niche. Nature Neuroscience *12*, 399-408.

Cheung, T.H., Quach, N.L., Charville, G.W., Liu, L., Park, L., Edalati, A., Yoo, B., Hoang, P., and Rando, T.A. (2012). Maintenance of muscle stem-cell quiescence by microRNA-489. Nature *482*, 524-528.

Close, J.L., Liu, J., Gumuscu, B., and Reh, T.A. (2006). Epidermal growth factor receptor expression regulates proliferation in the postnatal rat retina. Glia *54*, 94-104.

Connaughton, V.P., Graham, D., and Nelson, R. (2004). Identification and morphological classification of horizontal, bipolar, and amacrine cells within the zebrafish retina. J Comp Neurol *477*, 371-385.

Conte, I., Carrella, S., Avellino, R., Karali, M., Marco-Ferreres, R., Bovolenta, P., and Banfi, S. (2010). miR-204 is required for lens and retinal development via Meis2 targeting. Proc Natl Acad Sci U S A *107*, 15491-15496.

Cremisi, F. (2013). MicroRNAs and cell fate in cortical and retinal development. Frontiers in Cellular Neuroscience *7*, 141.

Crist, C.G., Montarras, D., and Buckingham, M. (2012). Muscle satellite cells are primed for myogenesis but maintain quiescence with sequestration of Myf5 mRNA targeted by microRNA-31 in mRNP granules. Cell Stem Cell *11*, 118-126.

Crist, C.G., Montarras, D., Pallafacchina, G., Rocancourt, D., Cumano, A., Conway, S.J., and Buckingham, M. (2009). Muscle stem cell behavior is modified by microRNA-27 regulation of Pax3 expression. Proc Natl Acad Sci U S A *106*, 13383-13387.

Damiani, D., Alexander, J.J., O'Rourke, J.R., McManus, M., Jadhav, A.P., Cepko, C.L., Hauswirth, W.W., Harfe, B.D., and Strettoi, E. (2008). Dicer inactivation leads to progressive functional and structural degeneration of the mouse retina. J Neurosci *28*, 4878-4887.

de Chevigny, A., Core, N., Follert, P., Gaudin, M., Barbry, P., Beclin, C., and Cremer, H. (2012). miR-7a regulation of Pax6 controls spatial origin of forebrain dopaminergic neurons. Nat Neurosci *15*, 1120-1126.

Decembrini, S., Bressan, D., Vignali, R., Pitto, L., Mariotti, S., Rainaldi, G., Wang, X., Evangelista, M., Barsacchi, G., and Cremisi, F. (2009). MicroRNAs couple cell fate and developmental timing in retina. Proc Natl Acad Sci U S A *106*, 21179-21184.

Del Debbio, C.B., Balasubramanian, S., Parameswaran, S., Chaudhuri, A., Qiu, F., and Ahmad, I. (2010). Notch and Wnt signaling mediated rod photoreceptor regeneration by Muller cells in adult mammalian retina. PloS one *5*, e12425.

Denli, A.M., Tops, B.B., Plasterk, R.H., Ketting, R.F., and Hannon, G.J. (2004). Processing of primary microRNAs by the Microprocessor complex. Nature *432*, 231-235.

Diao, Y., Guo, X., Jiang, L., Wang, G., Zhang, C., Wan, J., Jin, Y., and Wu, Z. (2013). miR-203, a tumor suppressor frequently down-regulated by promoter hypermethylation in Rhabdomyosarcoma. The Journal of Biological Chemistry *288*, 18923-18938.

Dotto, G.P. (2012). p63 and FGFR: when development meets proliferation. EMBO Molecular Medicine *4*, 165-167.

Dunmire, J.J., Lagouros, E., Bouhenni, R.A., Jones, M., and Edward, D.P. (2013). MicroRNA in aqueous humor from patients with cataract. Exp Eye Res *108*, 68-71.

Dyer, M.A., and Cepko, C.L. (2000). Control of Muller glial cell proliferation and activation following retinal injury. Nat Neurosci *3*, 873-880.

Fausett, B.V., and Goldman, D. (2006). A role for alpha1 tubulin-expressing Muller glia in regeneration of the injured zebrafish retina. J Neurosci *26*, 6303-6313.

Fimbel, S.M., Montgomery, J.E., Burket, C.T., and Hyde, D.R. (2007). Regeneration of inner retinal neurons after intravitreal injection of ouabain in zebrafish. J Neurosci *27*, 1712-1724.

Fischer, A.J., and Reh, T.A. (2000). Identification of a proliferating marginal zone of retinal progenitors in postnatal chickens. Dev Biol *220*, 197-210.

Fischer, A.J., and Reh, T.A. (2003). Potential of Muller glia to become neurogenic retinal progenitor cells. Glia *43*, 70-76.

Flynt, A.S., Li, N., Thatcher, E.J., Solnica-Krezel, L., and Patton, J.G. (2007). Zebrafish miR-214 modulates Hedgehog signaling to specify muscle cell fate. Nat Genet *39*, 259-263.

Forstemann, K., Tomari, Y., Du, T., Vagin, V.V., Denli, A.M., Bratu, D.P., Klattenhoff, C., Theurkauf, W.E., and Zamore, P.D. (2005). Normal microRNA maturation and germ-line stem cell maintenance requires Loquacious, a double-stranded RNA-binding domain protein. PLoS Biol *3*, e236.

Georgi, S.A., and Reh, T.A. (2010). Dicer is required for the transition from early to late progenitor state in the developing mouse retina. J Neurosci *30*, 4048-4061.

Gregory, R.I., Chendrimada, T.P., Cooch, N., and Shiekhattar, R. (2005). Human RISC couples microRNA biogenesis and posttranscriptional gene silencing. Cell *123*, 631-640.

Gregory, R.I., Yan, K.P., Amuthan, G., Chendrimada, T., Doratotaj, B., Cooch, N., and Shiekhattar, R. (2004). The Microprocessor complex mediates the genesis of microRNAs. Nature *432*, 235-240.

Grishok, A., Pasquinelli, A.E., Conte, D., Li, N., Parrish, S., Ha, I., Baillie, D.L., Fire, A., Ruvkun, G., and Mello, C.C. (2001). Genes and mechanisms related to RNA interference regulate expression of the small temporal RNAs that control C. elegans developmental timing. Cell *106*, 23-34.

Guo, S., Lu, J., Schlanger, R., Zhang, H., Wang, J.Y., Fox, M.C., Purton, L.E., Fleming, H.H., Cobb, B., Merkenschlager, M.*, et al.* (2010). MicroRNA miR-125a controls hematopoietic stem cell number. Proc Natl Acad Sci U S A *107*, 14229-14234.

Gwizdek, C., Bertrand, E., Dargemont, C., Lefebvre, J.C., Blanchard, J.M., Singer, R.H., and Doglio, A. (2001). Terminal minihelix, a novel RNA motif that directs polymerase III transcripts to the cell cytoplasm. Terminal minihelix and RNA export. The Journal of Biological Chemistry *276*, 25910-25918.

Gwizdek, C., Ossareh-Nazari, B., Brownawell, A.M., Doglio, A., Bertrand, E., Macara, I.G., and Dargemont, C. (2003). Exportin-5 mediates nuclear export of minihelix-containing RNAs. The Journal of Biological Chemistry *278*, 5505-5508.

Gwizdek, C., Ossareh-Nazari, B., Brownawell, A.M., Evers, S., Macara, I.G., and Dargemont, C. (2004). Minihelix-containing RNAs mediate exportin-5-dependent nuclear export of the double-stranded RNA-binding protein ILF3. The Journal of Biological Chemistry *279*, 884-891.

Hackler, L., Jr., Wan, J., Swaroop, A., Qian, J., and Zack, D.J. (2010). MicroRNA profile of the developing mouse retina. Invest Ophthalmol Vis Sci *51*, 1823-1831.

Han, J., Lee, Y., Yeom, K.H., Kim, Y.K., Jin, H., and Kim, V.N. (2004). The Drosha-DGCR8 complex in primary microRNA processing. Genes Dev *18*, 3016-3027.

Harris, W.A. (1997). Cellular diversification in the vertebrate retina. Curr Opin Genet Dev *7*, 651-658.

Hitchcock, P., Ochocinska, M., Sieh, A., and Otteson, D. (2004). Persistent and injury-induced neurogenesis in the vertebrate retina. Progress in Retinal & Eye Research *23*, 183-194.

Houbaviy, H.B., Murray, M.F., and Sharp, P.A. (2003). Embryonic stem cell-specific MicroRNAs. Dev Cell *5*, 351-358.

Hutvagner, G., McLachlan, J., Pasquinelli, A.E., Balint, E., Tuschl, T., and Zamore, P.D. (2001). A cellular function for the RNA-interference enzyme Dicer in the maturation of the let-7 small temporal RNA. Science *293*, 834-838.

Iida, A., Shinoe, T., Baba, Y., Mano, H., and Watanabe, S. (2011). Dicer plays essential roles for retinal development by regulation of survival and differentiation. Invest Ophthalmol Vis Sci *52*, 3008-3017.

Jackson, S.J., Zhang, Z., Feng, D., Flagg, M., O'Loughlin, E., Wang, D., Stokes, N., Fuchs, E., and Yi, R. (2013). Rapid and widespread suppression of self-renewal by microRNA-203 during epidermal differentiation. Development *140*, 1882-1891.

Jadhav, A.P., Roesch, K., and Cepko, C.L. (2009). Development and neurogenic potential of Muller glial cells in the vertebrate retina. Progress in Retinal and Eye Research *28*, 249-262.

Johns, P.R. (1977). Growth of the adult goldfish eye. III. Source of the new retinal cells. J Comp Neurol *176*, 343-357.

Johns, P.R., and Easter, S.S., Jr. (1977). Growth of the adult goldfish eye. II. Increase in retinal cell number. J Comp Neurol *176*, 331-341.

Judson, R.L., Babiarz, J.E., Venere, M., and Blelloch, R. (2009). Embryonic stem cell-specific microRNAs promote induced pluripotency. Nat Biotechnol *27*, 459-461.

Jusuf, P.R., Almeida, A.D., Randlett, O., Joubin, K., Poggi, L., and Harris, W.A. (2011). Origin and determination of inhibitory cell lineages in the vertebrate retina. J Neurosci *31*, 2549-2562.

Kanellopoulou, C., Muljo, S., Kung, A., Ganesan, S., Drapkin, R., Jenuwein, T., Livingston, D., and Rajewsky, K. (2005). Dicer-deficient mouse embryonic stem cells are defective in differentiation and centromeric silencing. Genes & Dev. *19*, 489-501.

Kapsimali, M., Kloosterman, W.P., de Bruijn, E., Rosa, F., Plasterk, R.H., and Wilson, S.W. (2007). MicroRNAs show a wide diversity of expression profiles in the developing and mature central nervous system. Genome Biol *8*, R173.

Karali, M., Peluso, I., Gennarino, V.A., Bilio, M., Verde, R., Lago, G., Dolle, P., and Banfi, S. (2010). miRNeye: a microRNA expression atlas of the mouse eye. BMC Genomics *11*, 715.

Karin, M., and Chang, L. (2001). AP-1--glucocorticoid receptor crosstalk taken to a higher level. The Journal of Endocrinology *169*, 447-451.

Karl, M.O., Hayes, S., Nelson, B.R., Tan, K., Buckingham, B., and Reh, T.A. (2008). Stimulation of neural regeneration in the mouse retina. Proc Natl Acad Sci U S A *105*, 19508-19513.

Karl, M.O., and Reh, T.A. (2010). Regenerative medicine for retinal diseases: activating endogenous repair mechanisms. Trends Mol Med *16*, 193-202.

Kassen, S.C., Ramanan, V., Montgomery, J.E., C, T.B., Liu, C.G., Vihtelic, T.S., and Hyde, D.R. (2007). Time course analysis of gene expression during light-induced photoreceptor cell death and regeneration in albino zebrafish. Developmental Neurobiology *67*, 1009-1031.

Ketting, R.F., Fischer, S., Bernstein, E., Sijen, T., Hannon, G.J., and Plasterk, R. (2001). Dicer functions in RNA interfence and in synthesis of small RNA involved in developmental timing in *C. elegans*. Genes & Dev. *15*, 2654-2659.

Kim, V.N., and Nam, J.W. (2006). Genomics of microRNA. Trends Genet *22*, 165-173.

Kloosterman, W.P., and Plasterk, R.H. (2006). The diverse functions of microRNAs in animal development and disease. Dev Cell *11*, 441-450.

Koboldt, D.C., Steinberg, K.M., Larson, D.E., Wilson, R.K., and Mardis, E.R. (2013). The next-generation sequencing revolution and its impact on genomics. Cell *155*, 27-38.

Kovacs, B., Lumayag, S., Cowan, C., and Xu, S. (2011). MicroRNAs in early diabetic retinopathy in streptozotocin-induced diabetic rats. Invest Ophthalmol Vis Sci *52*, 4402-4409.

Kozomara, A., and Griffiths-Jones, S. (2011). miRBase: integrating microRNA annotation and deep-sequencing data. Nucleic Acids Res *39*, D152-157.

Kuchenbauer, F., Morin, R.D., Argiropoulos, B., Petriv, O.I., Griffith, M., Heuser, M., Yung, E., Piper, J., Delaney, A., Prabhu, A.L.*, et al.* (2008). In-depth characterization of the microRNA transcriptome in a leukemia progression model. Genome Res *18*, 1787-1797.

La Torre, A., Georgi, S., and Reh, T.A. (2013). Conserved microRNA pathway regulates developmental timing of retinal neurogenesis. Proc Natl Acad Sci U S A *110*, E2362-2370.

Lagos-Quintana, M., Rauhut, R., Lendeckel, W., and Tuschl, T. (2001). Identification of novel genes coding for small expressed RNAs. Science *294*, 853-858.

Lagos-Quintana, M., Rauhut, R., Meyer, J., Borkhardt, A., and Tuschl, T. (2003). New microRNAs from mouse and human. Rna *9*, 175-179.

Lamba, D., Karl, M., and Reh, T. (2008). Neural Regeneration and Cell Replacement: A view from the eye. Cell Stem Cell *2*, 538-549.

Langmead, B., Trapnell, C., Pop, M., and Salzberg, S.L. (2009). Ultrafast and memory-efficient alignment of short DNA sequences to the human genome. Genome Biol *10*, R25.

Lee, H., and Kimelman, D. (2002). A dominant-negative form of p63 is required for epidermal proliferation in zebrafish. Dev Cell *2*, 607-616.

Lee, R.C., Feinbaum, R.L., and Ambros, V. (1993). The C. elegans heterochronic gene lin-4 encodes small RNAs with antisense complementarity to lin-14. Cell *75*, 843-854.

Lee, Y., Ahn, C., Han, J., Choi, H., Kim, J., Yim, J., Lee, J., Provost, P., Radmark, O., Kim, S.*, et al.* (2003). The nuclear RNase III Drosha initiates microRNA processing. Nature *425*, 415-419.

Lee, Y., Kim, M., Han, J., Yeom, K.H., Lee, S., Baek, S.H., and Kim, V.N. (2004). MicroRNA genes are transcribed by RNA polymerase II. Embo J *23*, 4051-4060.

Lena, A.M., Shalom-Feuerstein, R., Rivetti di Val Cervo, P., Aberdam, D., Knight, R.A., Melino, G., and Candi, E. (2008). miR-203 represses 'stemness' by repressing DeltaNp63. Cell Death Differ *15*, 1187-1195.

Lenkowski, J.R., Qin, Z., Sifuentes, C.J., Thummel, R., Soto, C.M., Moens, C.B., and Raymond, P.A. (2013). Retinal regeneration in adult zebrafish requires regulation of TGFbeta signaling. Glia *61*, 1687-1697.

Lewis, B.P., Burge, C.B., and Bartel, D.P. (2005). Conserved seed pairing, often flanked by adenosines, indicates that thousands of human genes are microRNA targets. Cell *120*, 15-20.

Liu, C., Teng, Z.Q., Santistevan, N.J., Szulwach, K.E., Guo, W., Jin, P., and Zhao, X. (2010). Epigenetic regulation of miR-184 by MBD1 governs neural stem cell proliferation and differentiation. Cell Stem Cell *6*, 433-444.

Livesey, F.J., and Cepko, C.L. (2001). Vertebrate neural cell-fate determination: lessons from the retina. Nat Rev Neurosci *2*, 109-118.

Loscher, C.J., Hokamp, K., Kenna, P.F., Ivens, A.C., Humphries, P., Palfi, A., and Farrar, G.J. (2007). Altered retinal microRNA expression profile in a mouse model of retinitis pigmentosa. Genome Biol *8*, R248.

Loscher, C.J., Hokamp, K., Wilson, J.H., Li, T., Humphries, P., Farrar, G.J., and Palfi, A. (2008). A common microRNA signature in mouse models of retinal degeneration. Exp Eye Res *87*, 529-534.

Lozano-Velasco, E., Contreras, A., Crist, C., Hernandez-Torres, F., Franco, D., and Aranega, A.E. (2011). Pitx2c modulates Pax3+/Pax7+ cell populations and regulates Pax3 expression by repressing miR27 expression during myogenesis. Dev Biol *357*, 165-178.

Lu, C., Zhang, J., Nie, Z., Chen, J., Zhang, W., Ren, X., Yu, W., Liu, L., Jiang, C., Zhang, Y.*, et al.* (2013). Study of microRNAs related to the liver regeneration of the whitespotted bamboo shark, Chiloscyllium plagiosum. BioMed Research International *2013*, 795676.

Lu, J., Guo, S., Ebert, B.L., Zhang, H., Peng, X., Bosco, J., Pretz, J., Schlanger, R., Wang, J.Y., Mak, R.H., *et al.* (2008). MicroRNA-mediated control of cell fate in megakaryocyte-erythrocyte progenitors. Dev Cell *14*, 843-853.

Lumayag, S., Haldin, C.E., Corbett, N.J., Wahlin, K.J., Cowan, C., Turturro, S., Larsen, P.E., Kovacs, B., Witmer, P.D., Valle, D., *et al.* (2013). Inactivation of the microRNA-183/96/182 cluster results in syndromic retinal degeneration. Proc Natl Acad Sci U S A *110*, E507-516.

Mahmoudi, T., Boj, S.F., Hatzis, P., Li, V.S., Taouatas, N., Vries, R.G., Teunissen, H., Begthel, H., Korving, J., Mohammed, S., *et al.* (2010). The leukemia-associated Mllt10/Af10-Dot1l are Tcf4/beta-catenin coactivators essential for intestinal homeostasis. PLoS Biol *8*, e1000539.

Masland, R.H. (2001). Neuronal diversity in the retina. Curr Opin Neurobiol *11*, 431-436.

Masland, R.H. (2012). The neuronal organization of the retina. Neuron *76*, 266-280.

Matranga, C., Tomari, Y., Shin, C., Bartel, D.P., and Zamore, P.D. (2005). Passenger-strand cleavage facilitates assembly of siRNA into Ago2-containing RNAi enzyme complexes. Cell *123*, 607-620.

Melton, C., Judson, R.L., and Blelloch, R. (2010). Opposing microRNA families regulate self-renewal in mouse embryonic stem cells. Nature *463*, 621-626.

Mensinger, A.F., and Powers, M.K. (2007). Visual function in regenerating teleost retina following surgical lesioning. Vis Neurosci *24*, 299-307.

Miska, E.A., Alvarez-Saavedra, E., Abbott, A.L., Lau, N.C., Hellman, A.B., McGonagle, S.M., Bartel, D.P., Ambros, V.R., and Horvitz, H.R. (2007). Most Caenorhabditis elegans microRNAs are individually not essential for development or viability. PLoS Genet *3*, e215.

Mitashov, V.I. (1997). Retinal regeneration in amphibians. Int J Dev Biol *41*, 893-905.

Miyoshi, N., Ishii, H., Nagano, H., Haraguchi, N., Dewi, D.L., Kano, Y., Nishikawa, S., Tanemura, M., Mimori, K., Tanaka, F., *et al.* (2011). Reprogramming of mouse and human cells to pluripotency using mature microRNAs. Cell Stem Cell *8*, 633-638.

Montgomery, J.E., Parsons, M.J., and Hyde, D.R. (2010). A novel model of retinal ablation demonstrates that the extent of rod cell death regulates the origin of the regenerated zebrafish rod photoreceptors. J Comp Neurol *518*, 800-814.

Morin, R.D., O'Connor, M.D., Griffith, M., Kuchenbauer, F., Delaney, A., Prabhu, A.L., Zhao, Y., McDonald, H., Zeng, T., Hirst, M., *et al.* (2008). Application of massively parallel sequencing to microRNA profiling and discovery in human embryonic stem cells. Genome Research *18*, 610-621.

Morris, J.P.t., and McManus, M.T. (2005). Slowing down the Ras lane: miRNAs as tumor suppressors? Sci STKE *2005*, pe41.

Moshiri, A., Close, J., and Reh, T.A. (2004). Retinal stem cells and regeneration. Int J Dev Biol *48*, 1003-1014.

Moshiri, A., McGuire, C.R., and Reh, T.A. (2005). Sonic hedgehog regulates proliferation of the retinal ciliary marginal zone in posthatch chicks. Dev Dyn *233*, 66-75.

Mutz, K.O., Heilkenbrinker, A., Lonne, M., Walter, J.G., and Stahl, F. (2013). Transcriptome analysis using next-generation sequencing. Curr Opin Biotechnol *24*, 22-30.

Nagashima, M., Barthel, L.K., and Raymond, P.A. (2013). A self-renewing division of zebrafish Muller glial cells generates neuronal progenitors that require N-cadherin to regenerate retinal neurons. Development *140*, 4510-4521.

Nelson, C.M., Ackerman, K.M., O'Hayer, P., Bailey, T.J., Gorsuch, R.A., and Hyde, D.R. (2013). Tumor necrosis factor-alpha is produced by dying retinal neurons and is required for Muller glia proliferation during zebrafish retinal regeneration. J Neurosci *33*, 6524-6539.

Nobuta, K., Lu, C., Shrivastava, R., Pillay, M., De Paoli, E., Accerbi, M., Arteaga-Vazquez, M., Sidorenko, L., Jeong, D.H., Yen, Y.*, et al.* (2008). Distinct size distribution of endogeneous siRNAs in maize: Evidence from deep sequencing in the mop1-1 mutant. Proc Natl Acad Sci U S A *105*, 14958-14963.

Noell, W.K., Walker, V.S., Kang, B.S., and Berman, S. (1966). Retinal damage by light in rats. Investigative Ophthalmology *5*, 450-473.

O'Donnell, K.A., Wentzel, E.A., Zeller, K.I., Dang, C.V., and Mendell, J.T. (2005). c-Myc-regulated microRNAs modulate E2F1 expression. Nature *435*, 839-843.

Olena, A.F., and Patton, J.G. (2010). Genomic organization of microRNAs. Journal of Cellular Physiology *222*, 540-545.

Olena, A.F., Rao, M., Thatcher, E. J., Patton, J. G. (2014). miR-216a regulates snx5, a novel Notch signaling pathway component, during zebrafish retinal development. Developmental Biology *Submitted*.

Ooto, S., Akagi, T., Kageyama, R., Akita, J., Mandai, M., Honda, Y., and Takahashi, M. (2004). Potential for neural regeneration after neurotoxic injury in the adult mammalian retina. Proc Natl Acad Sci U S A *101*, 13654-13659.

Organisciak, D.T., and Vaughan, D.K. (2010). Retinal light damage: mechanisms and protection. Progress in Retinal and Eye Research *29*, 113-134.

Otteson, D.C., and Hitchcock, P.F. (2003). Stem cells in the teleost retina: persistent neurogenesis and injury-induced regeneration. Vision Research *43*, 927-936.

Park, J.K., Kogure, T., Nuovo, G.J., Jiang, J., He, L., Kim, J.H., Phelps, M.A., Papenfuss, T.L., Croce, C.M., Patel, T.*, et al.* (2011). miR-221 silencing blocks hepatocellular carcinoma and promotes survival. Cancer Res *71*, 7608-7616.

Parsa, R., Yang, A., McKeon, F., and Green, H. (1999). Association of p63 with proliferative potential in normal and neoplastic human keratinocytes. The Journal of Investigative Dermatology *113*, 1099-1105.

Pasquinelli, A.E., Reinhart, B.J., Slack, F., Martindale, M.Q., Kuroda, M.I., Maller, B., Hayward, D.C., Ball, E.E., Degnan, B., Muller, P.*, et al.* (2000). Conservation of the sequence and temporal expression of let-7 heterochronic regulatory RNA. Nature *408*, 86-89.

Pei, Y.F., and Rhodin, J.A. (1970). The prenatal development of the mouse eye. The Anatomical Record *168*, 105-125.

Petriv, O.I., Kuchenbauer, F., Delaney, A.D., Lecault, V., White, A., Kent, D., Marmolejo, L., Heuser, M., Berg, T., Copley, M.*, et al.* (2010). Comprehensive microRNA expression profiling of the hematopoietic hierarchy. Proc Natl Acad Sci U S A *107*, 15443-15448.

Pinter, R., and Hindges, R. (2010). Perturbations of microRNA function in mouse dicer mutants produce retinal defects and lead to aberrant axon pathfinding at the optic chiasm. PloS one *5*, e10021.

Plasterk, R.H. (2006). Micro RNAs in animal development. Cell *124*, 877-881.

Pollak, J., Wilken, M.S., Ueki, Y., Cox, K.E., Sullivan, J.M., Taylor, R.J., Levine, E.M., and Reh, T.A. (2013). ASCL1 reprograms mouse Muller glia into neurogenic retinal progenitors. Development *140*, 2619-2631.

Powell, C., Grant, A.R., Cornblath, E., and Goldman, D. (2013). Analysis of DNA methylation reveals a partial reprogramming of the Muller glia genome during retina regeneration. Proc Natl Acad Sci U S A *110*, 19814-19819.

Poy, M.N., Eliasson, L., Krutzfeldt, J., Kuwajima, S., Ma, X., Macdonald, P.E., Pfeffer, S., Tuschl, T., Rajewsky, N., Rorsman, P.*, et al.* (2004). A pancreatic islet-specific microRNA regulates insulin secretion. Nature *432*, 226-230.

Qin, Z., and Raymond, P.A. (2012). Microarray-based gene profiling analysis of Muller glia-derived retinal stem cells in light-damaged retinas from adult zebrafish. Methods Mol Biol *884*, 255-261.

Ragusa, M., Caltabiano, R., Russo, A., Puzzo, L., Avitabile, T., Longo, A., Toro, M.D., Di Pietro, C., Purrello, M., and Reibaldi, M. (2013). MicroRNAs in vitreus humor from patients with ocular diseases. Mol Vis *19*, 430-440.

Rajaram, K., Harding, R., Bailey, T.J, Hyde, D.R., and Patton, J.G. (2014a). Dynamic miRNA Expression Patterns During Retina Regeneration in Zebrafish:
Loss of Dicer Inhibits Regeneration. Developmental Dynamics *Submitted*

Rajaram, K., Harding, R., Hyde, D.R., and Patton, J.G. (2014b). miR-203 regulates progenitor cell proliferation during adult zebrafish retina regeneration. Developmental Biology *In press*.

Ramachandran, R., Fausett, B.V., and Goldman, D. (2010). Ascl1a regulates Muller glia dedifferentiation and retinal regeneration through a Lin-28-dependent, let-7 microRNA signalling pathway. Nat Cell Biol *12*, 1101-1107.

Ramachandran, R., Zhao, X.F., and Goldman, D. (2011). Ascl1a/Dkk/beta-catenin signaling pathway is necessary and glycogen synthase kinase-3beta inhibition is sufficient for zebrafish retina regeneration. Proc Natl Acad Sci U S A *108*, 15858-15863.

Ramachandran, R., Zhao, X.F., and Goldman, D. (2012). Insm1a-mediated gene repression is essential for the formation and differentiation of Muller glia-derived progenitors in the injured retina. Nat Cell Biol *14*, 1013-1023.

Rand, T.A., Petersen, S., Du, F., and Wang, X. (2005). Argonaute2 cleaves the anti-guide strand of siRNA during RISC activation. Cell *123*, 621-629.

Rapaport, D.H., and Vietri, A.J. (1991). Identity of cells produced by two stages of cytogenesis in the postnatal cat retina. J Comp Neurol *312*, 341-352.

Rapp, L.M., and Williams, T.P. (1980). The role of ocular pigmentation in protecting against retinal light damage. Vision Res *20*, 1127-1131.

Reh, T.A., and Nagy, T. (1987). A possible role for the vascular membrane in retinal regeneration in Rana catesbienna tadpoles. Dev Biol *122*, 471-482.

Reichenbach, A., and Bringmann, A. (2013). New functions of Muller cells. Glia *61*, 651-678.

Reinhart, B.J., Slack, F.J., Basson, M., Pasquinelli, A.E., Bettinger, J.C., Rougvie, A.E., Horvitz, H.R., and Ruvkun, G. (2000). The 21-nucleotide let-7 RNA regulates developmental timing in Caenorhabditis elegans. Nature *403*, 901-906.

Rivetti di Val Cervo, P., Lena, A.M., Nicoloso, M., Rossi, S., Mancini, M., Zhou, H., Saintigny, G., Dellambra, E., Odorisio, T., Mahe, C.*, et al.* (2012). p63-microRNA feedback in keratinocyte senescence. Proc Natl Acad Sci U S A *109*, 1133-1138.

Roesch, K., Jadhav, A.P., Trimarchi, J.M., Stadler, M.B., Roska, B., Sun, B.B., and Cepko, C.L. (2008). The transcriptome of retinal Muller glial cells. J Comp Neurol *509*, 225-238.

Saeed, A.I., Sharov, V., White, J., Li, J., Liang, W., Bhagabati, N., Braisted, J., Klapa, M., Currier, T., Thiagarajan, M.*, et al.* (2003). TM4: a free, open-source system for microarray data management and analysis. BioTechniques *34*, 374-378.

Sanuki, R., Onishi, A., Koike, C., Muramatsu, R., Watanabe, S., Muranishi, Y., Irie, S., Uneo, S., Koyasu, T., Matsui, R.*, et al.* (2011). miR-124a is required for hippocampal axogenesis and retinal cone survival through Lhx2 suppression. Nat Neurosci *14*, 1125-1134.

Saul, K.E., Koke, J.R., and Garcia, D.M. (2010). Activating transcription factor 3 (ATF3) expression in the neural retina and optic nerve of zebrafish during optic nerve regeneration. Comparative biochemistry and physiology. Part A, Molecular & integrative physiology *155*, 172-182.

Scott, C.E., Wynn, S.L., Sesay, A., Cruz, C., Cheung, M., Gomez Gaviro, M.V., Booth, S., Gao, B., Cheah, K.S., Lovell-Badge, R.*, et al.* (2010). SOX9 induces and maintains neural stem cells. Nat Neurosci *13*, 1181-1189.

Sehm, T., Sachse, C., Frenzel, C., and Echeverri, K. (2009). miR-196 is an essential early-stage regulator of tail regeneration, upstream of key spinal cord patterning events. Dev Biol *334*, 468-480.

Selbach, M., Schwanhausser, B., Thierfelder, N., Fang, Z., Khanin, R., and Rajewsky, N. (2008). Widespread changes in protein synthesis induced by microRNAs. Nature *455*, 58-63.

Senoo, M., Pinto, F., Crum, C.P., and McKeon, F. (2007). p63 Is essential for the proliferative potential of stem cells in stratified epithelia. Cell *129*, 523-536.

Sidman, R.L. (1961). Histogenesis of mouse retina studies with thymidine-H3 (New York: Academic Press).

Slack, F.J., Basson, M., Liu, Z., Ambros, V., Horvitz, H.R., and Ruvkun, G. (2000). The lin-41 RBCC gene acts in the C. elegans heterochronic pathway between the let-7 regulatory RNA and the LIN-29 transcription factor. Mol Cell *5*, 659-669.

Slack, F.J., and Weidhaas, J.B. (2006). MicroRNAs as a potential magic bullet in cancer. Future Oncol *2*, 73-82.

Sonkoly, E., Wei, T., Pavez Lorie, E., Suzuki, H., Kato, M., Torma, H., Stahle, M., and Pivarcsi, A. (2010). Protein kinase C-dependent upregulation of miR-203 induces the differentiation of human keratinocytes. The Journal of Investigative Dermatology *130*, 124-134.

Stenkamp, D.L. (2007). Neurogenesis in the fish retina. International Review of Cytology *259*, 173-224.

Stone, L.S. (1950). Neural retina degeneration followed by regeneration from surviving retinal pigment cells in grafted adult salamander eyes. The Anatomical Record *106*, 89-109.

Subramanyam, D., Lamouille, S., Judson, R.L., Liu, J.Y., Bucay, N., Derynck, R., and Blelloch, R. (2011). Multiple targets of miR-302 and miR-372 promote reprogramming of human fibroblasts to induced pluripotent stem cells. Nat Biotechnol *29*, 443-448.

Sun, H., and Nathans, J. (2001). The challenge of macular degeneration. Scientific American *285*, 68-75.

Sun, K., and Lai, E.C. (2013). Adult-specific functions of animal microRNAs. Nat Rev Genet *14*, 535-548.

Sunkar, R., Zhou, X., Zheng, Y., Zhang, W., and Zhu, J.K. (2008). Identification of novel and candidate miRNAs in rice by high throughput sequencing. BMC Plant Biology *8*, 25.

Takeda, M., Takamiya, A., Jiao, J.W., Cho, K.S., Trevino, S.G., Matsuda, T., and Chen, D.F. (2008). alpha-Aminoadipate induces progenitor cell properties of Muller glia in adult mice. Invest Ophthalmol Vis Sci *49*, 1142-1150.

Taube, J.H., Malouf, G.G., Lu, E., Sphyris, N., Vijay, V., Ramachandran, P.P., Ueno, K.R., Gaur, S., Nicoloso, M.S., Rossi, S.*, et al.* (2013). Epigenetic silencing of microRNA-203 is required for EMT and cancer stem cell properties. Scientific Reports *3*, 2687.

Thatcher, E.J., Flynt, A.S., Li, N., Patton, J.R., and Patton, J.G. (2007). MiRNA expression analysis during normal zebrafish development and following inhibition of the Hedgehog and Notch signaling pathways. Dev Dyn *236*, 2172-2180.

Thatcher, E.J., and Patton, J.G. (2010). Small RNAs have a big impact on regeneration. RNA Biol *7*, 333-338.

Thatcher, E.J., Paydar, I., Anderson, K.K., and Patton, J.G. (2008). Regulation of zebrafish fin regeneration by microRNAs. Proc Natl Acad Sci USA *105*, 18384-18389.

Thomas, J.L., Nelson, C.M., Luo, X., Hyde, D.R., and Thummel, R. (2012). Characterization of multiple light damage paradigms reveals regional differences in photoreceptor loss. Exp Eye Res *97*, 105-116.

Thomas, J.L., and Thummel, R. (2013). A novel light damage paradigm for use in retinal regeneration studies in adult zebrafish. Journal of visualized experiments : JoVE, e51017.

Thummel, R., Enright, J.M., Kassen, S.C., Montgomery, J.E., Bailey, T.J., and Hyde, D.R. (2010). Pax6a and Pax6b are required at different points in neuronal progenitor cell proliferation during zebrafish photoreceptor regeneration. Exp Eye Res *90*, 572-582.

Thummel, R., Kassen, S.C., Enright, J.M., Nelson, C.M., Montgomery, J.E., and Hyde, D.R. (2008a). Characterization of Muller glia and neuronal progenitors during adult zebrafish retinal regeneration. Experimental Eye Research *87*, 433-444.

Thummel, R., Kassen, S.C., Montgomery, J.E., Enright, J.M., and Hyde, D.R. (2008b). Inhibition of Muller glial cell division blocks regeneration of the light-damaged zebrafish retina. Developmental Neurobiology *68*, 392-408.

Trimarchi, J.M., Stadler, M.B., and Cepko, C.L. (2008). Individual retinal progenitor cells display extensive heterogeneity of gene expression. PloS one *3*, e1588.

Truong, A.B., Kretz, M., Ridky, T.W., Kimmel, R., and Khavari, P.A. (2006). p63 regulates proliferation and differentiation of developmentally mature keratinocytes. Genes Dev *20*, 3185-3197.

Tsonis, P.A., Call, M.K., Grogg, M.W., Sartor, M.A., Taylor, R.R., Forge, A., Fyffe, R., Goldenberg, R., Cowper-Sal-lari, R., and Tomlinson, C.R. (2007). MicroRNAs and regeneration: Let-7 members as potential regulators of dedifferentiation in lens and inner ear hair cell regeneration of the adult newt. Biochemical and Biophysical Research Communications *362*, 940-945.

Valastyan, S., and Weinberg, R.A. (2011). Tumor metastasis: molecular insights and evolving paradigms. Cell *147*, 275-292.

Vihtelic, T.S., and Hyde, D.R. (2000). Light-induced rod and cone cell death and regeneration in the adult albino zebrafish (Danio rerio) retina. J Neurobiol *44*, 289-307.

Vihtelic, T.S., Soverly, J.E., Kassen, S.C., and Hyde, D.R. (2006). Retinal regional differences in photoreceptor cell death and regeneration in light-lesioned albino zebrafish. Exp Eye Res *82*, 558-575.

Viticchie, G., Lena, A.M., Cianfarani, F., Odorisio, T., Annicchiarico-Petruzzelli, M., Melino, G., and Candi, E. (2012). MicroRNA-203 contributes to skin re-epithelialization. Cell Death & Disease *3*, e435.

Viticchie, G., Lena, A.M., Latina, A., Formosa, A., Gregersen, L.H., Lund, A.H., Bernardini, S., Mauriello, A., Miano, R., Spagnoli, L.G.*, et al.* (2011). MiR-203 controls proliferation, migration and invasive potential of prostate cancer cell lines. Cell Cycle *10*, 1121-1131.

Walker, J.C., and Harland, R.M. (2009). microRNA-24a is required to repress apoptosis in the developing neural retina. Genes Dev *23*, 1046-1051.

Wan, J., Ramachandran, R., and Goldman, D. (2012). HB-EGF is necessary and sufficient for Muller glia dedifferentiation and retina regeneration. Dev Cell *22*, 334-347.

Wang, C., Wang, X., Liang, H., Wang, T., Yan, X., Cao, M., Wang, N., Zhang, S., Zen, K., Zhang, C.*, et al.* (2013). miR-203 Inhibits Cell Proliferation and Migration of Lung Cancer Cells by Targeting PKCalpha. PloS one *8*, e73985.

Wang, C., Zheng, X., Shen, C., and Shi, Y. (2012). MicroRNA-203 suppresses cell proliferation and migration by targeting BIRC5 and LASP1 in human triple-negative breast cancer cells. Journal of Experimental & Clinical Cancer Research : CR *31*, 58.

Wang, Y., Baskerville, S., Shenoy, A., Babiarz, J.E., Baehner, L., and Blelloch, R. (2008). Embryonic stem cell-specific microRNAs regulate the G1-S transition and promote rapid proliferation. Nat Genet *40*, 1478-1483.

Wang, Y., Medvid, R., Melton, C., Jaenisch, R., and Blelloch, R. (2007). DGCR8 is essential for microRNA biogenesis and silencing of embryonic stem cell self-renewal. Nat Genet *39*, 380-385.

Weber, A., Hochmann, S., Cimalla, P., Gartner, M., Kuscha, V., Hans, S., Geffarth, M., Kaslin, J., Koch, E., and Brand, M. (2013). Characterization of light lesion paradigms and optical coherence tomography as tools to study adult retina regeneration in zebrafish. PloS one *8*, e80483.

Wei, C., Salichos, L., Wittgrove, C.M., Rokas, A., and Patton, J.G. (2012). Transcriptome-wide analysis of small RNA expression in early zebrafish development. RNA *18*, 915-929.

Wenzel, A., Grimm, C., Marti, A., Kueng-Hitz, N., Hafezi, F., Niemeyer, G., and Reme, C.E. (2000). c-fos controls the "private pathway" of light-induced apoptosis of retinal photoreceptors. J Neurosci *20*, 81-88.

Wenzel, A., Grimm, C., Samardzija, M., and Reme, C.E. (2005). Molecular mechanisms of light-induced photoreceptor apoptosis and neuroprotection for retinal degeneration. Progress in Retinal and Eye Research *24*, 275-306.

Wienholds, E., Koudijs, M.J., van Eeden, F.J., Cuppen, E., and Plasterk, R.H. (2003). The microRNA-producing enzyme Dicer1 is essential for zebrafish development. Nat Genet *35*, 217-218.

Wightman, B., Ha, I., and Ruvkun, G. (1993). Posttranscriptional regulation of the heterochronic gene lin-14 by lin-4 mediates temporal pattern formation in C. elegans. Cell *75*, 855-862.

Wong, R.O.L., and Godinho, L. (2003). Development of the vertebrate retina (MIT Press).

Wu, D.M., Schneiderman, T., Burgett, J., Gokhale, P., Barthel, L., and Raymond, P.A. (2001). Cones regenerate from retinal stem cells sequestered in the inner nuclear layer of adult goldfish retina. Invest Ophthalmol Vis Sci *42*, 2115-2124.

Wu, J.H., Gao, Y., Ren, A.J., Zhao, S.H., Zhong, M., Peng, Y.J., Shen, W., Jing, M., and Liu, L. (2012). Altered microRNA expression profiles in retinas with diabetic retinopathy. Ophthalmic Research *47*, 195-201.

Xiao, C., Calado, D.P., Galler, G., Thai, T.H., Patterson, H.C., Wang, J., Rajewsky, N., Bender, T.P., and Rajewsky, K. (2007). MiR-150 controls B cell differentiation by targeting the transcription factor c-Myb. Cell *131*, 146-159.

Yang, A., Schweitzer, R., Sun, D., Kaghad, M., Walker, N., Bronson, R.T., Tabin, C., Sharpe, A., Caput, D., Crum, C.*, et al.* (1999). p63 is essential for regenerative proliferation in limb, craniofacial and epithelial development. Nature *398*, 714-718.

Yi, R., Poy, M.N., Stoffel, M., and Fuchs, E. (2008). A skin microRNA promotes differentiation by repressing 'stemness'. Nature *452*, 225-229.

Yin, V.P., Lepilina, A., Smith, A., and Poss, K.D. (2012). Regulation of zebrafish heart regeneration by miR-133. Dev Biol *365*, 319-327.

Yin, V.P., Thomson, J.M., Thummel, R., Hyde, D.R., Hammond, S.M., and Poss, K.D. (2008). Fgf-dependent depletion of microRNA-133 promotes appendage regeneration in zebrafish. Genes Dev *22*, 728-733.

Yoo, A.S., Sun, A.X., Li, L., Shcheglovitov, A., Portmann, T., Li, Y., Lee-Messer, C., Dolmetsch, R.E., Tsien, R.W., and Crabtree, G.R. (2011). MicroRNA-mediated conversion of human fibroblasts to neurons. Nature *476*, 228-231.

Young, R.W. (1985a). Cell differentiation in the retina of the mouse. The Anatomical Record *212*, 199-205.

Young, R.W. (1985b). Cell proliferation during postnatal development of the retina in the mouse. Brain Res *353*, 229-239.

Yu, X., Li, H., Jiang, X., Guo, L., Jiang, W., and Lu, S.H. (2013). MiR-203 inhibits the proliferation and self-renewal of esophageal cancer stem-like cells by suppressing stem renewal factor Bmi-1. Stem Cells and Development (available online)

Yu, Y.M., Gibbs, K.M., Davila, J., Campbell, N., Sung, S., Todorova, T.I., Otsuka, S., Sabaawy, H.E., Hart, R.P., and Schachner, M. (2011). MicroRNA miR-133b is essential for functional recovery after spinal cord injury in adult zebrafish. Eur J Neurosci *33*, 1587-1597.

Yurco, P., and Cameron, D.A. (2005). Responses of Muller glia to retinal injury in adult zebrafish. Vision Research *45*, 991-1002.

Zack, D.J., Dean, M., Molday, R.S., Nathans, J., Redmond, T.M., Stone, E.M., Swaroop, A., Valle, D., and Weber, B.H. (1999). What can we learn about age-related macular degeneration from other retinal diseases? Mol Vis *5*, 30.

Zhu, Q., Sun, W., Okano, K., Chen, Y., Zhang, N., Maeda, T., and Palczewski, K. (2011). Sponge transgenic mouse model reveals important roles for the microRNA-183 (miR-183)/96/182 cluster in postmitotic photoreceptors of the retina. The Journal of Biological Chemistry *286*, 31749-31760.